

**Structural, physical and genetic interactions
of the *i*-AAA protease Yme1 in
*Saccharomyces cerevisiae***

Inaugural-Dissertation

zur

Erlangung des Doktorgrades

der Mathematisch-Naturwissenschaftlichen Fakultät

der Universität zu Köln



vorgelegt von

Tanja Engmann

aus Iserlohn

Köln, 2009

Berichtersteller:

Professor Dr. Thomas Langer

Professor Dr. R. Jürgen Dohmen

Tag der mündlichen Prüfung: 20. Mai 2009

Abstract

The \hat{i} -AAA protease Yme1 is a highly conserved ATP-dependent AAA (ATPase Associated with various cellular Activities) protease anchored to the inner mitochondrial membrane where it mediates protein quality surveillance that is crucial for cell survival. In yeast, deletion of *YME1* is associated with pleiotropic phenotypes. However, the few known proteolytic substrates and interaction partners of the \hat{i} -AAA protease cannot explain the molecular basis of these phenotypes. Therefore, different approaches were used to define the function of the \hat{i} -AAA protease. First, affinity purification of a proteolytic inactive variant of Yme1 working as a substrate trap was employed and led to the identification of eight novel Yme1-interacting proteins that localise to different submitochondrial compartments. Subsequent analysis revealed that two interactors, Mcr1 and Mpm1, represent new proteolytic substrates of the \hat{i} -AAA protease. Hence, additional functions of the \hat{i} -AAA protease should be responsible for the other identified interactions. Second, insights into processes that require the function of the \hat{i} -AAA protease were obtained by a synthetic genetic array (SGA) approach using an assorted library of 96 non-essential mitochondrial gene deletions. 34 identified synthetic lethal interactions potentially link Yme1 to new functions like mitochondrial morphology, protein processing and lipid metabolism. Finally, the synthetic lethal interaction of *IMP1* and *YME1* was analysed by a high copy suppressor screening. This interaction is of particular interest, as all substrates of the Imp1 catalytic subunit of the IMP processing peptidase could be co-purified with the \hat{i} -AAA protease. The identified suppressor Pgc1, a key enzyme in glycolysis and gluconeogenesis, suggests a severe impairment of $\Delta yme1\Delta imp1$ cells in energy metabolism.

Moreover, in this thesis the substrate recognition by the \hat{i} -AAA protease was examined by mutational analysis. Recently, two substrate binding regions have been identified within Yme1: the CH-(C-terminal helices) and the NH-(N-terminal helices) region. In contrast to the NH-region, the molecular mechanism of substrate binding to the CH-region has not been studied so far. Here, the CH-region was not only identified to have a role in substrate binding and transfer to the proteolytic cavity, but also for the stabilisation of the \hat{i} -AAA protease complex.

Taken together, novel substrates and interaction partners of the \hat{i} -AAA protease were identified, pointing to additional functions of Yme1 independent of its proteolytic activity. As only few approaches have addressed the function of the \hat{i} -AAA protease in higher eukaryotes so far, it will be interesting to examine the relevance of these findings for mammals.

Table of contents

1	Introduction	1
1.1	Cellular compartmentation	1
1.2	Metabolic requirements of mitochondria	1
1.2.1	Role of mitochondria for the cellular energy metabolism	2
1.2.2	Mitochondrial lipids and ergosterol	3
1.3	Proteolytic systems controlling mitochondrial maintenance	9
1.4	ATP-dependent proteases.....	11
1.4.1	AAA ⁺ -proteases	12
1.4.2	Recognition and handling of substrate by AAA ⁺ -proteases.....	13
1.4.3	Mitochondrial AAA ⁺ -proteases.....	15
1.4.4	Substrate recognition by the <i>f</i> -AAA-proteases.....	16
1.4.5	Functions of the <i>f</i> and <i>m</i> -AAA proteases in mitochondria	18
1.4.6	The conserved <i>f</i> -AAA protease Yme1	20
1.5	Mitochondrial peptidases and mitochondrial protein import.....	22
1.6	Aims of the thesis	25
2	Materials and Methods	26
2.1	Molecular Biology Methods	26
2.1.1	Yeast expression plasmid	26
2.1.2	Plasmids for <i>in vitro</i> transcription and translation	28
2.2	Cell biology methods	29
2.2.1	Yeast strains and growth conditions	29
2.2.2	Yeast genetic procedures	35
2.3	Biochemistry Methods	36
2.3.1	Total protein isolation from <i>S. cerevisiae</i>	36
2.3.2	Preparation of cellular membranes from <i>S. cerevisiae</i>	36
2.3.3	Immunological detection of proteins.....	36
2.3.4	Procedures employing S ³⁵ -radiolabelled polypeptides.....	37
2.3.4.1	<i>In vitro</i> MPP-cleavage assay.....	37
2.3.4.2	Import and import-chase of S ³⁵ -radioalbled polypeptides into isolated mitochondria	38
2.3.5	Co-immunoprecipitation	38
2.3.6	Blue native polyacrylamide gel electrophoresis (BN-PAGE)	39
2.3.7	Ni-NTA affinity chromatography of mitochondrial extracts	39
2.3.8	Lipid analysis	40
2.3.8.1	Lipid isolation.....	40
2.3.8.2	Thin Layer Chromatography (TLC).....	41
2.3.9	Miscellaneous.....	41
3	Results	42

3.1	Initial substrate binding to the CH-region of the <i>i</i> -AAA protease Yme1.....	42
3.1.1	Mutational analysis of the α -17 and α -18 helices of the CH-region of Yme1 in regard to substrate binding and degradation	43
3.1.1.1	<i>In vivo</i> activity of CH-mutant variants of Yme1.....	44
3.1.1.2	Cox2 binding to Yme1 CH-mutant variants.....	46
3.1.1.3	Degradation of Cox2 in Δ <i>sco1</i> Δ <i>yme1</i> harbouring CH-mutant variants of Yme1	47
3.1.2	Effects of C-terminal truncations of the CH-region of Yme1 on substrate degradation and complex formation of the <i>i</i> -AAA protease.....	48
3.1.2.1	<i>In vivo</i> activity of C-terminal truncation mutants of Yme1	49
3.1.2.2	Degradation of Cox2 in Δ <i>sco1</i> Δ <i>yme1</i> and Δ <i>imp1</i> Δ <i>yme1</i> harbouring C-terminal truncation mutants of Yme1.....	50
3.1.2.3	Complex formation of C-terminally truncated Yme1 mutants.....	51
3.2	Identification of binding partners of the <i>i</i> -AAA protease Yme1.....	53
3.2.1	Maturation of the <i>i</i> -AAA protease subunits Yme1 from different species.....	53
3.2.1.1	<i>In vivo</i> processing of Yme1 in mutants of different processing peptidases.....	54
3.2.1.2	Processing of <i>in vitro</i> translated ³⁵ S- radiolabelled Yme1 orthologs by purified MPP	55
3.2.1.3	<i>In vivo</i> activity of N-terminally tagged <i>i</i> -AAA protease.....	56
3.2.2	Affinity purification of a proteolytically inactive variant of Yme1	57
3.2.3	Co-immunoprecipitation of Yme1 from strains harbouring HA-tagged versions of Yme1-interacting proteins.....	59
3.2.4	Correlation of Δ <i>yme1</i> phenotypes to the phenotypes of Yme1-interacting proteins	62
3.2.5	Effects of the <i>i</i> -AAA protease on Yme1-interacting proteins	63
3.2.5.1	Steady state levels of Yme1-interacting proteins in the presence or absence of Yme1.....	63
3.2.5.2	<i>In organello</i> import of <i>in vitro</i> translated Mcr1, Mpm1, Gep1 and Qcr2 into isolated wild type and Δ <i>yme1</i> mitochondria.....	64
3.2.5.3	<i>i</i> -AAA protease dependent degradation of Mcr1, Mpm1 and Phb1	66
3.2.5.4	<i>In organello</i> import of <i>in vitro</i> translated Pda1 and Pdb1 into isolated wild type and Δ <i>yme1</i> mitochondria.....	68
3.2.6	Variations in expression of Yme1-interacting proteins and their influence on Δ <i>yme1</i>	69
3.2.6.1	Effects of Gep1 overexpression in wild type and Δ <i>yme1</i> cells	69
3.2.6.2	Overexpression of Mcr1 in wild type and Δ <i>yme1</i>	70
3.2.7	Effects of Δ <i>yme1</i> on cellular ergosterol levels.....	71
3.3	Analysis of genetic interactions of the <i>i</i> -AAA protease Yme1	74
3.3.1	Analysis of genetic interactions of Δ <i>yme1</i> with a deletion library of assorted mitochondrial proteins.....	74
3.3.1.1	Phenotypic analysis of Δ <i>yme1</i> synthetic lethal interactors	77
3.3.2	High copy suppressor screening for synthetic lethal interactors of Yme1.....	78
3.3.2.1	Identification of genes suppressing the synthetic lethality of Δ <i>yme1</i> Δ <i>imp1</i>	79
3.3.2.2	Suppression of Δ <i>yme1</i> phenotypes by suppressors of Δ <i>yme1</i> Δ <i>imp1</i>	81
4	Discussion	82
4.1	Role of the CH-region of the <i>i</i> -AAA protease Yme1 in substrate binding.....	82

4.1.1	Initial substrate binding by the CH-region of the <i>f</i> -AAA protease Yme1	82
4.1.2	CH-dependent degradation of substrates by the <i>f</i> -AAA protease Yme1	84
4.1.3	Structural importance of the CH-region of Yme1.....	86
4.2	Processing of the <i>f</i> -AAA protease Yme1	86
4.3	Novel interaction partners of the <i>f</i> -AAA protease Yme1	88
4.3.1	Possible function of the <i>f</i> -AAA protease Yme1 in sorting and assembly of the mitochondrial proteins Qcr2, Pda1 and Pdb1	89
4.3.2	New substrates of the <i>f</i> -AAA protease: Mpm1 and Mcr1	91
4.3.3	The <i>f</i> -AAA protease Yme1 functionally interacts with Gep1	93
4.4	Genetic interaction of the <i>f</i> -AAA protease Yme1	95
4.4.1	Synthetic lethality of the <i>f</i> -AAA protease Yme1 – more than just an consequence of mtDNA loss.....	95
4.4.2	New implications for Yme1 function	96
4.4.3	High copy suppressor screen of $\Delta yme1\Delta imp1$	98
4.5	Impact of the <i>f</i> -AAA protease Yme1 on cellular and mitochondrial lipid levels....	99
4.5.1	Depletion of Yme1 changes mitochondrial phospholipids levels.....	99
4.5.2	A potential influence of Yme1 on cellular ergosterol distribution.....	100
5	Zusammenfassung.....	103
6	References	105
7	List of abbreviations	123
8	Attachment	124
9	Danksagung.....	125
10	Eidesstattliche Erklärung	126
11	Lebenslauf	127

1 Introduction

1.1 Cellular compartmentation

The concept of eukaryotic compartmentation enables the segregation of specific biochemical reactions to distinct environments for the purpose of biochemical efficiency and restricted dispersion of intermediate reaction products. This is of particular importance for subsequent conversions of substrates, accomplished during metabolic processes and proteolytic events. Local enrichments are either achieved by formation of complexes that cluster specific sets of enzymes or enclosure of reactions by membranes resulting in defined aqueous environments. While prokaryotic cells do not show enclosed membrane structures, eukaryotic cells comprise a complex intracellular compartmentalisation. One of these intracellular compartments is the mitochondrion. Mitochondria, as chloroplasts, are surrounded by two membranes which, according to the endosymbiotic theory, originate from invasion of a α -proteobacterium into a primordial eukaryotic cell (Wallace, 2007). These two membranes configure four mitochondrial subcompartments: Outer mitochondrial membrane, intermembrane space, inner mitochondrial membrane and the matrix space. Within the mitochondria, fundamental cellular processes are conducted which render this organelle essential for most eukaryotic cells. In fact, several diseases are associated with defects in mitochondria (Chan, 2006; Lin and Beal, 2006; Wallace, 2007) underlining the essential function of this organelle. Consequently, maintenance of mitochondrial integrity and function is crucial for an eukaryotic cell. It is therefore not surprising, that the inherited proteolytic quality control system of mitochondrial ancestors is conserved (Koppen and Langer, 2007) and that a number of accessory defence systems have evolved (Tatsuta and Langer, 2008).

1.2 Metabolic requirements of mitochondria

Mitochondria do not only adapt their activity to different physiological demands, but they are in addition able to modulate their subcellular distribution to local cellular requirements. The latter is accomplished by the formation of a reticulated mitochondrial network which responds to cellular needs by constant fission and fusion events, thereby optimising mitochondrial performance (Cervený et al., 2007; Detmer and Chan, 2007; Hoppins et al., 2007). The most prominent metabolic reactions within mitochondria of *S. cerevisiae* are the citric acid cycle (also known as TCA or Krebs cycle), the process of oxidative phosphorylation

and the biosynthesis of amino acids (in mammals also β -oxidation of fatty acids). Moreover, mitochondria are the site of heme and Fe/S cluster biosynthesis (Hamza, 2006; Lill and Muhlenhoff, 2006; Lill and Muhlenhoff, 2008) and involved in the intermediary metabolism, calcium homeostasis and apoptosis (Chan, 2006; McBride et al., 2006). The maintenance of all of these processes is crucial for the survival of an organism.

1.2.1 Role of mitochondria for the cellular energy metabolism

Under aerobic conditions, mitochondria can serve as the major site of ATP production of the cell, harbouring the constituents of the citric acid cycle and the oxidative phosphorylation within the matrix space and the inner mitochondrial membrane, respectively. The mitochondria dependent energy production is also called respiration. Conversely, in the absence of oxygen cells undergo fermentation, a process that does not require the function of mitochondria. Glucose is the main source of energy utilised in both processes. However, yeast and other eukaryotic cells do not strictly depend on the availability of glucose; they are able to adapt their metabolic system to different carbon sources, but only under aerobic conditions. In the presence of glucose, most energy is generated by cytosolic glycolysis. Only upon utilisation of non-fermentable carbon sources, such as glycerol or lactate, the mitochondrial oxidative metabolism is fully activated. Non-fermentable carbon sources usually need to be remodeled before they can serve as a source of energy. Such enzymatic activities are partially present within mitochondria. Glycerol is processed within the cytosol to glycerol-3-phosphate by Gut1 (Pavlik et al., 1993). After glycerol-3-phosphate is internalised into mitochondria, it is converted into dihydroxy-acetate-phosphate (DAH-phosphate) that can enter the cytosolic glycolysis or gluconeogenesis processes (Sprague and Cronan, 1977). The mitochondrial enzyme producing DAH-phosphate is known as glycerol 3-phosphate dehydrogenase, Gut2, and is localized to the inner mitochondrial membrane (Rijken et al., 2007; Ronnow and Kielland-Brandt, 1993). Lactate, another non-fermentable carbon source, is converted within the mitochondria to pyruvate that can enter glycolysis or gluconeogenesis. Within yeast mitochondria, one L-lactate dehydrogenase (cytochrome *b2*) Cyb2 (Lodi and Ferrero, 1993) and two D-lactate dehydrogenase, Dld1 and Dld2 (Chelstowska et al., 1999; Rojo et al., 1998) are present. In addition, mitochondria contain enzymes that are able to connect different metabolic pathways. One important representative is the multienzyme pyruvate dehydrogenase complex that resides in the matrix space of mitochondria. The enzyme is composed of two E1 proteins Pda1 and Pdb1, the E2 core protein Lat1, the E3 protein Lpd1 and the protein X component Pdx1 (Pronk et al., 1996). The important function of this mitochondrial complex is the oxidative

decarboxylation of internalised pyruvate into acetyl CoA and CO₂, thereby linking glycolysis to the citric acid cycle. In general, the citric acid cycle is responsible for the complete conversion of nutrients, thus producing NADH and FADH₂ molecules that are utilised during oxidative phosphorylation, as well as GTP. Furthermore, biosynthetic components, like amino acids, relevant for diverse cellular elements are initialised via the citric acid cycle.

Therefore, the mitochondria do not only present the most efficient site of cellular ATP production, but are also involved in utilisation of alternative carbon sources. In addition, pathways within the mitochondria enable the supply/allocation of components originally used for energy production in the biogenesis of diverse cellular constituents like amino acid, fatty acids and heme (porphyrine) precursors.

1.2.2 Mitochondrial lipids and ergosterol

Although mitochondrial functions have been analysed extensively over the past decades, the role of lipids within this organelle has only more recently attracted the attention of research. Just like proteins, lipids are also important for the biogenesis and maintenance of mitochondria. In respect to cellular lipid supply, mitochondria are of particular interest, as they are involved in the biogenesis of some lipid species (Voelker, 2004). Yeast mitochondria usually comprise glycerophospholipids (phospholipids) and to a lower extent the yeast specific sterol ergosterol (Zinser and Daum, 1995). However, in contrast to other cellular membranes no sphingolipids are found in mitochondrial membranes.

Commonly, phospholipids are composed of a phosphatidic acid element that is attached to variable head groups. The phosphatidic acid element contains a glycerol backbone which attaches to one phosphate and two fatty acids through ester bonds (Fig. 1.1). The variable head groups of phospholipids include choline, ethanolamine, serine, inositol and glycerol (van Meer et al., 2008). A phospholipid exclusively present within mitochondria is cardiolipin (Jakovcic et al., 1971). In contrast to other phospholipids, cardiolipin is a polyglycerophospholipid and contains two phosphatidic acid moieties that are linked via a glycerol bridge and harbour altogether four fatty acids (Fig. 1.1) (Schlame, 2008).

The two most abundant phospholipids within yeast mitochondria are phosphatidylethanolamine (PE) and phosphatidylcholine (PC) (Zinser and Daum, 1995). Whereas PC is only imported into mitochondria, PE can also be generated within mitochondria. The inner mitochondrial membrane protein Psd1 produces the majority of cellular PE by conversion of phosphatidylserine (PS) to PE (Clancey et al., 1993). Alternatively PE is produced from PS at the golgi-apparatus by Psd2 (Trotter and Voelker, 1995). Both PE and PC can also be synthesised via the Kennedy-pathway (Kent, 1995). However, the PE and PC species

synthesised through this pathway make only minor contributions to mitochondrial phospholipids (Birner et al., 2001). Another cellular compartment essential for the biogenesis of phospholipids is a specialised fraction of the endoplasmic reticulum (ER) called the MAM (mitochondria associated membrane) fraction. Here, the two MAM proteins Pem1 and Pem2 are required for conversion of PE to PC (Zinser et al., 1991). Furthermore, Cds1 produces CDP-diacylglycerol (CDP-DAG) from phosphatidic acid (PA) that is required for the generation of phosphatidylserine (PS) and phosphatidylinositol (PI) in the MAMs (Achleitner et al., 1999; Gaigg et al., 1995). Cds1 is also present in the inner mitochondrial membrane where it plays a role in the production of cardiolipin (Kuchler et al., 1986). PA is synthesised in mitochondria by a two-step acylation of glycerol-3-phosphate at the outer membrane of mitochondria (Athenstaedt and Daum, 1999).

Cardiolipin (CL) is the third most abundant phospholipid (14,6%) present in mitochondria. Unlike PE and PC, CL is enriched in the inner mitochondrial membrane and not distributed equally between the two mitochondrial membranes (Schlame, 2008). Consistently, the synthesis of cardiolipin takes place in the inner membrane of mitochondria. After CDP-DAG is produced by Cds1, it is further processed by Pgs1 to phosphatidylglycerolphosphate (PGP) (Chang et al., 1998). Then, dephosphorylation occurs by a still unknown enzyme. The resulting phosphatidylglycerol (PG) is converted by the cardiolipin synthase, Crd1, to CL (Chang et al., 1998; Tuller et al., 1998). In addition, so-called remodelling processes postsynthetically modify the acylchain composition of CL. One enzyme responsible for such remodelling is the transacetylase Taz1 that is localised to the inner leaflet of the outer mitochondrial membrane (Claypool et al., 2006). Interest in the functional role of Taz1 has increased when frequent mutations in the human homolog have been identified in patients suffering from Barth Syndrome (Bione et al., 1996). In yeast, CL is also required for a variety of cellular functions like ageing, apoptosis, mitochondrial protein import, mitochondrial bioenergetics, translational regulation and cell wall biosynthesis (Joshi et al., 2008).

Although phospholipids produced in mitochondria are often transferred to different sites within the cell before they can fulfil their function, not much is known about the exact transport mechanisms of these lipids within and from mitochondria. It is conceivable that most phospholipids laterally diffuse through membrane continuities. Further, Met30 has been demonstrated to be required for transport of PS from MAMs into mitochondria (Choi et al., 2006). Thus, distinct transport molecules might exist. In general, most membrane transports are facilitated by the vesicular transport system. However, mitochondria are not connected to this system and might thus have different mechanisms for the allocation of these phospholipids to the rest of the cell. The unique lipid composition of mitochondria could have resulted from the detachment of the organelle from the vesicular transport system. Instead

of depending on the internalisation of certain lipid species, the mitochondria might rather rely on the lipids produced by themselves.

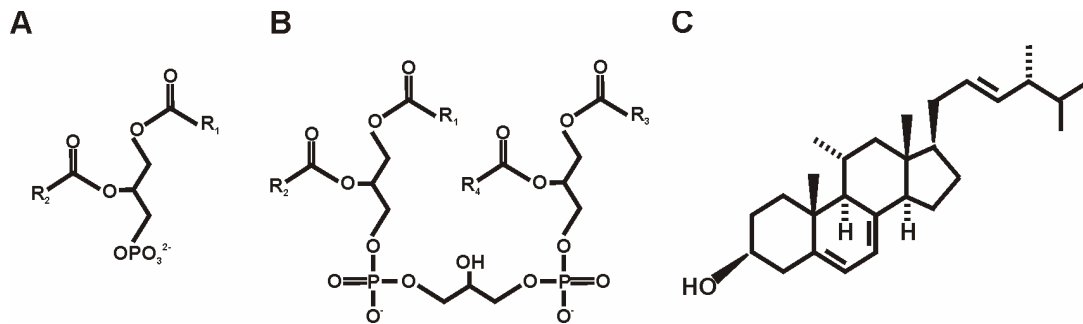


Figure 1.1 Lipid components within mitochondria. (A) Glycerophospholipids. The glycerol backbone is bound to two variable fatty acids (R_1 and R_2) and a phosphate. Variable headgroup are choline, ethanolamine, serine, inositol and glycerol. (B) Polyglycerophospholipids. Two glycerol backbones are linked with two phosphates by a glycerol bridge between the two phosphate moieties. Four variable fatty acids can be attached here. The predominant polyglycerophospholipid in mitochondria is cardiolipin. (C) Sterols. Ergosterol, the sterol found in yeast like *S. cerevisiae*, is shown.

Another lipid found in mitochondria but originating from synthesis in the ER is ergosterol. Sterols are composed of a cholestane basis to which different side chains can be attached at the C-17 residue (Fig. 1.1) (Moss, 1989). Biosynthesis of ergosterol is a fairly complex procedure that involves 22 different enzymatic activities (Daum et al., 1998). The biosynthetic pathway of ergosterol formation can be split into two parts. The first part, commonly called the mevalonate or isoprenoid pathway, is initiated with two acetyl CoA molecules that are processed to farnesyl pyrophosphate. In the second part of ergosterol biosynthesis, farnesyl pyrophosphate is converted to ergosterol. Deletions of the enzymes required for the earlier step of the ergosterol biosynthesis are lethal. Conversely, the absence of the enzymes facilitating the last eight steps is not lethal, although the produced intermediates cannot substitute for ergosterol (Daum et al., 1998). The reason for this discrepancy is not understood. Most steps within the biosynthetic pathway of ergosterol are performed within the ER (Zinser et al., 1993) and only a subset of enzymatic activities is found in mitochondria. Erg10, an acetoacetyl CoA thiolase facilitating the first step of the ergosterol biosynthesis, is localised to both the cytoplasm and mitochondria (Kornblatt and Rudney, 1971). Additionally, the two outer mitochondrial membrane proteins Ncp1 and Mcr1 are involved in the reduction of the cytochrome P450 family member Erg11 (Lamb et al., 1999; Sutter and Loper, 1989), for which an ER localisation is proposed (Ott et al., 2005). Hence, no direct participation of mitochondria in ergosterol biosynthesis is evident. Nevertheless, ergosterol biosynthesis requires molecular oxygen and is thus depending on the mitochondrial heme production regulating the molecular oxygen content of the cell. The

oxygen dependent steps in the ergosterol biosynthesis are the epoxidation of squalene and the desaturation and demethylation of lanosterol (Hata et al., 1981; Lorenz et al., 1986). As a result, yeast is only able to produce ergosterol under aerobic conditions. Under anaerobic conditions, however, yeast is sterol auxotroph and depends on the exogenous supply of this essential cellular compound (Lewis et al., 1985; Lorenz and Parks, 1991). Accordingly, uptake mechanisms of ergosterol have been identified (Fig. 1.2). This uptake depends on an impaired heme biosynthesis and is hence restricted to anaerobic conditions, a phenomenon also referred to as 'aerobic sterol exclusion' (Lorenz et al., 1986) that is not well understood. Consequently, under aerobic conditions ergosterol is synthesised endogenously and no uptake is possible, whereas under anaerobic conditions endogenous synthesis is impaired and the essential uptake of exogenous ergosterol is induced via the transcription factor Ucp2 (Crowley et al., 1998). Resulting expression of Pdr11 and Aus1, two ATP-binding cassette transporters, leads to the ATP-dependent uptake of the exogenous ergosterol (Wilcox et al., 2002) and thereby ensures cell survival.

Ergosterol is unequally distributed throughout different membranes and the incorporation of sterol intermediates is not favoured (Daum et al., 1998). Ergosterol is most abundant in the plasma membrane and in secretory particles (Zinser and Daum, 1995). Further, lipid particles, microsomes and the inner membrane of mitochondria contain ergosterol (Schneiter et al., 1999). Surprisingly, the site of ergosterol biosynthesis, the ER, contains a relatively low ergosterol content implying an efficient postsynthetic depletion and trafficking of the sterol to a distinct location (Fig. 1.2). Ergosterol resides in cellular compartments in form of free ergosterol (plasma membrane). Another form of ergosterol, steryl ester, resembles the storage form of ergosterol and its intermediates and is predominantly found together with triacylglycerol (TAG) in lipid particles (Czabany et al., 2007; Czabany et al., 2008). Conversion of ergosterol and its intermediates to the storable ester form is achieved by Are1 and Are2 at the expense of acetyl CoA (Zweytick et al., 2000). Stored steryl ester are mobilised upon requirement by the action of the steryl ester hydrolases Tgl1, Yeh1 and Yeh2 (Köffel et al., 2005; Wagner et al., 2009). As hydrolysis of steryl esters occurs at different cellular localisations, a role of lipid particles in trafficking of ergosterol cannot be excluded. However, the major sterol trafficking between the ER and the plasma membrane has been demonstrated to occur via vesicular or non-vesicular pathways (Raychaudhuri and Prinz, 2006; Sullivan et al., 2006). In the non-vesicular pathway, translocation of sterols from the ER to the plasma membrane is based on the decreased chemical potential of sterol after its binding to other kinds of lipids within the plasma membrane. As these sterol moieties are not able to diffuse within the gradient between the sterol rich plasma membrane and the sterol poor ER, successive incorporation of ergosterol into the already sterol enriched

compartment is achieved. The non-vesicular pathway was identified in experiments utilising Brefeldin A for disruption of the vesicular pathway where no impairment of sterol trafficking was obvious (Baumann et al., 2005). Within this pathway, oxysterol binding proteins (OSH) are responsible for the transport of sterols through the hydrophilic environment (Beh et al., 2009; Wang et al., 2005). Additional lipid transfer proteins have been identified in mammals (Prinz, 2007). In yeast, additional factors are found to influence the cellular distribution of sterols. Altered intracellular sterol is observed in the absence of Arv1, Ptc1 and Plc1 (Fei et al., 2008; Tinkelenberg et al., 2000). Their exact function, however, is not understood.

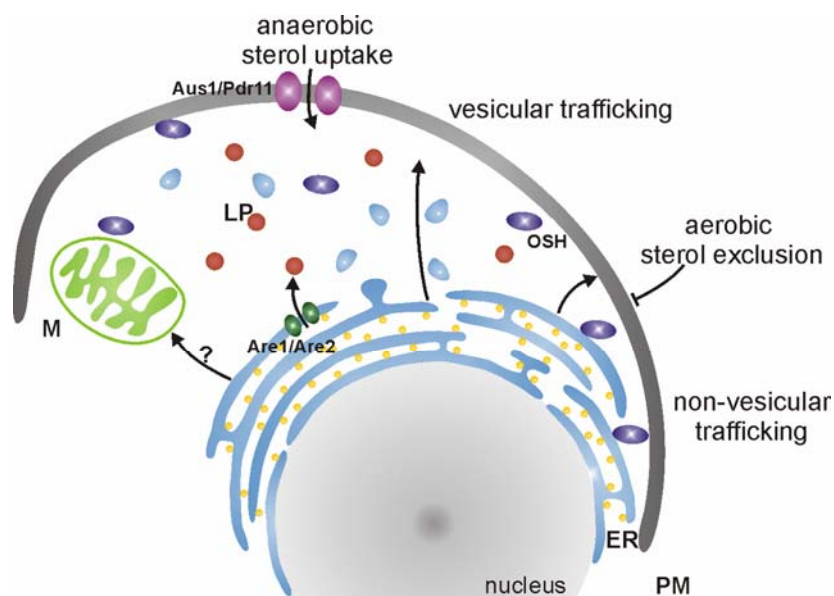


Figure 1.2 Uptake and trafficking of cellular ergosterol. Uptake of exogenous sterol in yeast is only facilitated under anaerobic conditions by the two ATP-binding cassette transporters Aus1 and Pdr11 localised to the plasma membrane (PM). Under aerobic conditions the supply of ergosterol is restricted to intracellular synthesis, a phenomenon called "aerobic sterol exclusion". The major site of sterol synthesis is the endoplasmic reticulum (ER). Ergosterol trafficking occurs over vesicular and non-vesicular pathways. The later involves the action of oxysterol binding proteins (OSH). Both trafficking pathways mainly mediate the translocation of ergosterol between ER and PM. The mechanism by which ergosterol is transported to mitochondria (M) is, however, not understood. Storage of ergosterol and intermediates in their steryl ester form is mediated by Are1 and Are2 which compose lipid particles (LP) in the ER. PM, plasma membrane; ER, endoplasmic reticulum; M, mitochondria; LP, lipid particle; OSH, oxysterol binding proteins.

As mitochondria are not connected to the vesicular transport system of the cell, import of sterols into the organelle must also be achieved by a non-vesicular pathway. In yeast, no components involved in this process have been identified yet. The movement of sterols between the inner and outer mitochondrial membrane has in any case been shown to depend on the presence of ATP and the membrane potential (Tuller and Daum, 1995). In

contrast, adrenal mammalian tissue contains two mitochondrial outer membrane proteins responsible for sterol transport into mitochondria. The peripheral benzodiazepine receptor (PBR) contains a cholesterol binding domain and is highly expressed in steroidogenic cells (Papadopoulos et al., 1997; Papadopoulos et al., 1997). The steroid acute regulatory protein (STAR) mediates the translocation of cholesterol from the outer mitochondrial membrane to the inner mitochondrial membrane (Miller, 2007). The exact mode of action by which STAR facilitates sterol transport is still under debate.

Although sterols represent extremely expensive metabolic components, they account for a substantial amount of the cellular lipids. As cells acquiesce the complexity and cost of sterol biosynthesis, the function of sterols must be crucial for the viability of eukaryotic cells, and irreplaceable by any other cellular lipid component (Parks et al., 1995). Most studies defining the role of sterol in eukaryotic membranes have been performed in yeast. Here, ergosterol functions in bulk membrane formation influencing the rigidity and permeability of the membrane (Abe and Hiraki, 2009; Kleinhans et al., 1979; Lees et al., 1979). In this line, sterols participate in the formation of detergent resistant membranes (DRM) (Cerneus et al., 1993). Ergosterol is implicated in a variety of other function in yeast, that will not be discussed in detail here. Moreover, a function in membrane packing of phospholipids by the mammalian sterol cholesterol is described (Ikonen, 2008; McConnell and Radhakrishnan, 2003). Further, coinciding ergosterol has a protective effect against phospholipid peroxidation (Wiseman et al., 1993; Wiseman et al., 1993) occurring for example upon stroke.

Most of the proposed functions of ergosterol are based on the analysis of the plasma membrane moiety of this lipid. However, similar roles in sorting and organisation by ergosterol may be expected in mitochondria where the majority of lipid is represented by phospholipids. One proposed regulatory role of ergosterol is the maintenance and/or biogenesis of mitochondrial morphology (Altmann and Westermann, 2005). Whether the underlying events leading to the disturbed mitochondrial morphology are based on alterations of mitochondrial or cellular ergosterol levels is not clear. The exact function of ergosterol in mitochondria remains up to date unknown. In contrast, mammalian cells are depending on mitochondria for the synthesis of steroids (steroidogenesis). For this purpose, conversion of internalised cholesterol to pregnenolone, the rate limiting step of steroidogenesis, is achieved by the action of cytochrome P450_{scc} (CPY11A1) (Miller, 2007). The STAR lipid transfer proteins play a crucial role in this process by delivering cholesterol from the outer to the inner mitochondrial membrane. The essential role of this mitochondrial process is evident in mammals that suffer from congenital lipid adrenal hyperplasia that is associated with mutations in STAR or P450_{scc} (Miller, 1997; Yang et al., 1993). Additional

metabolic reactions are performed on internalised 11-decorticoesterone (DOC) and 11-deoxycortisol (DOCHL). Nevertheless, other functions of mitochondrial sterol in mammals and in yeast remain to be elucidated, as well as the mitochondrial transport of sterols in yeast.

1.3 Proteolytic systems controlling mitochondrial maintenance

Different lines of defence assuring the integrity of mitochondria have evolved (Tatsuta and Langer, 2008). On tissue level, cells with damaged mitochondria can undergo apoptosis to prevent for example subsequent damage of adjacent cells. On an organellar level, the mitochondrial integrity can be controlled by complete removal of damaged organelles by mitophagy (Kim et al., 2007), an autophagy related process. This event will lead to the turnover of the ~1000 known mitochondrial proteins (Mootha et al., 2003; Sickmann et al., 2003; Taylor et al., 2003). A more economic process is the restoration of function by fusion of damaged mitochondria with intact neighbouring mitochondria (Detmer and Chan, 2007). Mitochondria display a dynamic network structure that is subjected to constant fission and fusion events accomplished by intricate molecular machines (Hoppins et al., 2007). Although restoring mitochondrial function, the fusion process does not ensure removal of damaged structures and does not explain the different turnover rates seen for mitochondrial proteins (Augustin et al., 2005; Russell et al., 1980). Hence, a different defence system has to exist on the level of mitochondria. Indeed, mitochondria contain an elaborate proteolytic system distributed throughout the different compartments of the organelle (Koppen and Langer, 2007). In *S. cerevisiae*, as well as in higher eukaryotes, this system is mainly built up by ATP-dependent proteases and oligopeptidases (Fig. 1.3). Representative of the yeast ATP-dependent proteases are Pim1 that acts together with Hsp78 (Röttgers et al., 2002) and the two AAA-proteases, the *i*-AAA and the *m*-AAA protease (Van Dyck and Langer, 1999). Yeast oligopeptidases are Mop112 and Prd1. In general, the term oligopeptidases refers to the ability of those peptidases to degrade peptides that result from degradation of polypeptides by other proteases further to amino acids (Desautels and Goldberg, 1982; Young et al., 2001). In case of Mop112 and Prd1 this protease is predominantly the *i*-AAA protease (Kambacheld et al., 2005).

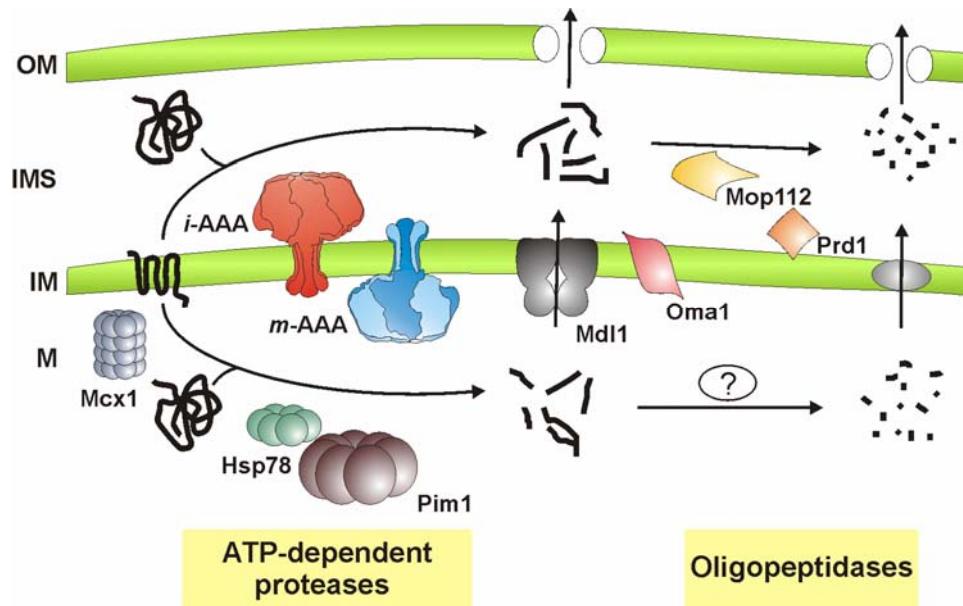


Figure 1.3 The proteolytic system of mitochondria in *S. cerevisiae*. Two classes of peptidases can be distinguished within mitochondria: ATP-dependent proteases and oligopeptidases. Additional peptidases like Oma1 exist. Both ATP-dependent proteases and the metallopeptidase Oma1 generate peptides within the mitochondrial matrix space (M) that are either directly released over the inner mitochondrial membrane (IM) into the intermembrane space (IMS) via the peptide transporter Mdl1 or are degraded further to amino acids by a so far unknown peptidase. Peptides can also be generated within the intermembrane space by the *i*-AAA protease. Then, peptides can either be released from mitochondria through the outer mitochondrial membrane (OM) or their breakdown to amino acids is facilitated by Mop112 and Prd1. See text for details.

Furthermore, peptide export has been described for yeast mitochondria depending on the ABC-transporter Mdl1 (Young et al., 2001) that is localised to the inner mitochondrial membrane. A signalling function of released peptides on nuclear gene expression of mitochondrial genes has been proposed (Arnold et al., 2006; Young et al., 2001). Within the mitochondria Mdl1 transports peptides from the matrix site to the intermembrane space, where both Mop112 and Prd1 reside. Therefore, the complete breakdown of cleaved mitochondrial targeting sequences and other peptides originally generated in the matrix space by the two oligopeptidases is plausible (Kambacheld et al., 2005; Moberg et al., 2003; Stahl et al., 2002). As deletion of both oligopeptidases is associated with mild phenotypes (Kambacheld et al., 2005), the two oligopeptidases might not be essential for breakdown of the vast majority of peptides generated by processing of mitochondrial targeting sequences in the matrix. Besides, peptides in the intermembrane space can be released freely and additional matrix oligopeptidases might exist. Furthermore, the two oligopeptidases are connected to the quality control of mitochondrial proteins since turnover occurs for 5% to 10% of all mitochondrial proteins (Augustin et al., 2005; Kambacheld et al., 2005). Moreover, yeast contains the metallopeptidase Oma1, an integral inner membrane protein

with a catalytic site that is facing the matrix space (Käser et al., 2003). Oma1 shows overlapping function with the *m*-AAA protease in quality control of inner membrane proteins by cleavage of misfolded polytopic membrane proteins at multiple sites (Käser et al., 2003). In higher eukaryotes, an additional intermembrane space serine proteases exist, HtrA2 (Omi) (Hegde et al., 2002). Diseases are not only related to mutations within the respective genes of HtrA2, but the serine protease has been linked to Parkinson disease (Martins et al., 2004; Plun-Favreau et al., 2007). Besides, mutations within the human ortholog of the *m*-AAA protease cause an autosomal recessive form of hereditary spastic paraplegia (HSP) (Casari et al., 1998). In conclusion, a concerted working mode of all proteases, the ATP-dependent proteases, oligopeptidases and other proteases like Oma1 or HtrA will facilitate quality surveillance within the mitochondria and therefore assures their function and maintenance.

1.4 ATP-dependent proteases

ATP-dependent proteases are conserved from bacteria to man. In eukaryotes, ATP-dependent proteases are required for a variety of cellular processes (Ogura and Wilkinson, 2001; Tucker and Sallai, 2007). In *Escherichia coli* four of ATP-dependent proteases, Lon, FtsH, Clp and HslUV can be distinguished (Gottesman, 2003). ATP-dependent proteases are members of the AAA⁺ (ATPases associated with various cellular activities) family of Walker type P-loop ATPases (Ammelburg et al., 2006; Hanson and Whiteheart, 2005). Proteins belonging to that class are characterised by the presence of a homologous ATPase domain referred to as AAA domain and function as molecular chaperones. The AAA domain is often accompanied by a proteolytic domain responsible for subsequent degradation of the unfolded substrate. Depending on the type of protease, the AAA domain and the proteolytic domain are expressed as one or two polypeptide chains. Furthermore, different proteolytic classes of the ATP-dependent proteases are described: Lon and Clp proteases for example represent serine proteases (Van Dyck et al., 1994; Wang et al., 1997), whereas FtsH is a metalloprotease (Tomoyasu et al., 1993). The functional protease is usually assembled into a hexameric or heptameric core ring structure that buries the proteolytic sites inside a proteolytic chamber (Sauer et al., 2004; Schmidt et al., 1999; Zwickl et al., 2000). This kind of assembly produces a high local density of proteolytic sites beneficial for substrate degradation, but also restricts the access to the proteolytic site and thereby restrains proteolysis by the ATP-dependent proteases (Prakash and Matouschek, 2004; Sauer et al., 2004; Schmidt et al., 1999; Singh et al., 2000). Moreover, functions independent of the

proteolytic activity have been indicated for the AAA domains of ATP-dependent proteases (Suzuki et al., 1997; Tatsuta et al., 2007).

1.4.1 AAA⁺-proteases

The active form of AAA⁺-proteases is established by assembly of their subunits into a hexameric or heptameric ring structure (Hanson and Whiteheart, 2005; Schmidt et al., 1999). This ring shaped structure creates an inner proteolytic cavity and is required for a coordinated function of AAA domains (Ishikawa et al., 2004; Kim and Kim, 2003; Wang et al., 2001; Xia et al., 2004; Zhang et al., 2000). In general, the AAA domain of each oligomer contributes the following functional key elements: the Walker A and B motif, the sensor-1 and sensor-2 motif and the arginine finger (Hanson and Whiteheart, 2005; Tucker and Sallai, 2007). Within the protein sequence of a subclass of the AAA⁺-proteases, the so-called AAA proteases, the sensor-1 motif and the arginine finger are mapped to the highly conserved region, called the second region of homology (SRH) (Lupas and Martin, 2002) (Fig. 1.4). Functionally, the Walker A motif is required for binding of ATP by directly interacting with the phosphate moiety of ATP (Neuwald et al., 1999). The bound ATP is then subsequently hydrolysed to ADP by residues of the Walker B motif, where an aspartate coordinates the essential Mg²⁺ ion while a glutamate activates a water molecule for the nucleophilic attack (Hanson and Whiteheart, 2005; Iyer et al., 2004). Sensor-1 and sensor-2 motif, as well as the arginine finger, also play a role in ATP binding and hydrolysis (Hanson and Whiteheart, 2005; Hishida et al., 2004; Karata et al., 1999; Ogura et al., 2004). For the action of the arginine finger and the sensor-2 motif, the formation of the ring structure is essential, because only in this configuration these elements are able to protrude into the ATPase domain of the neighbouring subunit and contact the bound nucleotide (Ogura et al., 2004). The universal function of the AAA domain is the implementation of energy derived from ATP hydrolysis into a conformational change of the molecule, driving substrate unfolding and translocation (Martin et al., 2008). Apparently, not just hydrolysis of ATP, but also binding and release of the nucleotide seem to generate the driving force for the conformational change (Wang et al., 2001). Different modes of ATP hydrolysis within the ring structure are discussed (Martin et al., 2005; Moffitt et al., 2009; Ogura and Wilkinson, 2001).

The concept of a proteolytic chamber also enables selective and entire degradation of substrates by AAA⁺-protease. Depending on the type of AAA⁺-protease the proteolytic chamber is either exclusively built up of the proteolytic domain or a participation of the AAA domain in the formation of the chamber is seen (Bieniossek et al., 2006).

Furthermore, the specific properties of prokaryotic Clp, Lon and FtsH proteases are introduced here, as orthologs of these proteases are found in mitochondria (Chapter 1.4.3). The caseinolytic protease ClpP resembles only a proteolytic subunit that is found to assemble with variable AAA subunits (mostly ClpA and ClpX) to different AAA⁺-protease constellations (Yu and Houry, 2007). Both Lon and FtsH proteases express the proteolytic and the AAA subunit in one polypeptide chain. All three proteases assemble into ring structures and a substrate entry and degradation mechanism similar to that of other AAA⁺-proteases is conceivable. Distinct structural features of Lon are the amino terminal N-domain and the proposed substrate sensor and discriminatory domain (SSD) (Licht and Lee, 2008). FtsH proteases contain an SRH domain and are therefore the only AAA protease of the three compared AAA⁺-proteases (Lupas and Martin, 2002). Moreover, FtsH proteases are integral membrane protein with two transmembrane domains situated within the N-terminal region of the protein adjacent to the AAA domain (Ito and Akiyama, 2005). The membrane bound state of FtsH proteases raises the question of how substrates are recognised and degraded. Substrate binding and translocation are crucial processes for the functionality of all AAA⁺-proteases and will be addressed in the following paragraph.

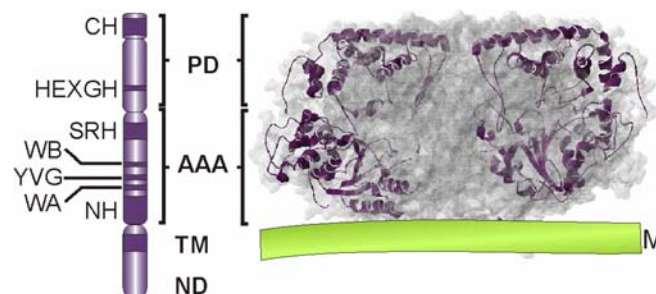


Figure 1.4 Structure of AAA protease domains and their orientation relative to the membrane. Conserved domains and motifs are indicated on the left side. Domains of the FtsH protease are projected into the predicted hexameric structure based on the crystal structure of *Thermus thermophilus* (Suno et al., 2006). ND, N-terminal domain; TM, transmembrane region; AAA, AAA domain; NH, N-terminal helix; WA, Walker A motif; YVG, central pore loop; WB, Walker B motif; SRH, second region of homology; PD, proteolytic domain; HEXGH, proteolytic center; CH, C-terminal helix; M, membrane. The figure is adapted from (Graef et al., 2008).

1.4.2 Recognition and handling of substrate by AAA⁺-proteases

Substrate engagement by the different AAA⁺-proteases occurs by a certain substrate recognition motif on the substrate, over an adaptor protein of the protease or to a specific site within the protease. Then, binding and hydrolysis of ATP will induce conformational changes that lead to an unfolding of the substrate. Finally, translocation of the substrate will

enable its subsequent degradation within the proteolytic cavity. The proposed rate limiting steps during the whole process are the unfolding and translocation of the substrate (Kenniston et al., 2003).

Here, the mechanism for substrate engagement of prokaryotic Clp, Lon and FtsH are described. Recognition elements within the substrate mediate its first contact with the protease. Accordingly, terminal or internal consensus sequences have been identified in Clp and FtsH substrates. One of the best characterised consensus sequences is the *ssrA* tag. It consists of 11 amino acids that are added C-terminally to proteins that are arrested during translation (Gottesman, 2003; Keiler et al., 1996). Sequence comparison of additional Clp substrates allowed the identification of five terminal recognition elements (Flynn et al., 2003). Also, latent terminal recognition sequences are known; for example the LexA repressor generates new C-terminal and N-terminal ends by an autocatalytic process that serve as recognition sequences for ClpXP (Neher et al., 2003). A consensus sequence has not been identified for Lon proteases, but substrate engagement is also initiated within certain recognition elements (Nishii et al., 2002; Ondrovicova et al., 2005; von Janowsky et al., 2005). Further, internal sequences can act as recognition elements for substrates engagement by the Clp and FtsH proteases under certain conditions (Hoskins et al., 2002; Okuno et al., 2006). Protease adaptor proteins are best known for Clp proteases, where the AAA subunit (ClpA or ClpX) has to be connected to the proteolytic subunit ClpP to form the functional AAA⁺-protease (Yu and Houry, 2007). The function of the AAA⁺-protease ClpAP is inhibited by ClpS (Guo et al., 2002; Zeth et al., 2002); in contrast ClpXP function is stimulated by SspB (Bolon et al., 2004; Levchenko et al., 2000). Functional stimulation of FtsH is achieved by the DnaK/DnaJ/GroE chaperone system (Tatsuta et al., 2000). No such adaptors are known for bacterial Lon. Lastly, substrate engagement can be influenced by recognition elements within the protease itself. Within the Clp proteases the substrate recognition elements are localised to the AAA subunits, ClpA or ClpX. Both proteins harbour an accessory N-terminal domain (N-domain) that is activated upon assembly of the ring-like structure. Zn²⁺ binding elements of one subunit have to dimerise with the element in the adjacent subunit (Hinnerwisch et al., 2005; Singh et al., 2001; Wojtyra et al., 2003; Xia et al., 2004). Moreover, an involvement of the central pore structure of the AAA domain in substrate binding is suggested (Hinnerwisch et al., 2005). Within the sequence of FtsH substrate binding element have not been identified.

One striking feature of AAA⁺-proteases is their ability to unfold a bound substrate with the help of the AAA domain prior to its degradation by the proteolytic domain. This process is referred to as 'protein unfolding-coupled translocation' and is based on studies in HslUV (Wang et al., 2001; Wang et al., 2001). A threading mode of substrate translocation is

proposed in which local denaturation of the substrate protein is caused by a pulling force that originates from conformational changes of the AAA domain induced by ATP hydrolysis. Crucial for this process are conserved residues (XVG) within a loop structure that resides in the pore of the AAA domain of the AAA⁺-proteases (Wang et al., 2001). In respect to substrate unfolding, an intriguing property of FtsH proteases is their capability to extract polypeptide chains from the lipid bilayer for degradation (Ito and Akiyama, 2005). However, the unfoldase activity of FtsH has been shown to be limited (Herman et al., 2003). Hence, AAA⁺-proteases have not only developed efficient systems for substrate engagement but also for substrate translocation.

1.4.3 Mitochondrial AAA⁺-proteases

Mitochondria contain representatives of Clp, Lon and FtsH proteases of which here the respective yeast proteins are described. Mcx1 is a ClpX homolog that is localised to the matrix space of mitochondria (Fig.1.1), where it is proposed to function as a chaperone (Van Dyck et al., 1998) as no ClpP homologs are present in yeast mitochondria. Additional studies, however, reveal only a minor impact of Mcx1 on the aggregation and disaggregation of proteins (von Janowsky et al., 2006).

Pim1 belongs to the Lon family of proteases and resides within the matrix space of mitochondria (Suzuki et al., 1994; Van Dyck et al., 1994; Wagner et al., 1994) where it forms a heptameric ring structure (Stahlberg et al., 1999). Most substrates are subjected to Pim1 degradation after exposure of denatured protein segments (Ondrovicova et al., 2005; von Janowsky et al., 2005). Subsequent degradation depends on the substrates solubility that is assured by the assisting chaperone Hsp78 under heat stress (Röttgers et al., 2002; von Janowsky et al., 2006). A function of Pim1 is the quality control of mitochondrial matrix proteins under stress conditions like heat stress or oxidative damage (Bota and Davies, 2002). However, this function does not directly explain the loss of respiration of a $\Delta pim1$ strain (Suzuki et al., 1994). Elucidation of this phenotype is provided by the potential function of Pim1 in mtDNA maintenance that might be based on the non-selective binding of mitochondrial Lon proteases to DNA (Liu et al., 2004).

Two FtsH family members are present within the inner membrane of yeast mitochondria: the *i*-AAA proteases active in the intermembrane space and the *m*-AAA proteases active in the matrix space (Fig.1.3). Based on structural analysis of bacterial homologs, both proteases constitute a typical barrel-shaped membrane embedded ring structure of an FtsH protease and exhibit a narrow axial pore and a proteolytic cavity (Ito and Akiyama, 2005). A unique attribute of the *m*-AAA protease is the formation of a hetero-oligomeric assembly of two

closely related subunits, Yta10 and Yta12. In contrast, the *i*-AAA protease comprises only one subunit, Yme1. Similar to other FtsH proteases, both the *i*-AAA and *m*-AAA protease harbour an HEXGH motif typical for members of the M41 family of metallopeptidase (Rawlings and Barrett, 1995). Within the proteolytic center of FtsH the two histidines coordinate the Zn^{2+} metal ion together with a structurally proximal aspartate residue (Bieniossek et al., 2006). Nucleophilic cleavage of the peptide bonds is facilitated by activation of a water molecule by the glutamate residue. In addition, the ability of FtsH proteases to extract proteins from a lipid bilayer is conserved for the *i* and *m*-AAA protease. First, both proteases are capable of degrading integral membrane proteins that expose at least an unfolded 20 amino acid segment on either site of the inner mitochondrial membrane (Leonhard et al., 2000); moreover, direct evidence for a membrane dislocation mechanism of the *m*-AAA protease was recently provided (Tatsuta et al., 2007). Though, the molecular details of this dislocation mechanism are elusive, they point to a crucial role of the transmembrane domains of the proteases (Korbelt et al., 2004). Elements within the substrate sequence responsible for its binding to the protease seem to be only characterised by their unfolding state representing a rather degenerate strategy of substrate recognition. Within the sequence of the protease the already mentioned distinct regions, the NH- and CH-region, seem to regulate efficient, but specific binding of substrates to the *i*-AAA proteases.

1.4.4 Substrate recognition by the *i*-AAA-proteases

A sophisticated substrate recognition system is responsible for defined degradation of substrates by AAA proteases in mitochondria. Plainly relying on unstructured, exposed sequence elements of the substrate, the AAA proteases appear to be able to identify specific substrates. This is of particular importance as both AAA proteases are ATP-dependent proteases which are to a certain extent able to actively unfold substrates which might enable unselective and potentially harmful proteolysis. On the other hand, mitochondrial AAA proteases are embedded into the lipid bilayer and hence, restricted in their orientation toward a substrate protein. Therefore, substrate recognition by these proteases most likely requires a substantially different mechanism than the one described for their soluble counterparts.

Within the structure of the *i*-AAA protease two distinct substrate binding sites have been identified: the NH-(N-terminal helices) region, located at the surface of the AAA domain, and the CH-(C-terminal helices) region, exposed at the surface of the proteolytic domain and by that on top of the cylindrical structure of the *i*-AAA protease (Graef et al., 2008) (Fig. 1.5). The ~ 40 amino acid long NH-region is positioned in close proximity to the inner

mitochondrial membrane, making it an ideal element to encounter substrates protruding from the membrane. Structurally, it consists of helical structure build up by highly negatively charged amino acids that are required for substrate binding to this region (Graef and Langer, 2006). The independent/autonomous action of the NH-region in substrate binding is supported by *in vitro* studies of C-terminally truncated Yme1 molecules (Leonhard et al., 1999). Within the process of degradation, substrates are reported to first bind to the NH-region, before they are encountered by the central pore loops to be subsequently transferred to the proteolytic center (Graef and Langer, 2006).

The second substrate binding site the CH-region appears more suitable for binding of soluble substrates to the \bar{i} -AAA protease, as it is located rather distantly from the inner mitochondrial membrane. The structure of the CH-region is built up by three helices the α -16, α -17 and α -18 helix of Yme1 at the top and side of the catalytic chamber of the \bar{i} -AAA protease (Graef et al., 2007). In respect to substrate binding and degradation, two different mechanisms are described for the CH-region, a CH-dependent and a CH-independent mechanism.

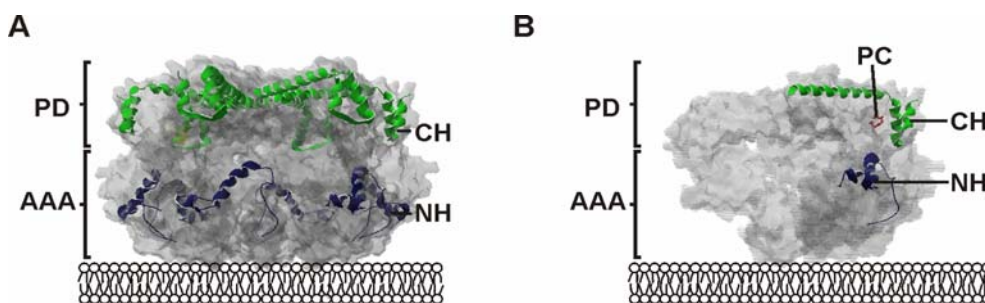


Figure 1.5 Initial substrate binding sites of the \bar{i} -AAA protease. (A) Within the cylindrical structure of the AAA protease (grey) the substrate binding sites are exposed in a lattice like assembly at the outer surface of the protease. The NH-region (blue) resides at the surface of the AAA domain, whereas the CH-region (green) is part of the proteolytic domain. (B) Open structure revealing the relative position of CH-region (green), NH-region (blue) and the proteolytic center (red). Here the different domains within the crystal structure of the related AAA protease of *Thermotoga maritima* are shown (U. Baumann personal communication). PD, proteolytic domain; AAA, AAA domain; NH, N-terminal helices; CH, C-terminal helices, PC, proteolytic center.

As an example, the degradation of cytochrome *c* oxidase 2 (Cox2) is described which can take place in a CH-dependent as well as in a CH-independent manner. CH-independent degradation of Cox2 is observed for fully folded Cox2 where the NH-region serves as a backup for initial substrate binding site (Graef et al., 2007). Any interference with the folding status of Cox2 renders its degradation CH-dependent (Graef et al., 2007). So, whether the degradation of a substrate occurs in a CH-dependent or CH-independent manner seems to be influenced by the folding state of a substrate and its localisation relative to the membrane. In this line, soluble or peripherally attached substrate proteins are thought to be degraded in a CH-dependent manner, whereas substrates proteins that are completely

folded and tightly attached or inserted into the membrane might be degraded CH-independent. The exact mechanism determining the CH-dependent or CH-independent degradation of a substrate remains elusive. Autonomous substrate binding to the CH-region has been determined by *in vitro* binding studies (Graef et al., 2007).

Although the existence of two independent substrate binding sites might have evolved to achieve an enhanced recognition of substrates with different properties, the relevance of these two binding sites within the degradation process is far from being understood. During degradation, substrates first have to bind to the protease before being encountered by the central pore loops for further translocation to the inner cavity for degradation. For the NH-region such a mechanism is already implied (Graef and Langer, 2006). In contrast, there is no evidence for substrate translocation from the CH-region to the central pore loops. As the CH-region is situated rather distant to the central pore loops substrates might first bind to the NH-region before they are encountered by the central pore loops. Alternatively, additional substrate entry pathways to the proteolytic center could exist for substrates that are bound to this region. Therefore, analysis of substrate transition mechanisms after binding of substrates to the CH-region is awaited. The fact that the *i*-AAA protease is membrane embedded could again make the mechanism more complicated in comparison to soluble AAA proteases.

1.4.5 Functions of the *i*- and *m*-AAA proteases in mitochondria

Various functions have been described for the two mitochondrial AAA proteases (Fig. 1.6). Both the *i*-AAA and the *m*-AAA protease are required for mitochondrial protein quality surveillance of inner membrane proteins (Leonhard et al., 2000) on which they show overlapping function. One argument for this overlap of function is the synthetic lethality seen for simultaneous deletion of both proteases (Lemaire et al., 2000; Leonhard et al., 2000) that is also underlining the essential role of the proteases for cellular function. Moreover, the presence of either of the proteases is demonstrated to be sufficient for complete degradation of a certain substrate protein (Leonhard et al., 2000). Furthermore, prohibitins are found to assemble with the *m*-AAA protease into a high molecular weight complex in the inner mitochondrial membrane, where they negatively regulate the quality control function of the *m*-AAA protease (Steglich et al., 1999).

In addition to its quality control function, the *m*-AAA protease is involved in the processing of nuclearly encoded mitochondrial proteins (Esser et al., 2002; Nolden et al., 2005). One such mitochondrial protein is MrpL32, a subunit of the large particle of the mitochondrial ribosome. After mitochondrial import of MrpL32, the *m*-AAA protease processes the protein

to its mature form and by that allows the completion of a functional mitochondrial ribosome formation. Why the proteolytic action of the *m*-AAA protease on MrpL32 does not lead to complete degradation of the protein remains to be elucidated. The function of the *m*-AAA protease in processing of MrpL32 explains the respiratory deficiency of a strain depleted of the *m*-AAA protease subunits, as a lack of mitochondrial translation results in a loss of respiratory complexes (Nolden et al., 2005).

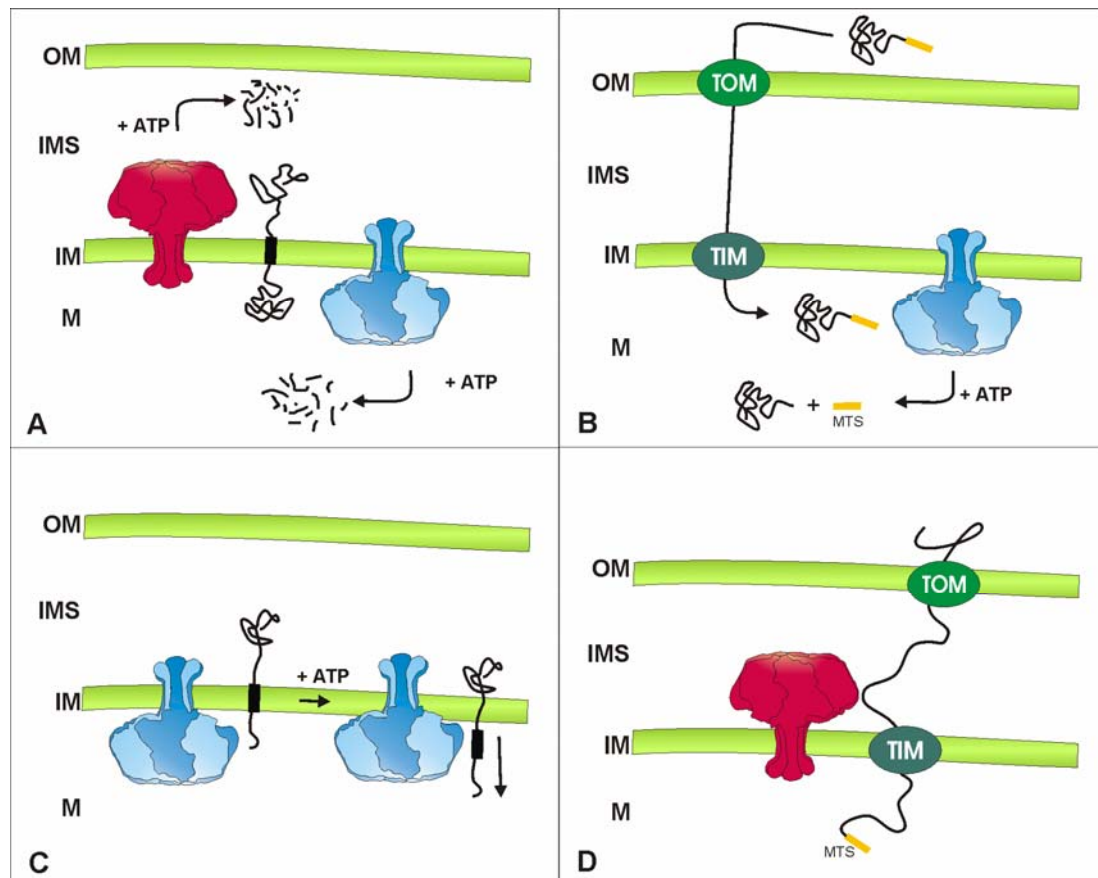


Figure 1.6 Versatile functions of the *i*- and *m*-AAA proteases of mitochondria. (A) Quality control surveillance. Misfolded polypeptides are degraded to peptides after their dislocation from the membrane. The membrane topology of substrates determines the involvement of either *i*-AAA (red) or *m*-AAA protease (blue) which exert overlapping substrate specificity (Leonhard et al., 2000). **(B)** Protein processing. The *m*-AAA protease mediates processing of nuclear encoded mitochondrial proteins resulting in their activation (Esser et al., 2002; Nolden et al., 2005). Maturation of the ribosomal protein MrpL32 by the *m*-AAA protease enables ribosomal assembly within mitochondria (Nolden et al., 2005). **(C)** Membrane dislocation. Ccp1 is dislocated by the *m*-AAA protease in an ATP-dependent manner allowing its intramembrane cleavage by the rhomboid protease Pcp1 (Tatsuta et al., 2007). **(D)** Protein import. The *i*-AAA protease is required for import of heterologously expressed, mammalian PNPase into the mitochondrial intermembrane space (Rainey et al., 2006). OM, outer mitochondrial membrane; IMS, intermembrane space; IM, inner mitochondrial membrane; M, matrix space. The figure is adapted from (Graef et al., 2008).

Moreover, membrane dislocation events are demonstrated for the *m*-AAA protease (Tatsuta et al., 2007). The *m*-AAA protease is required for maturation of cytochrome *c* peroxidase

(Ccp1) (Esser et al., 2002), a reactive oxygen scavenger in the intermembrane space that contains a bipartite import sequence for its posttranslational import into mitochondria (Kaput et al., 1982). Upon import into mitochondria, Ccp1 is matured by subsequent action of the *m*-AAA protease and the ATP-dependent rhomboid protease Pcp1 (Esser et al., 2002; Tatsuta et al., 2007). This process strictly depends on the presence of the *m*-AAA protease, as intramembrane cleavage by Pcp1 can only occur after membrane dislocation of Ccp1 by the *m*-AAA protease which renders the cleavage site of Ccp1 accessible for Pcp1 (Tatsuta et al., 2007). Also for the *i*-AAA protease a non-proteolytic function is suggested. Mitochondrial import of mammalian PNPase expressed heterologously in yeast requires the *i*-AAA protease (Rainey et al., 2006). PNPase binding to the *i*-AAA protease subunit Yme1 promotes the translocation of PNPase across the outer mitochondrial membrane. This function is impaired if the proteolytic activity of Yme1 is inhibited, although Yme1 is not able to degrade PNPase under these conditions. Whether the action of Yme1 in import of PNPase resembles the membrane dislocation event seen for the *m*-AAA protease in case of Ccp1 remains unclear at this point.

Thus, additional functions independent of the proteolytic activity of the mitochondrial AAA proteases have been identified (Graef et al., 2008) highlighting the relevance of these proteases for additional mitochondrial processes involving housekeeping and regulatory roles during mitochondrial biogenesis. Nevertheless, they are required for quality control of mitochondrial membrane proteins. Therefore, combination of the activity of Pim1 and the two AAA proteases defines an elaborate system of mitochondrial quality control that assures maintenance of mitochondrial function.

1.4.6 The conserved *i*-AAA protease Yme1

The *i*-AAA protease is best studied in the yeast *S. cerevisiae*. Here, the homo-oligomer is composed of Yme1 subunits that assemble into a proposed hexameric structure localised to the inner mitochondrial membrane with their catalytic domains facing the intermembrane space (Leonhard et al., 1999). Unexpectedly, analysis of the complex by gelfiltration experiment and blue native gel electrophoresis reveals a complex size that does not resemble an assembly of only six subunits. It is therefore conceivable that other components are involved in the assembly of the native complex. Two proteins influencing the complex size of the *i*-AAA protease are the yeast specific adaptors Mgr1 and Mgr3 (Dunn et al., 2008). The complex size of the *i*-AAA protease is reduced in the absence of either *MGR1* or *MGR3* and degradation of model substrates is decreased. However, both proteins are not shown to be involved in degradation of the substrate Cox2 and their deletion resembles only

one of the known $\Delta yme1$ phenotypes, the dependence on mitochondrial DNA (mtDNA) (Dunn et al., 2006). In general, the deletion of *YME1* is connected to pleiotrophic phenotypes. The already noted dependence of cells on mtDNA in the absence of Yme1 is also described as 'petite negative' phenotype (Chen and Clark-Walker, 1999; Thorsness and Fox, 1993). Furthermore, $\Delta yme1$ cells are respiratory incompetent at elevated temperature and not able to grow on glucose-rich medium at lower temperature (Thorsness et al., 1993). Deletion of *YME1* also induces an aberrant mitochondrial morphology and an increased mitochondrial turnover via the vacuole which also results in transfer of mtDNA to the nucleus (Campbell et al., 1994; Campbell and Thorsness, 1998; Thorsness and Fox, 1993). More recently, the function of Yme1 has been linked to ergosterol and longevity. $\Delta yme1$ cells are deficient for uptake of ergosterol under anaerobic growth condition (Reiner et al., 2006). As ergosterol biosynthesis requires molecular oxygen uptake of ergosterol is essential under those conditions (Parks et al., 1995). The connection of Yme1 to longevity is based on studies monitoring the replicative lifespan of cells in the absence of *YME1* (Francis et al., 2007; Palermo et al., 2007). Further, *YME1* is deleted in life-extending mutants of which many show a decreased cytosolic protein synthesis (Wang et al., 2008). The resulting double mutants exhibit a loss of extended lifespan, linking the function of Yme1 to a role in longevity.

Species	Name	% identity to <i>S. cerevisiae</i> Yme1
<i>H. sapiens</i>	YME1L1	52%
<i>M. musculus</i>	Yme1l1	51.8%
<i>R. norvegicus</i>	Yme1l1	51.8%
<i>C. elegans</i>	M03C11.5	51.6%
<i>S. pombe</i>	SPCC965.04c	47.8%
<i>C. albicans</i>	YME1	67.3%

Table 1.1 Homology of Yme1 orthologs. Yme1 orthologs exist in *Homo sapiens*, *Mus musculus*, *Rattus norvegicus*, *Caenorhabditis elegans*, *Schizosaccharomyces pombe* and *Candida albicans*. Their respective protein names and relative homology to Yme1 from *S. cerevisiae* are depicted here. Source: BIOBASE Knowledge Library.

According to the vast number of phenotypes associated with the loss of the \hat{A} AAA protease, this protein, although present within mitochondria, participates in many cellular processes. Nonetheless, the described phenotypes cannot be directly linked to so far identified mitochondrial interaction partners (Mgr1 and Mgr3) or proteolytic substrates of the \hat{A} AAA

protease. Besides Cox2 (Leonhard et al., 1996; Nakai et al., 1995; Pearce and Sherman, 1995; Weber et al., 1996), the \hat{i} -AAA protease is also involved in the degradation of Nde1 (Augustin et al., 2005) and Phb1/2 (Kambacheld et al., 2005). Hence, in order to explain the molecular mechanisms causing the pleiotropic phenotypes of a $\Delta yme1$ strain, the identification of additional interaction partners and substrates is required.

Yme1 is expressed throughout the eukaryotic kingdom and described orthologs show a high sequence identity (Tab. 1.1), speaking for a general importance of the \hat{i} -AAA protease in cellular function. The high degree of similarity is also supported by complementation studies of yeast, where expression of YME1L1 restored the respiratory deficiency of $\Delta yme1$ at elevated temperature (Shah et al., 2000). The human homolog YME1L1 has been demonstrated to process the mitochondrial fusion component OPA1 at a specific site (Griparic et al., 2007; Song et al., 2007). Furthermore, stabilisation of another OPA1 isoform is apparent upon downregulation of YME1L1, pointing to its degradation by the protease (Guillery et al., 2008). OPA1 is the human homolog of Mgm1. In yeast, processing of Mgm1 is less complex and shown to be mediated by Pcp1 (Sesaki et al., 2006; Sesaki et al., 2003). Although yeast cells exhibit a mitochondrial morphology defect in the absence of Yme1, the \hat{i} -AAA protease seems not to be involved in the processing of Mgm1 (Campbell et al., 1994). It would be interesting to see if other phenotypes found for the yeast homolog Yme1 can be observed in higher eukaryotes.

1.5 Mitochondrial peptidases and mitochondrial protein import

Mitochondrial processing peptidases are predominantly important for the cleavage of mitochondrial targeting sequences generating the active, matured form of a protein in different mitochondrial subcompartments (Koppen and Langer, 2007). Usually targeting sequences consist of 10-80 amino acids at the N-terminus of a protein. These sequences are rich in positively charged amino acids and are able to form amphipatic helical structures (Song et al., 1998). In addition, internal targeting sequences exist, but their nature remains largely elusive (Folsch et al., 1996). Further, bipartite import sequences can be found, that require that action of two peptidases for full maturation (Hartl et al., 1987). Prior to their processing, the respective precursor proteins have to be imported into mitochondria. The import of proteins into mitochondria is achieved by an elaborate system of translocases located in inner and outer mitochondrial membrane (reviewed in (Bolender et al., 2008; Neupert and Herrmann, 2007)) (Fig. 1.6).

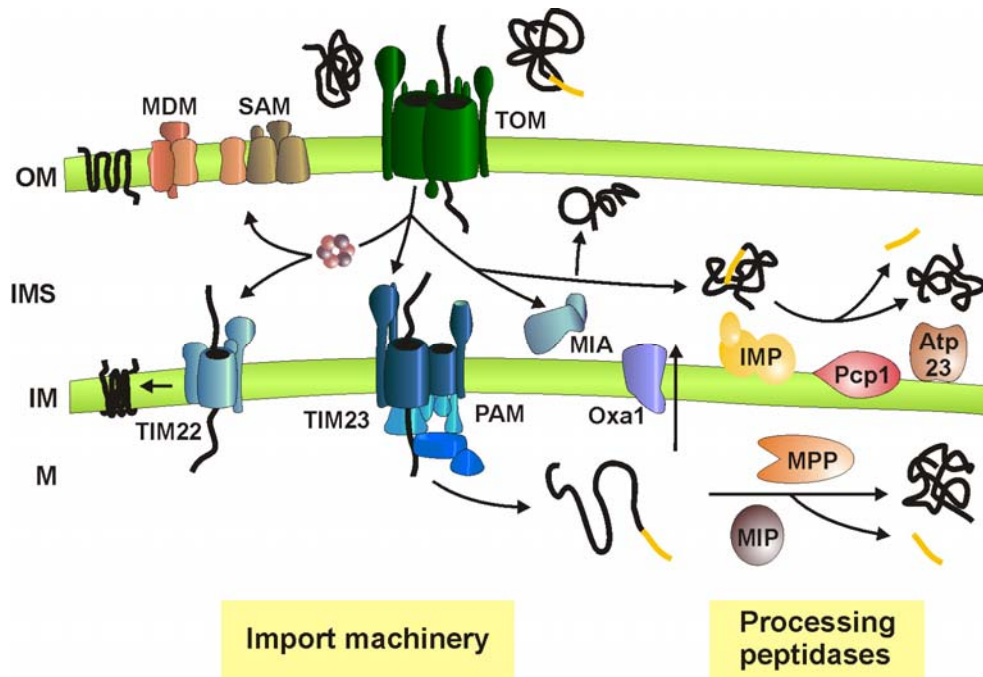


Figure 1.6 The mitochondrial protein import machinery and its connection to mitochondrial processing peptidases in *S. cerevisiae*. After translocation of proteins through the TOM (translocase of the outer membrane) complex proteins enter different pathways. β -barrel proteins are assembled into the outer membrane (OM) by the action of the SAM (sorting and assembly machinery) and the MDM (mitochondrial distribution morphology) complex. Intermembrane space proteins can be oxidised and assembled by Mia40 (mitochondrial intermembrane space import and assembly). Inner mitochondrial membrane and carrier proteins are translocated through the inner mitochondrial membrane (IM) and are assembled by the TIM23 or TIM22 (translocase of the inner membrane) complex, respectively. Import of matrix proteins is facilitated by the Tim23 complex. After import into the matrix (M) proteins are either translocated through the inner mitochondrial membrane via Oxa1 or are processed by MPP (mitochondrial processing peptidase) or MIP (mitochondrial intermediate peptidase). Proteins imported into the intermembrane space (IMS) are processed by IMP (inner membrane protease), Pcp1 or Atp23.

Three major mitochondrial processing peptidases exist in the matrix space and the inner mitochondrial membrane of mitochondria (Gakh et al., 2002). Within the matrix space the peptidases MPP (mitochondrial processing peptidase) and MIP (mitochondrial intermediate peptidase) ensure maturation of imported precursor proteins (Hawlitsek et al., 1988; Kalousek et al., 1988; Yang et al., 1988). The yeast MPP peptidase is a hetero-dimer of Mas1 and Mas2 that is essential for cell survival (Yaffe et al., 1985). The conserved metallopeptidase is highly homologous to non-catalytic subunits of the cytochrome *c* reductase (Gencic et al., 1991; Schulte et al., 1989). Therefore, it is not surprising that MPP is a bi-functional protein in some organisms (Glaser and Dessi, 1999). The monomeric metallopeptidase MIP is composed of Oct1 in yeast (Chew et al., 1996; Kalousek et al., 1988) and requires octapeptides for the cleavage of precursor proteins (Isaya et al., 1992). The severe phenotypes associated with inactivation of the gene point to an important regulatory role of the peptidase (Isaya et al., 1994). The catalytic domain of the membrane

embedded hetero-oligomeric IMP complex is facing the intermembrane space (Pratje and Guiard, 1986; Schneider et al., 1991). The two catalytic subunits Imp1 and Imp2 contain serine peptidase specific dyads (Dalbey et al., 1997; Nunnari et al., 1993; Schneider et al., 1994) and are homologous to bacterial leader peptidase and thylakoid processing peptidases (Behrens et al., 1991; Halpin et al., 1989). They are accompanied by the non-catalytic subunit Som1 (Bauerfeind et al., 1998; Esser et al., 1996) that is binding to Imp1 and might modulate its substrate specificity, as only a subset of Imp1 substrates is depending on the presence of Som1 in processing by the IMP peptidase (Jan et al., 2000; Liang et al., 2004). The IMP peptidase is required for processing of several nuclearly encoded proteins, as well as the mitochondrially encoded subunit 2 of cytochrome *c* oxidase (Cox2) (Burri et al., 2005; Esser et al., 2004). One intriguing characteristic of the IMP peptidase is the distinct substrate specificity of the two physically connected catalytic subunits Imp1 and Imp2 (Nunnari et al., 1993) that is based on their ability to recognise different substrate cleavage sites (Luo et al., 2006). However, substrate specific cleavage sites are not necessarily conserved, for example the cleavage site of the human NADH cytochrome *c* reductase does not resemble one described for the yeast homolog Mcr1 (Tomatsu et al., 1989).

Besides those three processing peptidases, the mitochondrial rhomboid protease Pcp1 (Esser et al., 2002; Herlan et al., 2003), the *m*-AAA protease (Yta10/Yta12) (Esser et al., 2002; Nolden et al., 2005) and the metallopeptidase Atp23 (Osman et al., 2007; Zeng et al., 2007) have been shown to mediate the processing of specific precursor proteins. The membrane embedded serine peptidase Pcp1 is a member of the rhomboid protease family (Freeman, 2008). Pcp1 is involved in processing of the reactive oxygen scavenger cytochrome *c* peroxidase (Ccp1) (Esser et al., 2002) and the dynamin like GTPase Mgm1 (Herlan et al., 2003). The later is a component of the mitochondrial fusion machinery and links Pcp1 function to mitochondrial morphogenesis. The conserved metallopeptidase Atp23 is required for assembly of the ATP synthase subunit Atp6. It facilitates not only its cleavage, but also its insertion into the membrane embedded F_0 -subunit of the ATP synthase (Osman et al., 2007; Zeng et al., 2007). The *m*-AAA protease is required for maturation of Ccp1 and MrpL32 (Nolden et al., 2005; Tatsuta et al., 2007), and the general impairment of processing of MrpL32 explains the apparent phenotype in the absence of the *m*-AAA protease. Therefore, the processing function of the *m*-AAA protease is crucial for the cell.

1.6 Aims of the thesis

The highly conserved ATP-dependent *f*-AAA protease Yme1 is a crucial player in the protein quality control system of mitochondria. Two distinct substrate binding sides within the *f*-AAA protease have been identified, the CH-region and the NH-region. Furthermore, substrates have been found to be degraded in a CH-dependent or CH-independent manner, always requiring the presence of the NH-region. Substrate binding to the NH-region could be shown to depend on the presence of negatively charged amino acids in a helical structure adjacent to the inner mitochondrial membrane. However, the molecular requirements of initial substrate recognition by the CH-region remain to be elucidated. To address this question the initial binding of substrates to distinct residues or areas within the CH-region of Yme1 will be examined by mutational analysis. In this respect, the identification of additional substrates will also be useful.

The absence of a functional *f*-AAA protease Yme1 in yeast cells leads a broad range of severe defects including impaired respiratory growth and mitochondrial morphogenesis. However, the underlying molecular mechanisms are far from being understood, due to limited knowledge of its proteolytic substrates and interaction partners. In order to identify novel substrates or interaction partners, affinity purification of the endogenous *f*-AAA protease from the convenient yeast system will be performed. For this purpose, a proteolytic inactive but structurally intact variant of Yme1 will be used that specifically enriches for proteolytic substrates which might interact only transiently with the protease. In addition to this biochemical approach, a genetic approach will be applied. A synthetic genetic array (SGA) will be conducted for the identification of processes which require the function of the *f*-AAA protease. Here, the viability of double mutants with a deletion of the *f*-AAA protease Yme1 in combination with a deletion of another non-essential gene will be determined. In general, the loss of viability of a double mutant indicates the genetic interaction of the two deleted genes that act in related processes. Moreover, new functions of the *f*-AAA protease should be identified by the subsequent implementation of a high copy suppressor screening of a subset of determined synthetic lethal interaction of *YME1*.

2 Materials and Methods

2.1 Molecular Biology Methods

Standard procedures in molecular biology were performed according to compiled protocols (Sambrook and Russell, 2001). Used enzymes were purchased from NEB (New England Biolabs) and Roche. DNA purification kits were purchased from Macherey-Nagel. Suppliers for (the used) chemicals were Sigma, Merck and Roth unless stated otherwise.

2.1.1 Yeast expression plasmid

For functional analysis of the CH-region of Yme1, the plasmid pVT100U-Yme1 was used as template for mutagenesis by polymerase chain reaction (PCR) based on the "QuikChange side-directed mutagenesis kit" procedure (Stratagene). Degenerated primers (TL3174-TL3193) allowed the exchange of two subsequent residues within the α -17 and α -18 helix of the CH-region of Yme1 for alanine or glycine: K681G/K682G, E685A/L686G, H687A/R688A, L689G/A690G, Q681A/G692A, L693G/I694G, E695A/Y696A, A701G/I794G, H702H/E703A, and E705A/Q706A (for oligonucleotide sequences see Tab. 3). Truncations of the CH-region of Yme1 were generated by introducing nonsense mutations into two neighbouring codons. Yme1 ^{Δ 709-747} was lacking all residues following the CH-region of Yme1 (TL4258/TL4259), the variant Yme1 ^{Δ 698-747} did not include the α -18 helix of the CH-region (TL4592/4593), the variant Yme1 ^{Δ 681-747} did not contain the α -18 helix of the CH-region (TL4594/4595), and the variant Yme1 ^{Δ 651-747} did not include any part of the CH-region (TL4596/4596).

Purification of Yme1 was based on a hexahistidine (6HIS) tag that was fused to the N-terminal or C-terminal end of the mature protein. For the variant harbouring a C-terminal 6HIS tag, the *YME1* coding sequence with the endogenous promoter is amplified from pRS314-Yme1 and pRS314-Yme1^{E541Q} using the oligonucleotides TL2358 and TL2360 (Graef and Langer, 2006). The PCR fragment was cut with *Bg*II (within the promoter region of *YME1*) and *Eco*RI and cloned into the *Bam*HI and *Eco*RI restriction sites of pRS314. To introduce N-terminal 6HIS in between the mitochondrial targeting sequence and the mature version of the Yme1 protein (between Yme1^{E50} and Yme1^{K51}), mutagenesis PCR was performed with pRS314-Yme1 and pRS314-Yme1^{E541Q} (Graef and Langer, 2006). For galactose-based overexpression, the *YME1* gene was amplified from genomic DNA using the oligonucleotides TL4261 and TL4263, cut with the restriction enzymes *Eco*RI and *Bg*II and cloned into the *Eco*RI and *Bam*HI restriction sites of pYX113. For constitutive overexpression, the *MCR1* gene was cut after amplification from genomic DNA

(TL2644/TL2645) with *EcoRI/XbaI* and cloned into the *EcoRI/NheI* restriction sites of the TPI-promoter containing pXY142. Candidate genes for the suppression of the synthetic lethality of $\Delta yme1\Delta imp1$ cells, *PGK1*, *YLR218c*, *PET54* and *MIC14*, were excised from the corresponding Yep13 library plasmid and cloned into YEplac181 to test the suppressive effect of the single gene expressed under its native promoter.

Table 2.1 Yeast expression constructs used in this study.

Plasmid	Reference
pVT100U-Yme1	(Klanner et al., 2001)
pVT100U-Yme1 ^{K681G/K682G}	this study
pVT100U-Yme1 ^{E685A/L686G}	this study
pVT100U-Yme1 ^{H687A/R688A}	this study
pVT100U-Yme1 ^{L689G/A690G}	this study
pVT100U-Yme1 ^{Q691A/G692A}	this study
pVT100U-Yme1 ^{L693G/I694G}	this study
pVT100U-Yme1 ^{E695A/Y696A}	this study
pVT100U-Yme1 ^{A701G/I704G}	this study
pVT100U-Yme1 ^{H702A/E703A}	this study
pVT100U-Yme1 ^{E705A/Q706A}	this study
pVT100U-Yme1 ^{$\Delta 709-747$}	this study
pVT100U-Yme1 ^{$\Delta 698-747$}	this study
pVT100U-Yme1 ^{$\Delta 681-747$}	this study
pVT100U-Yme1 ^{$\Delta 651-747$}	this study
pVT100U-Yme1 ^{$\Delta 52-198$}	unpublished, M. Graef
pRS314	(Sikorski and Hieter, 1989)
pRS314-Yme1	(Graef and Langer, 2006)
pRS314-Yme1 ^{E541Q}	PhD thesis M. Graef
pRS314-Yme1-6HIS	this study
pRS314-Yme1 ^{E541Q} -6HIS	this study
pRS314-Yme1 ⁽¹⁻⁵⁰⁾ -6HIS-Yme1 ⁽⁵¹⁻⁷⁴⁷⁾	this study
pRS314-Yme1 ⁽¹⁻⁵⁰⁾ -6HIS-Yme1 ⁽⁵¹⁻⁷⁴⁷⁾ -E541Q	this study
pXY113	Novagen
pXY113-Yme1	this study
pXY142	Novagen
pYX142-Mcr1	this study
YEplac181	(Gietz and Sugino, 1988)

Plasmid	Reference
YEplac181-GAL-Gep1-myc	unpublished, C. Potting
YEplac181-Pgk1	this study
YEplac181-Ylr218c	this study
YEplac181-Pet54	this study
YEplac181-Mic14	this study
pFA6a-kanMX6	(Longtine et al., 1998)
pFA6a-3HA-kanMX6	(Longtine et al., 1998)
pAG25	(Goldstein and McCusker, 1999)
pYM14	(Janke et al., 2004)

2.1.2 Plasmids for *in vitro* transcription and translation

For the generation of *in vitro* synthesised polypeptides, the pGEM4 vector system (Promega) was used. PCR-based insertion of the Kozak consensus sequence [(GCC)(A/G)CC ATG] preceding the start codon (Kozak, 1987) and restriction sites allowed cloning of the different genes into the pGEM4 vector. *In vitro* production of RNA was driven by the SP6-promoter for all used constructs.

Table 2.2 List of plasmids for *in vitro* transcription and translation used in this study.

Plasmid	Reference
pGEM4	Promega
pGEM4-Phb1	(Kambacheld et al., 2005)
pGEM4-Yme1	T. Langer
pGEM4-IAP-1	(Klanner et al., 2001)
pGEM4-YME1L1	G. Pellechia
pGEM4-Yme1l1	J. Majczak
pGEM4-Mcr1	this study
pGEM4-Mpm1	this study
pGEM4-Gep1	this study
pGEM4-Qcr2	this study
pGEM4-Pda1	this study
pGEM4-Pdb1	this study

2.2 Cell biology methods

2.2.1 Yeast strains and growth conditions

All studies were performed in the yeast *S. cerevisiae*; all strains (Tab. 2.4) were derived from W303 (Thomas and Rothstein, 1989) or BY4743 (Brachmann et al., 1998). Growth of yeast strains was performed according to standard protocols in complete (YP) or synthetic (SC) media (Sherman, 2002) supplemented with 2% (w/v) glucose or galactose, as indicated. Additional supplements for complete media were 3% (v/v) glycerol (YPG), EtBr (25 µg/ml) and nystatin (50 U/ml). For isolation of mitochondria, yeast cells were grown in lactate medium (Tatsuta and Langer, 2007). Creation of PCR-based genomic integrations was based on homologous recombination strategies (Goldstein and McCusker, 1999; Janke et al., 2004; Longtine et al., 1998). Single deletion strains not listed in Table 2.4 were derived from the Euroscarf collection (Winzeler et al., 1999). Diploid double deletion strains were derived from crossings of $\Delta yme1::NAT$ (YTE108) with single strains from the Euroscarf collection (Winzeler et al., 1999).

Table 2.3 Oligonucleotides used in this study.

Primer	Description	Sequence (5'-3')
TL852	disruption of <i>YME1</i>	TTATAATACATTGTGGATAGAACGAAAACAGAGACGTGATAGATGCGTACGCTGCAGGTCGAC
TL853	disruption of <i>YME1</i>	TTGAGGTAGGTTCCCTTCATACGTTTAACTTCTTAGAATAAAATCAATCGATGAATTCGAGCTCG
TL2214	disruption of <i>MGR1</i>	TCCTCCATTCCCTCTCCTTTTCCAATTACCGTAATAAAAAGCGGATCCCCGGTTAATTAA
TL2358	cloning of <i>YME1</i> -6HIS into pRS314	GATCTTAGCATTGCGAATTCTTATTCAATGGTGATGGTGATGGTGATGGTGCA TTTAACATTGTAGGAA
TL2359	cloning of <i>YME1</i> into pRS314	TAGCATTGAGCGGCTGTCT
TL2378	disruption of <i>MGR1</i>	TTAATATACGCACGGTACAACCTAAGCAATCCGCAAAGACCTGATATCATCGATGAATTC
TL2391	C-terminal HA-tagging of <i>GEP1</i>	AAATATTGACTTGTGTTAGAGACGCATACAACCACGAAAATCGATATCCCCGGGTTAATTAA
TL2392	C-terminal HA-tagging of <i>GEP1</i>	GTAGTATGCAGTGCCATGCGGGATCAAGGAATTTGTATCTGAA TTCGAGCTCGTTTAAAC
TL2630	disruption of <i>IMP1</i>	AATAAGACAGTGAATCATCCAACAGTGTACAATACCAGGGCGTACGCTGCAGGT
TL2631	disruption of <i>IMP1</i>	ATTGCGTATCGAACCGTCCCAGAAGGGCTTGTCAAAAATGATCGATGAATTCGAGCT
TL2644	cloning of <i>MCR1</i>	GCACCGGAATTCCGCGCCCATGTTTTCCAGATTATCCAG
TL2645	cloning of <i>MCR1</i>	CGTCGCTCTAGAGCGTTAAAATTTGAAAACCTTGGTCCTTGGAGTA

Primer	Description	Sequence (5' - 3')
TL2822	C-terminal tagging of <i>MCR1</i>	GAACAATTTGGGCTACTCCAAGGACCAAGTTTTCAAATTTTCGGATCCCCGGGTTAATTAA
TL2823	C-terminal tagging of <i>MCR1</i>	GATCCGAAATTAATAAAAAATATCAATTACTTTCTCCATGCCTGATATCATCGATGAATTC
TL2824	C-terminal tagging of <i>QCR2</i>	CGTCGGTGATGTTTCCAAGTCCATATTTGGACGAATTGCGGATCCCCGGGTTAATTAA
TL2825	C-terminal tagging of <i>QCR2</i>	ATTTGCCTTTAGTTTTTCGTTTTGTACAAATACTTTCTCTCTGATATCATCGATGAATTC
TL3174	5'- <i>yme1</i> ^{K681G/K682G} mutagenesis primer	CAAGAAGACTATTAAGTGGGGGAAATGTTGAGCTACATAG
TL3175	3'- <i>yme1</i> ^{K681G/K682G} mutagenesis primer	CTATGTAGCTCAACATTTCCCCCAGTTAATAGTCTTCTTG
TL3176	5'- <i>yme1</i> ^{E685A/L686G} mutagenesis primer	CTCCAAGAAAAATGTTTCGGGGACATAGACTTGCGCAAG
TL3177	3'- <i>yme1</i> ^{E685A/L686G} mutagenesis primer	CTTGCGCAAGTCTATGTCCCCGAACATTTTTCTTGGAG
TL3178	5'- <i>yme1</i> ^{H687A/R688A} mutagenesis primer	GAAAAATGTTGAGCTACGTCGACTTGCGCAAGGTCTTATTG
TL3179	3'- <i>yme1</i> ^{H687A/R688A} mutagenesis primer	CAATAAGACCTTGCGCAAGTCGACGTAGCTCAACATTTTTTC
TL3180	5'- <i>yme1</i> ^{L689G/A690G} mutagenesis primer	GTTGAGCTACATAGAGGTGGGCAAGGTCTTATTGAATATG
TL3181	3'- <i>yme1</i> ^{L689G/A690G} mutagenesis primer	CATATTCATAAGACCTTGCCACCTCTATGTAGCTCAAC
TL3182	5'- <i>yme1</i> ^{Q691A/G692A} mutagenesis primer	GCTACATAGACTTGCGCGACGTCTTATTGAATATGAAAC
TL3183	3'- <i>yme1</i> ^{Q691A/G692A} mutagenesis primer	GTTTCATATTCATAAGACGTGCGCAAGTCTATGTAGC
TL3184	5'- <i>yme1</i> ^{L693G/I694G} mutagenesis primer	CATAGACTTGCGCAAGGTGGTGGTGAATATGAAACTCTAG
TL3185	3'- <i>yme1</i> ^{L693G/I694G} mutagenesis primer	CTAGAGTTTCATATTCACCACCACCTTGCGCAAGTCTATG
TL3186	5'- <i>YME1</i> ^{E695A/Y696A} mutagenesis primer	GCGCAAGGTCTTATTCGACGTGAAACTCTAGATGC
TL3187	3'- <i>yme1</i> ^{E695A/Y696A} mutagenesis primer	GCATCTAGAGTTTCACGTGCAATAAGACCTTGCGC
TL3188	5'- <i>yme1</i> ^{A701G/I704G} mutagenesis primer	GAATATGAAACTCTAGATGGCCACGAAGGCGAACAAGTTTGTAAG
TL3189	3'- <i>yme1</i> ^{A701G/I704G} mutagenesis primer	CTTTACAACTTGTTTCGCTTCGTGGCCATCTAGAGTTTCATATTC
TL3190	5'- <i>yme1</i> ^{H702A/E703A} mutagenesis primer	GAAACTCTAGATGCCCGCCGAATCGAACAAGTTTGTAAG

Primer	Description	Sequence (5' - 3')
TL3191	3'- <i>yme1</i> ^{H702A/E703A} mutagenesis primer	CTTTACAAACTTGTTCGATTCCGGCGGGCATCTAGAGTTTC
TL3192	5'- <i>yme1</i> ^{E705A/Q706A} mutagenesis primer	GATGCCACGAAATCCGACGAGTTTGTAAAGGTTAATAG
TL3193	3'- <i>yme1</i> ^{E705A/Q706A} mutagenesis primer	CTATTAACCTTTACAAACTCGTCGGATTTCTGTTGGGCATC
TL3819	5'- <i>yme1</i> ^{E50-6HIS-K51} mutagenesis primer	GATCAAAGAAGTTCTACCGTTTTTATTCTGAACACCATCACCATCACCAT AAGAATAGCGGTGAAATGCCTCCTAAGAAG
TL3820	3'- <i>yme1</i> ^{E50-6HIS-K51} mutagenesis primer	CTTCTTAGGAGGCATTTACCGCTATTCTTATGGTGATGGTGATGGTGT TCAGAATAAAAACGGTAGAACTTCTTTGATC
TL4252	cloning of <i>GEP1</i>	CCGGAATTCGGGCGTGTCAAAAAAATGCTGTTTCCGTTGA
TL4253	cloning of <i>GEP1</i>	CCGGAATTCGGATGAACGTTTCAAAAATACTTG
TL4254	cloning of <i>MPM1</i>	GCACCGGAATTCGGCCGCATGGGCTTTTATGAAGGCGATG
TL4255	cloning of <i>MPM1</i>	CGCTCTAGAGCGCTAATTGTCTTCGTCAACACTCACCAC
TL4258	5'- <i>yme1</i> ^{Δ709-747} mutagenesis primer	CGAACAAGTTTGTAAAGGTTAATAACTGGACAACTGAAAAC
TL4259	3'- <i>yme1</i> ^{Δ709-747} mutagenesis primer	GTTTTCAGTTTGTCCAGTTATTAACCTTTACAACTTGTTCG
TL4261	cloning of <i>YME1</i>	CGAAGATCTTCATCATGCATTTAACATTGTAGG
TL4263	cloning of <i>YME1</i>	CCGGAATTCGGATGAACGTTTCAAAAATACTTG
TL4293	disruption of <i>MPM1</i>	GGACAAGAAAGACAAAGGAAACCGACAAACCGTTTACTCGATCGGATCC CCGGGTTAATTAA
TL4294	C-terminal tagging of <i>MPM1</i>	CCCCAGGTGAAGCATAAAGTGGTGAGTGTTGACGAAGACAATCGGATCC CCGGGTTAATTAA
TL4295	C-terminal tagging and disruption of <i>MPM1</i>	GCATATTGTGAAGATATGAGTAAAAAAGGAAACGAAAATATGTCCTG ATATCATCGATGAATTC
TL4519	C-terminal tagging of <i>PDA1</i>	GATACTTGGGACTTCAAAAAGCAAGGTTTTGCCTCTAGGGATCGGATCC CCGGGTTAATTAA
TL4520	C-terminal tagging of <i>PDA1</i>	CATGCGATCACAGCACTATTATTTTATTTTCTTACGATTTAAGAATTC GAGCTCGTTTAAAC
TL4522	C-terminal tagging of <i>PDB1</i>	CTCCAACCATCGTTAAAGCTGTCAAAGAAGTCTTGTCAATTGAACGGATC CCCGGTTAATTAA
TL4523	C-terminal tagging of <i>PDB1</i>	CCCTATCTCCTTCTTCTCCTTCTTATTGGATTGAAGTTTATGAATTC GAGCTCGTTTAAAC
TL4592	5'- <i>yme1</i> ^{Δ698-747} mutagenesis primer	CAAGGTCTTATTGAATATTAATAACTAGATGCCACGAAATC
TL4593	3'- <i>yme1</i> ^{Δ698-747} mutagenesis primer	GATTCGTGGGCATCTAGTTATTAATATTCAATAAGACCTTG
TL4594	5'- <i>yme1</i> ^{Δ681-747} mutagenesis primer	GAAGACTATTAACCTAAGTAATAAGTTGAGCTACATAGAC

Primer	Description	Sequence (5' - 3')
TL4595	3' - <i>yme1</i> ^{Δ681-747} mutagenesis primer	GTCTATGTAGCTCAACTTACTTAGTTAATAGTCTTC
TL4596	5' - <i>yme1</i> ^{Δ651-747} mutagenesis primer	CAGAAAATTGGGAATCTTGATAAAATAAGATTCGCGATATTGC
TL4597	3' - <i>yme1</i> ^{Δ651-747} mutagenesis primer	GCAATATCGCGAATCTTATTTTATCAAGATTCCCAATTTTCTG
TL4824	cloning of <i>PDA1</i>	GCACCGGAATTCCGCGCCCATGCTTGCTGCTTCATTCAAACG
TL4825	cloning of <i>PDA1</i>	TCCCCCGGGGGGATTAATCCCTAGAGGCAAAACCTTGC
TL4826	cloning of <i>PDB1</i>	GCACCGGAATTCCGCGCCCATGTTTTCCAGACTGCCAAC
TL4827	cloning of <i>PDB1</i>	TCCCCCGGGGGGATTAATTCAATTGACAAGACTTCTTTG

Table 2.4 Yeast strains used in this study. Strains are listed in order of appearance.

#	Name	Genotype	Reference
	W303-1B	<i>MATα ade2-1 his3-11,15 leu2,112 trp1-1 ura3-52 can1-100</i>	(Thomas and Rothstein, 1989)
YCK10	<i>Δyme1::HIS</i>	<i>MATα ade2-1 his3-11,15 leu2,112 trp1-1 ura3-52 can1-100 yme1::HIS3MX6</i>	(Klanner et al., 2001)
YTE45	<i>Δyme1 + Yme1</i>	<i>MATα ade2-1 his3-11,15 leu2,112 trp1-1 ura3-52 can1-100 yme1::HIS3MX6 + pVT100U-Yme1</i>	this study
YTE55	<i>Δyme1 + Yme1</i> ^{K681G/K682G}	<i>MATα ade2-1 his3-11,15 leu2,112 trp1-1 ura3-52 can1-100 yme1::HIS3MX6 + pVT100U-Yme1</i> ^{K681G/K682G}	this study
YTE56	<i>Δyme1 + Yme1</i> ^{E685A/L686G}	<i>MATα ade2-1 his3-11,15 leu2,112 trp1-1 ura3-52 can1-100 yme1::HIS3MX6 + pVT100U-Yme1</i> ^{E685A/L686G}	this study
YTE57	<i>Δyme1 + Yme1</i> ^{H687A/R688A}	<i>MATα ade2-1 his3-11,15 leu2,112 trp1-1 ura3-52 can1-100 yme1::HIS3MX6 + pVT100U-Yme1</i> ^{H687A/R688A}	this study
YTE58	<i>Δyme1 + Yme1</i> ^{L689G/A690G}	<i>MATα ade2-1 his3-11,15 leu2,112 trp1-1 ura3-52 can1-100 yme1::HIS3MX6 + pVT100U-Yme1</i> ^{L689G/A690G}	this study
YTE59	<i>Δyme1 + Yme1</i> ^{Q691A/G692A}	<i>MATα ade2-1 his3-11,15 leu2,112 trp1-1 ura3-52 can1-100 yme1::HIS3MX6 + pVT100U-Yme1</i> ^{Q691A/G692A}	this study
YTE60	<i>Δyme1 + Yme1</i> ^{L693G/I694G}	<i>MATα ade2-1 his3-11,15 leu2,112 trp1-1 ura3-52 can1-100 yme1::HIS3MX6 + pVT100U-Yme1</i> ^{L693G/I694G}	this study
YTE61	<i>Δyme1 + Yme1</i> ^{E695A/Y696A}	<i>MATα ade2-1 his3-11,15 leu2,112 trp1-1 ura3-52 can1-100 yme1::HIS3MX6 + pVT100U-Yme1</i> ^{E695A/Y696A}	this study
YTE62	<i>Δyme1 + Yme1</i> ^{A701G/I704G}	<i>MATα ade2-1 his3-11,15 leu2,112 trp1-1 ura3-52 can1-100 yme1::HIS3MX6 + pVT100U-Yme1</i> ^{A701G/I704G}	this study
YTE63	<i>Δyme1 + Yme1</i> ^{H702A/E703A}	<i>MATα ade2-1 his3-11,15 leu2,112 trp1-1 ura3-52 can1-100 yme1::HIS3MX6 + pVT100U-Yme1</i> ^{H702A/E703A}	this study

#	Name	Genotype	Reference
YTE64	$\Delta yme1 + Yme1^{E705A/Q706A}$	<i>MATα ade2-1 his3-11,15 leu2,112 trp1-1 ura3-52 can1-100 yme1::HIS3MX6 + pVT100U-Yme1^{E705A/Q706A}</i>	this study
	$\Delta sco1 \Delta yme1$	<i>MATα ade2-1 his3-11,15 leu2,112 trp1-1 ura3-52 can1-100 sco1::KanMX6 yme1::HIS3MX6</i>	unpublished M. Graef
YTE87	$\Delta sco1 \Delta yme1 + Yme1$	<i>MATα ade2-1 his3-11,15 leu2,112 trp1-1 ura3-52 can1-100 sco1::KanMX6 yme1::HIS3MX6 + pVT100U-Yme1</i>	this study
YTE 71-80	$\Delta sco1 \Delta yme1 + Yme1^{K681G/K682G} - Yme1^{E705A/Q706A}$	<i>MATα ade2-1 his3-11,15 leu2,112 trp1-1 ura3-52 can1-100 sco1::KanMX6 yme1::HIS3MX6 + pVT100U-Yme1^{K681G/K682G} - pVT100U-Yme1^{E705A/Q706A}</i>	this study
YTE92	$\Delta yme1 + Yme1^{\Delta 709-747}$	<i>MATα ade2-1 his3-11,15 leu2,112 trp1-1 ura3-52 can1-100 yme1::HIS3MX6 + pVT100U-Yme1^{\Delta 709-747}</i>	this study
YTE132	$\Delta yme1 + Yme1^{\Delta 698-747}$	<i>MATα ade2-1 his3-11,15 leu2,112 trp1-1 ura3-52 can1-100 yme1::HIS3MX6 + pVT100U-Yme1^{\Delta 698-747}</i>	this study
YTE133	$\Delta yme1 + Yme1^{\Delta 681-747}$	<i>MATα ade2-1 his3-11,15 leu2,112 trp1-1 ura3-52 can1-100 yme1::HIS3MX6 + pVT100U-Yme1^{\Delta 681-747}</i>	this study
YTE134	$\Delta yme1 + Yme1^{\Delta 651-747}$	<i>MATα ade2-1 his3-11,15 leu2,112 trp1-1 ura3-52 can1-100 yme1::HIS3MX6 + pVT100U-Yme1^{\Delta 651-747}</i>	this study
YTE93	$\Delta sco1 \Delta yme1 + Yme1^{\Delta 709-747}$	<i>MATα ade2-1 his3-11,15 leu2,112 trp1-1 ura3-52 can1-100 sco1::KanMX6 yme1::HIS3MX6 + pVT100U-Yme1^{\Delta 709-747}</i>	this study
YTE 135-137	$\Delta sco1 \Delta yme1 + Yme1^{\Delta 698-747} - Yme1^{\Delta 651-747}$	<i>MATα ade2-1 his3-11,15 leu2,112 trp1-1 ura3-52 can1-100 sco1::KanMX6 yme1::HIS3MX6 + pVT100U-Yme1^{\Delta 709-747} - pVT100U-Yme1^{\Delta 651-747}</i>	this study
YTE125	$\Delta imp1 \Delta yme1$	<i>MATα ade2-1 his3-11,15 leu2,112 trp1-1 ura3-52 can1-100 imp1::NAT yme1::HIS3MX6</i>	this study
YTE 138-142	$\Delta imp1 \Delta yme1 + Yme1^{\Delta 709-747} - Yme1^{\Delta 651-747}$	<i>MATα ade2-1 his3-11,15 leu2,112 trp1-1 ura3-52 can1-100 imp1::NAT yme1::HIS3MX6 + pVT100U-Yme1^{\Delta 709-747} - pVT100U-Yme1^{\Delta 651-747}</i>	this study
	<i>mas1ts</i>	<i>MATα leu2 his3 phoC phoE mas1^{ts}</i>	(Yaffe and Schatz, 1984)
YKO200	$\Delta yta10 \Delta yta12$	<i>MATα ade2-1 his3-11,15 leu2,112 trp1-1 ura3-52 can1-100 yta10::HIS3MX6 yta12::KanMX6</i>	(Koppen et al., 2007)
YTE25	$\Delta yme1 + Yme1$	<i>MATα ade2-1 his3-11,15 leu2,112 trp1-1 ura3-52 can1-100 yme1::HIS3MX6 + pRS314-Yme1</i>	this study
YTE26	$\Delta yme1 + Yme1^{E541Q}$	<i>MATα ade2-1 his3-11,15 leu2,112 trp1-1 ura3-52 can1-100 yme1::HIS3MX6 + pRS314-Yme1^{E541Q}</i>	this study
YTE28	$\Delta yme1 + Yme1\text{-6HIS}$	<i>MATα ade2-1 his3-11,15 leu2,112 trp1-1 ura3-52 can1-100 yme1::HIS3MX6 + pRS314-Yme1-6HIS</i>	this study
YTE29	$\Delta yme1 + Yme1^{E541Q}\text{-6HIS}$	<i>MATα ade2-1 his3-11,15 leu2,112 trp1-1 ura3-52 can1-100 yme1::HIS3MX6 + pRS314-Yme1^{E541Q}-6HIS</i>	this study

#	Name	Genotype	Reference
YTE88	$\Delta yme1 +$ Yme1 ⁽¹⁻⁵⁰⁾ -6HIS -Yme1 ⁽⁵¹⁻⁷⁴⁷⁾	<i>MATα ade2-1 his3-11,15 leu2,112 trp1-1 ura3-52</i> <i>can1-100 yme1::HIS3MX6</i> + pRS314-Yme1 ⁽¹⁻⁵⁰⁾ -6HIS-Yme1 ⁽⁵¹⁻⁷⁴⁷⁾	this study
YTE89	$\Delta yme1 +$ Yme1 ⁽¹⁻⁵⁰⁾ -6HIS -Yme1 ⁽⁵¹⁻⁷⁴⁷⁾ - E541Q	<i>MATα ade2-1 his3-11,15 leu2,112 trp1-1 ura3-52</i> <i>can1-100 yme1::HIS3MX6</i> + pRS314-Yme1 ⁽¹⁻⁵⁰⁾ -6HIS-Yme1 ⁽⁵¹⁻⁷⁴⁷⁾ -E541Q	this study
YTE36	$\Delta yme1 +$ Yme1 ^(Δ52-198)	<i>MATα ade2-1 his3-11,15 leu2,112 trp1-1 ura3-52</i> <i>can1-100 yme1::HIS3MX6</i> + pRS314-Yme1 ^(Δ52-198)	unpublished, M. Graef
YTE39	W303-Qcr2-HA	<i>MATα ade2-1 his3-11,15 leu2,112 trp1-1 ura3-52</i> <i>can1-100 QCR2-3HA (KanMX6)</i>	this study
YTE40	$\Delta yme1$ - Qcr2-HA	<i>MATα ade2-1 his3-11,15 leu2,112 trp1-1 ura3-52</i> <i>can1-100 yme1::HIS3MX6 QCR2-3HA (KanMX6)</i>	this study
YTE41	W303-Mcr1-HA	<i>MATα ade2-1 his3-11,15 leu2,112 trp1-1 ura3-52</i> <i>can1-100 MCR1-3HA (KanMX6)</i>	this study
YTE42	$\Delta yme1$ - Mcr1-HA	<i>MATα ade2-1 his3-11,15 leu2,112 trp1-1 ura3-52</i> <i>can1-100 yme1::HIS3MX6 MCR1-3HA (KanMX6)</i>	this study
YTE98	W303-Gep1-HA	<i>MATα ade2-1 his3-11,15 leu2,112 trp1-1 ura3-52</i> <i>can1-100 GEP1-6HA (KanMX6)</i>	this study
YTE99	$\Delta yme1$ - Gep1-HA	<i>MATα ade2-1 his3-11,15 leu2,112 trp1-1 ura3-52</i> <i>can1-100 yme1::HIS3MX6 GEP1-6HA (KanMX6)</i>	this study
YTE100	W303-Mpm1- HA	<i>MATα ade2-1 his3-11,15 leu2,112 trp1-1 ura3-52</i> <i>can1-100 MPM1-3HA (KanMX6)</i>	this study
YTE101	$\Delta yme1$ - Mpm1-HA	<i>MATα ade2-1 his3-11,15 leu2,112 trp1-1 ura3-52</i> <i>can1-100 yme1::HIS3MX6 MPM1-3HA (KanMX6)</i>	this study
YTE128	W303-Pda1-HA	<i>MATα ade2-1 his3-11,15 leu2,112 trp1-1 ura3-52</i> <i>can1-100 PDA1-3HA (KanMX6)</i>	this study
YTE129	$\Delta yme1$ - Pda1-HA	<i>MATα ade2-1 his3-11,15 leu2,112 trp1-1 ura3-52</i> <i>can1-100 yme1::HIS3MX6 PDA1-3HA (KanMX6)</i>	this study
YTE130	W303-Pdb1-HA	<i>MATα ade2-1 his3-11,15 leu2,112 trp1-1 ura3-52</i> <i>can1-100 PDB1-3HA (KanMX6)</i>	this study
YTE131	$\Delta yme1$ - Pdb1-HA	<i>MATα ade2-1 his3-11,15 leu2,112 trp1-1 ura3-52</i> <i>can1-100 yme1::HIS3MX6 PDB1-3HA (KanMX6)</i>	this study
YTE105	$\Delta yme1$ -Mpm1- HA + Yme1 ^{E541Q}	<i>MATα ade2-1 his3-11,15 leu2,112 trp1-1 ura3-52</i> <i>can1-100 yme1::HIS3MX6 MPM1-3HA (KanMX6)</i> + pRS314-Yme1 ^{E541Q}	this study
YTE106	$\Delta yme1$ -Mcr1- HA + Yme1 ^{E541Q}	<i>MATα ade2-1 his3-11,15 leu2,112 trp1-1 ura3-52</i> <i>can1-100 yme1::HIS3MX6 MCR1-3HA (KanMX6)</i> + pRS314-Yme1 ^{E541Q}	this study
YTE107	$\Delta yme1$ -Qcr2- HA + Yme1 ^{E541Q}	<i>MATα ade2-1 his3-11,15 leu2,112 trp1-1 ura3-52</i> <i>can1-100 yme1::HIS3MX6 QCR2-3HA (KanMX6)</i> + pRS314-Yme1 ^{E541Q}	this study

#	Name	Genotype	Reference
YTE142	$\Delta yme1$ -Mpm1-HA + pYX113	<i>MATα ade2-1 his3-11,15 leu2,112 trp1-1 ura3-52 can1-100 yme1::HIS3MX6 MPM1-3HA (KanMX6) + pYX113</i>	this study
YTE143	$\Delta yme1$ -Mcr1-HA + pYX113	<i>MATα ade2-1 his3-11,15 leu2,112 trp1-1 ura3-52 can1-100 yme1::HIS3MX6 MCR1-3HA (KanMX6) + pYX113</i>	this study
YTE144	$\Delta yme1$ -Mpm1-HA	<i>MATα ade2-1 his3-11,15 leu2,112 trp1-1 ura3-52 can1-100 yme1::HIS3MX6 MPM1-3HA (KanMX6) + pXY113-Yme1</i>	this study
YTE145	$\Delta yme1$ -Mcr1-HA + Gal-Yme1	<i>MATα ade2-1 his3-11,15 leu2,112 trp1-1 ura3-52 can1-100 yme1::HIS3MX6 MCR1-3HA (KanMX6) + pXY113-Yme1</i>	this study
YTE146	W303 + pYX142	<i>MATα ade2-1 his3-11,15 leu2,112 trp1-1 ura3-52 can1-100 + pYX142</i>	this study
YTE147	$\Delta yme1$ + pXY142	<i>MATα ade2-1 his3-11,15 leu2,112 trp1-1 ura3-52 can1-100 yme1::HIS3MX6 + pYX142</i>	this study
YTE148	W303 + pYX142-Mcr1	<i>MATα ade2-1 his3-11,15 leu2,112 trp1-1 ura3-52 can1-100 + pYX142-Mcr1</i>	this study
YTE149	$\Delta yme1$ + pXY142-Mcr1	<i>MATα ade2-1 his3-11,15 leu2,112 trp1-1 ura3-52 can1-100 yme1::HIS3MX6 + pYX142-Mcr1</i>	this study
YTE108	$\Delta yme1::NAT$	<i>MATα his3Δ1 leu2Δ0 lys3Δ0 ura3Δ0 yme1::NAT</i>	this study
YTE117	$\Delta imp1\Delta yme1$ + Yme1	<i>MATα his3Δ1 leu2Δ0 met15Δ0 ura3Δ0, lys3Δ0 imp1::KanMX, yme1::NAT + pVT100U-Yme1</i>	this study
YTE150	$\Delta imp1\Delta yme1$ + YEplac181	<i>MATα his3Δ1 leu2Δ0 met15Δ0 ura3Δ0, lys3Δ0 imp1::KanMX, yme1::NAT + YEplac181</i>	this study
YTE151	$\Delta imp1\Delta yme1$ + Pgc1	<i>MATα his3Δ1 leu2Δ0 met15Δ0 ura3Δ0, lys3Δ0 imp1::KanMX, yme1::NAT + YEplac181-Pgc1</i>	this study
YTE152	$\Delta imp1\Delta yme1$ + Ylr218c	<i>MATα his3Δ1 leu2Δ0 met15Δ0 ura3Δ0, lys3Δ0 imp1::KanMX, yme1::NAT + YEplac181-Ylr218c</i>	this study
YTE153	$\Delta imp1\Delta yme1$ + Pet54	<i>MATα his3Δ1 leu2Δ0 met15Δ0 ura3Δ0, lys3Δ0 imp1::KanMX, yme1::NAT + YEplac181-Pet54</i>	this study
YTE154	$\Delta imp1\Delta yme1$ + Mic14	<i>MATα his3Δ1 leu2Δ0 met15Δ0 ura3Δ0, lys3Δ0 imp1::KanMX, yme1::NAT + YEplac181-Mic14</i>	this study

2.2.2 Yeast genetic procedures

DNA was introduced into yeast cell with the lithium acetate/single-stranded carrier DNA/polyethylene glycol method (Gietz and Woods, 2002). The Synthetic Genetic Analysis (SGA) was accomplished as described previously (Tong et al., 2001). Confirmation of synthetic lethal interactions was achieved by sporulation and tetrad dissection. For the identification of high copy suppressors of the synthetic lethal interactions, a Yep13 high-copy

genomic library was employed. Double deletion strains harbouring a pVT100U-Yme1 plasmid were transformed with the library. After growth at 30°C on SD-Leu, plates were replicated onto plates containing 5'FOA (1 mg/ml) for counterselection of the pVT100U-Yme1 plasmid. Suppressing genes were identified through isolation of Yep13 plasmids from yeast, transformation of the corresponding plasmids into *E. coli* cells and subsequent cloning of the single genes into the YEplac181.

2.3 Biochemistry Methods

2.3.1 Total protein isolation from *S. cerevisiae*

Total protein samples were prepared by alkaline extraction (Yaffe and Schatz, 1984). 3 OD₆₀₀ units yeast cells were sedimented by centrifugation for 1 min at 16.000 *g* and washed once with 500µl H₂O. The cell pellet was resuspended in 300 µl H₂O and 50 µl of lysis buffer [1.85 M NaOH, 7.4% (v/v) β-mercaptoethanol, 10 mM PSMF; 5% (v/v) ethanol] were added. After incubation for 10 min at 4°C, the total cellular proteins were precipitated with TCA (Tatsuta and Langer, 2007) and subjected to SDS-PAGE (Lämmli, 1970) and Western-Blot (Towbin et al., 1979). Precipitated cellular proteins corresponding to 0.2-0.3 OD₆₀₀ units were used for SDS-PAGE.

2.3.2 Preparation of cellular membranes from *S. cerevisiae*

In order to prepare of cellular membranes, including the mitochondrial fraction, 10 OD₆₀₀ units yeast cells were harvested by centrifugation (1 min, 16.000 *g*, 4°C). After resuspending the cell pellet in 300 µl SHKCl buffer [0.6 M Sorbitol, 50 mM HEPES/KOH pH 7.4, 80 mM KCl, 2 mM PMSF] and supplying the sample with 200 µl glass-beads (Ø 0.5 mm), cells were opened by five repetitive cycles of mixing (30 sec, Vortex) and cooling on ice (30 sec). Subsequent addition of 400 µl SHKCl buffer and centrifugation (3 min, 500 *g*, 4°C) allowed the removal of glass-beads and unbroken cells. The cellular membrane fraction was separated from the soluble fraction by centrifugation (20 min, 12.000 *g*, 4°C) and used for further analysis by SDS-PAGE (Lämmli, 1970) and Western blot (Towbin et al., 1979). When starting with 200 OD₆₀₀ units yeast cells, 3 ml SHKCl and 3 g of glass-beads were used.

2.3.3 Immunological detection of proteins

All steps for immunological detection were performed in TBS buffer [10 mM Tris/HCl pH 7.4, 150 mM NaCl]. Blocking of nitrocellulose and PVDF membrane was performed with 5% (w/v) milk powder dissolved in TBS. For incubation with the protein-specific antiserum, 1%

(w/v) milk powder was added and for the incubation of horseradish-peroxidase coupled antibodies specific for different immunoglobulin Gs 5% (w/v) milk powder and a dilution of 1:10.000 were used. The peroxidase activity on the membranes could be detected after incubation for 1 min with a 1:1 mixture of chemiluminescence reagents [solution 1: 100 mM Tris/HCl pH 8.5, 0.44 µg/ml luminol, 150 µg/ml *p*-coumaric acid; solution 2: 100 mM Tris/HCl pH 8.5, 1.8% (v/v) H₂O₂]. Emission signals were captured by exposure to light-sensitive X-ray films (Super RX, Fuji).

Table 2.5 Antibodies used in this study listed in order of appearance.

Antisera	Epitope	Dilution	Reference
α-Yme1	N-terminal peptide (amino acid 55-65) of Yme1 from <i>S. cerevisiae</i>	1:10.000	(Leonhard et al., 1996)
α-Cox2	whole protein of Cox2 from <i>S. cerevisiae</i>	1:1.000	
α-Tom40	C-terminal peptide of Tom40 from <i>S. cerevisiae</i>	1:20.000	
α-Mge1	C-terminal peptide of Mge1 from <i>S. cerevisiae</i>	1:10.000	(Schneider et al., 1994)
α-Cyb2	whole protein of Cyb2 from <i>S. cerevisiae</i>	1:2.000	
α-HA (3F10)	YPYDVPDYA	1:3.000	Roche
α-Mcr1	whole protein of Mcr1 from <i>S. cerevisiae</i>	1:2.000	(Hahne et al., 1994)
α-Myc (9B11)	EQKLISEEDL	1:1.000	Cell Signaling Technology

2.3.4 Procedures employing S³⁵-radiolabelled polypeptides

In organello translation of mitochondrial translation products and *in vitro* transcription and translation of polypeptides were performed as previously described (Brandt, 1991; Tatsuta and Langer, 2007). TNT-based S³⁵-radiolabelled polypeptides were produced using the TNT[®]-Sp6 Coupled Reticulocyte Lysate System according to the manufacturer's protocols (Promega).

2.3.4.1 *In vitro* MPP-cleavage assay

Purification of recombinant MPP from *E. coli* expressing a single mRNA encoding α-MPP and an N-terminally hexahistidine-tagged β-MPP (vector pVG18) was operated as established (Luciano et al., 1997), using Ni-NTA sepharose (1 ml HiTrap™ Chelating HP column, GE Healthcare) connected to an FPLC/HPLC system (ÄKTA, GE Healthcare).

In vitro cleavage by MPP was performed using 10% (v/v) of S³⁵-radiolabelled precursor protein. Incubation at 30°C in cleavage buffer [20 mM HEPES/KOH pH 7.4, 50 mM NaCl, 1

mM ZnCl₂, 5 mM MgCl₂, 1 mM ATP, 24.4 µg purified MPP protein] was performed for 20 min. One third of the sample was subjected to SDS- PAGE (Lämmli, 1970) and Western blot (Towbin et al., 1979) followed by autoradiography.

2.3.4.2 Import and import-chase of S³⁵-radioalabeled polypeptides into isolated mitochondria

The import reaction was carried out as previously described (Tatsuta and Langer, 2007). Different percentages of S³⁵-radiolabelled polypeptides were used for import reactions [3-5% (v/v) of total reaction]. For removal of non-imported S³⁵-radiolabelled polypeptides final concentrations of 20 µg/µl (import) or 50 µg/µl (import-chase) trypsin were used; the import reaction was performed 10 min on ice and stopped by addition of STI (1 mg/ml final concentration) and subsequent incubation for 5 min on ice. Samples were separated by SDS-PAGE (Lämmli, 1970) prior to analysis by Western blot (Towbin et al., 1979) and autoradiography.

2.3.5 Co-immunoprecipitation

For co-immunoprecipitation antibodies were coupled to Protein A Sepharose™ CL-4B (PAS) beads (GE Healthcare). Beads were equilibrated with wash buffer [150 mM KAc pH 7.4, 30 mM Tris/HCl pH 7.4, 4 mM MgAc, 1 mM PMSF, 0,125% (w/v) DDM or 0,1% (w/v) digitonin. Separation of PAS-beads from the liquid phase was achieved by centrifugation (1 min, 16.000 *g*, 4°C). To couple the antibody to the PAS-beads 12.5 µl antibody in 400 µl wash buffer were mixed 1 h at 4°C with 1 mg PAS-beads (ratio of PAS-beads to antibody was retained with increasing amounts of PAS beads). After removal of unbound antibody by two washing steps, PAS-beads were incubated with the protein lysate for 2 h at 4°C. Subsequent washing with wash buffer (twice) and 10 mM Tris/HCl pH 7.4 removed loosely bound material and detergent from the PAS-beads. Antibody and bound proteins were eluted by Laemmli buffer prior to analysis of the samples by SDS-PAGE (Lämmli, 1970) and Western blot (Towbin et al., 1979).

Protein lysates of different purification procedures were used for precipitation. Solubilisation was performed in 150 mM KAc pH 7.4, 30 mM Tris/HCl pH 7.4, 4 mM MgAc, 1 mM PMSF, 0,5% (w/v) DDM or 1% (w/v) digitonin. Isolated mitochondria (160 µg) were solubilised after *in organello* translation (Chapter 2.3.4) at a concentration of 5 mg/ml at 4°C and shaking at 1.400 rpm for 30 min. Crude cellular membrane samples from 200 OD₆₀₀ units yeast cells were solubilised in 1.25 ml buffer at 4°C and 1.400 rpm for 30 min. For both

samples, separation of insoluble material was achieved by centrifugation (15 min, 18.000 *g*, 4°C).

For co-immunoprecipitations of Yme1, an antiserum directed against the N-terminal part of the protein was used (Leonhard et al., 1996). Co-immunoprecipitations of HA-tagged proteins were performed with Anti-HA High Affinity (clone 3F10, Roche).

2.3.6 Blue native polyacrylamide gel electrophoresis (BN-PAGE)

The principal of the blue native polyacrylamide gel electrophoresis (BN-PAGE) has been described previously (Schägger, 2001; Schägger and von Jagow, 1991). Samples for BN-PAGE were obtained by preparation of cellular membranes (Chapter 2.3.2) from 10 OD₆₀₀ units of yeast cells. The cellular membrane fraction was solubilised in 20 µl solubilisation buffer [50 mM NaCl, 5 mM 6-aminohexanoic acid, 50 mM imidazole/HCl pH 7.4, 50 mM KP_i buffer pH 7.4, 10% (v/v) glycerol] containing 0.5% (w/v) DDM. Agitation for 20 min at 4°C and 1.400rpm was followed by centrifugation (15 min, 18.000 *g*, 4°C) to remove non-solubilised remnants. 18 µl of the solubilised sample were mixed with 2 µl of 2% (w/v) coomassie G-250 (in solubilisation buffer). The samples were separated at 4°C by BN-PAGE with a polyacrylamide concentration gradient ranging from 3 to 11% (w/v). Gels were run at 50 V in deep blue cathode buffer [50 mM tricine, 7.5 mM imidazole, 0.02% (w/v) coomassie G-250] and anode buffer [25 mM imidazole/HCl pH 7.0] until the sample had completely entered the gel. Thereafter, the deep blue cathode buffer was replaced by cathode buffer without coomassie G-250 and the electrophoresis was continued for 3 h at 300 V. Western blotting of proteins was performed with PVDF membranes that were beforehand equilibrated in methanol. Marker proteins were thyroglobulin (667 kDa) and ferritin (440 kDa).

2.3.7 Ni-NTA affinity chromatography of mitochondrial extracts

Isolated mitochondria from yeast strains harbouring a proteolytically inactive variant of the Yme1 protein containing a C-terminal (Yme1^{E541Q}-6HIS) or N-terminal (Yme1⁽¹⁻⁵⁰⁾-6HIS - Yme1⁽⁵¹⁻⁷⁴⁷⁾-E541Q) hexahistidine tag were subjected to Ni-NTA affinity chromatography. Purification was performed using Ni-NTA sepharose (1 ml HiTrap™ Chelating HP column) connected to an FPLC/HPLC system (ÄKTA). Mitochondria harbouring an inactive variant of Yme1 without hexahistidine tag (Yme1^{E541Q}) served as a negative control for both purifications. For both, the C-terminally and the N-terminally tagged Yme1, the same buffer conditions were used for solubilisation [0.5% (w/v) DDM, 150 mM KAc pH 7.4, 30 mM Tris/HCl pH 7.4, 4 mM MgAc, 1x Complete w/o EDTA Proteinase-Inhibitor (Roche), 1 mM PMSF, 20 mM imidazole/HCl pH 7.4 – additionally 10% (v/v) glycerol for Yme1⁽¹⁻⁵⁰⁾-6HIS -

Yme1^{(51-747)-E541Q}]. Although the protein concentration during solubilisation was different (2.5 mg/ml for Yme1^{E541Q}-6HIS, 4 mg/ml for Yme1⁽¹⁻⁵⁰⁾-6HIS -Yme1^{(51-747)-E541Q}), mitochondrial extracts were obtained with both conditions starting from 40 mg of isolated mitochondria. The affinity purification of both proteins was essentially the same, but optimised for the purification of Yme1⁽¹⁻⁵⁰⁾-6HIS-Yme1^{(51-747)-E541Q}. Therefore, the used chromatography conditions will be described separately: for the Yme1^{E541Q}-6HIS, loading was performed with 20 mM imidazole at a flow rate of 1 ml/min. Then, the flow rate was set to 0.3 ml/min for all following steps. After washing with 10 CV (Column Volumes) of buffer containing 150 mM imidazole and 3 CV 175 mM imidazole washing, the Yme1 protein was eluted with 300 mM imidazole. For Yme1⁽¹⁻⁵⁰⁾-6HIS-Yme1^{(51-747)-E541Q}, the mitochondrial extract was loaded with an imidazole concentration of 100 mM and a flow rate of 0.3 ml/min. Subsequent washings with buffer containing 150 mM imidazole at a flow rate of 0.8 ml/min were followed by a linear increase of the imidazole concentration to 750 mM during 10 CV at a flow rate of 0.3 ml/min. For both purifications the elution fractions containing the Yme1 proteins were pooled, subjected to TCA-precipitation (Tatsuta and Langer, 2007) and loaded on a 7-20% (w/v) gradient SDS-PAGE that was later stained with colloidal coomassie (Neuhoff et al., 1990). PMF (peptide mass fingerprint) analysis of protein bands extracted from the SDS-PAGE was performed with the help of the CMMC (Center for Molecular Medicine, University of Cologne, Stefan Müller and Julia Hommer) or the CECAD (Cologne Excellence Cluster on Cellular Stress Response and Aging-associated Disease, Tobias Lamkemeyer).

2.3.8 Lipid analysis

2.3.8.1 Lipid isolation

Lipids were extracted from sphaeroplast or isolated mitochondria. For isolation of lipids from whole cells, a preincubation with DTT buffer [13 mM DTT (dithiothreitol), 100 mM Tris/HCl pH 7.4] and lysis buffer [1,2 M sorbitol, 20 mM KPi pH 7.4, 1,7 mg/g (weight) lyticase] produced sphaeroplasts. 25 mg sphaeroplasts or 1 mg isolated mitochondria in 50 µl SEM buffer [250 mM sucrose, 10 mM MOPS pH 7.2, 1 mM EDTA] were mixed with 1.5 ml chloroform:methanol [2:1 (v/v)] and incubated at RT and 1.600 rpm for 60 min. Subsequently, 300 µl of H₂O were added and the sample was mixed for 60 sec on a Vortex mixer. The aqueous and the solvent phase were separated by centrifugation (5 min, 200 *g*, RT). The solvent phase was washed twice with 250 µl H₂O:methanol [1:1 (v/v)] and dried under constant air stream. Lipids were dissolved in chloroform and the phospholipid concentration was determined as previously described (Rouser et al., 1970).

2.3.8.2 Thin Layer Chromatography (TLC)

Loading of TLC plates (HPTLC Silica gel 60 F₂₅₄, Merck) was performed with the Linomat 5 (Camag) after activation with 1,8% (w/v) boric acid (in ethanol) (Vaden et al., 2005). The TLC plates were developed with cyclohexane:ethylacetate [3:1 (v/v)] using the Automatic Developing Chamber (Camag). TLC plates were stained with 470 mM CuSO₄ in 8,5% (v/v) *o*-phosphoric acid followed by incubation at 180°C for 10 min. As marker lipids served ergosterol, cholesterol, cholesterylsterate and cholesterylpalmitate.

2.3.9 Miscellaneous

Isolation of mitochondria was accomplished according to compiled protocols (Tatsuta and Langer, 2007).

3 Results

3.1 Initial substrate binding to the CH-region of the *f*-AAA protease Yme1

The *f*-AAA protease is an ATP-dependent protease composed of Yme1 subunits that are inserted into the inner membrane of mitochondria. Previous characterisation of substrate interaction with the *f*-AAA protease demonstrated a dependence of substrate binding and degradation on the surface exposed CH- and NH-region of the *f*-AAA protease (Graef and Langer, 2006; Graef et al., 2007). The NH-region is part of the AAA domain of Yme1, which is required for its proteolytic activity and hence the *in vivo* function of the protease (Graef and Langer, 2006). Structurally the CH-region is composed of three α -helices that situate at the top and side of the catalytic chamber facing the intermembrane space (Fig. 3.1) (Graef et al., 2007). The role of the CH-region is more complex, as two different modes of substrate binding and degradation can be distinguished: a CH-dependent and a CH-independent. A CH-independent mechanism of binding and degradation is shown for the assembled cytochrome *c* oxidase subunit 2 (Cox2), where both processes occur via the NH-region. In contrast, non assembled Cox2 is bound and degraded in a CH-dependent manner (Graef et al., 2007). As one of the major differences between the two forms of Cox2 is their relative localization within the membrane, and the proximity of the NH- and CH-region of Yme1 to the membrane varies, substrate binding to either site might be stimulated by the substrates' distance to the membrane. Generally, the binding of substrates to the CH- or NH-region can occur independently from each other.

Here, the possible requirement of distinct regions or residues within the CH-region of Yme1 for the initial engagement of substrates was examined (Fig. 3.1). Up to date, only the requirement of the complete CH-region in binding and degradation of substrates has been analysed (Graef et al., 2007). It is hence not clear whether single residues or distinct areas within the CH-region are sufficient for binding of substrates to the *f*-AAA protease Yme1.

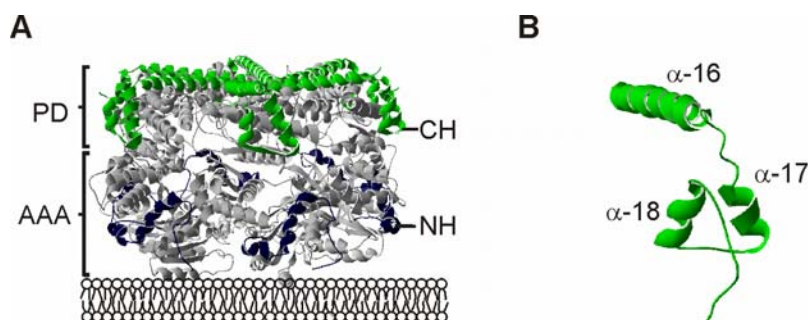


Figure 3.1 CH- and NH-regions within the structure of the *i*-AAA protease Yme1.

(A) Initial substrate binding sites of the *i*-AAA protease. NH- (N-terminal helices) and CH- (C-terminal helices) substrate binding regions of the *i*-AAA protease form a lattice-like structure at the surface of the predicted proteolytic cylinder of AAA proteases. **(B)** Helices within the CH-region of the *i*-AAA protease. α -16 is positioned at the surface of the predicted proteolytic cylinder, whereas α -17 and α -18 build up a lateral aligning U-like structure. Shown are the corresponding structures within the crystal structure of the related AAA protease of *T. maritima* (A) (U. Baumann, personal communication), *T. thermophilus* (B) FtsH (Sunno et al., 2006).

Further, the possible involvement of distinct areas or single residues in the progress of degradation by the protease was examined, as no exact mechanism of substrate transmission is described for substrates that are bound to the CH-region of the *i*-AAA protease Yme1. The comparison of the mutants' ability to bind and degrade substrates allows the identification of residues responsible for substrate transmission. For this purpose, pair wise point mutations were introduced into the α -17 and α -18 helices of the CH-region of Yme1 and the three helices building up the CH-region were subsequently removed using C-terminal deletions.

3.1.1 Mutational analysis of the α -17 and α -18 helices of the CH-region of Yme1 in regard to substrate binding and degradation

The analysis of specific residues and their role in substrate binding and degradation is based on the introduction of pair wise mutations into the sequence of the α -17 and α -18 helices of the CH-region of Yme1. Generally, more or less uncharged amino acid residues were exchanged with glycine, whereas charged amino acids were replaced by alanine. Changing amino acid residues to either glycine or alanine produced the following CH-mutant variants of Yme1: α -17- Yme1^{K681G/682G}, Yme1^{E685A/L686G}, Yme1^{H687A/R688A}, Yme1^{L689G/A690G}, Yme1^{Q691A/G692A}, Yme1^{L693G/I694G}, Yme1^{E695A/Y696A}; α -18- Yme1^{A701G/I704G}, Yme1^{H702A/E703A}, Yme1^{E705A/Q706A}. The general activity of the Yme1 CH-mutants is reflected by their ability to complement known $\Delta yme1$ phenotypes – in the absence of *YME1* cells are not able to grow

without mtDNA, on non-fermentable carbon source at elevated temperature and they show a drastically reduced fitness on glucose containing media at reduced temperature (Thorsness and Fox, 1993; Thorsness et al., 1993; Weber et al., 1995). $\Delta yme1$ cells containing a plasmid-derived wild type variant of Yme1 (endogenous promoter) can fully complement for the loss of the genomic deletion of *YME1* which is not the case for expression of the proteolytic inactive variant of Yme1 (Leonhard et al., 1996; Weber et al., 1996). Thus, complementation of $\Delta yme1$ by the mutated variants of Yme1 reveals the general *in vivo* activity of the protein, however, it does not correlate with the substrate binding and degradation capacity of Yme1 CH-region hybrid variants (Graef et al., 2007). Further, the direct binding and degradation of Cox2 was monitored. Cox2 is one of the three mitochondrial encoded core subunits of the cytochrome *c* oxidase (COX) complex (Herrmann and Funes, 2005). If Cox2 is not assembled into the COX complex it is degraded in a Yme1 dependent manner (Nakai et al., 1995; Pearce and Sherman, 1995; Weber et al., 1996). Therefore, the ability of CH-mutant variants of Yme1 to bind and degrade Cox2 gives a direct hint for a possible role of the mutated residues in substrate engagement by the *i*-AAA protease.

3.1.1.1 *In vivo* activity of CH-mutant variants of Yme1

To test the *in vivo* activity of the CH-mutant variants $\Delta yme1$ cells expressing Yme1^{K681G/682G}, Yme1^{E685A/L686G}, Yme1^{H687A/R688A}, Yme1^{L689G/A690G}, Yme1^{Q691A/G692A}, Yme1^{L693G/I694G}, Yme1^{E695A/Y696A}, Yme1^{A701G/I704G}, Yme1^{H702A/E703A} and Yme1^{E705A/Q706A} were grown on YPD, YPD containing EtBr or YPG. Addition of EtBr to the medium triggers the loss of mtDNA. An inability to grow under this condition is referred to as a petite negative phenotype (Chen and Clark-Walker, 1999). Loss of growth on YPG medium with glycerol as a non-fermentable carbon source reflects the respiratory competence of cells. Complementation of $\Delta yme1$ with Yme1 hybrid mutants does not support the strict dependence on the CH-region of Yme1 for *in vivo* function of the *i*-AAA protease (Graef et al., 2007). Therefore, no direct link of CH-dependent binding and degradation to the *in vivo* activity of the *i*-AAA protease is obvious. Nevertheless, efficient substrate binding is important for the proteolytic function of the *i*-AAA protease within mitochondria, and the proteolytic function is known to be a required *in vivo* function of the *i*-AAA protease Yme1. Hence, testing the *in vivo* activity of the CH-mutant variants might give an idea about the effect the mutation has on degradation of bound substrates.

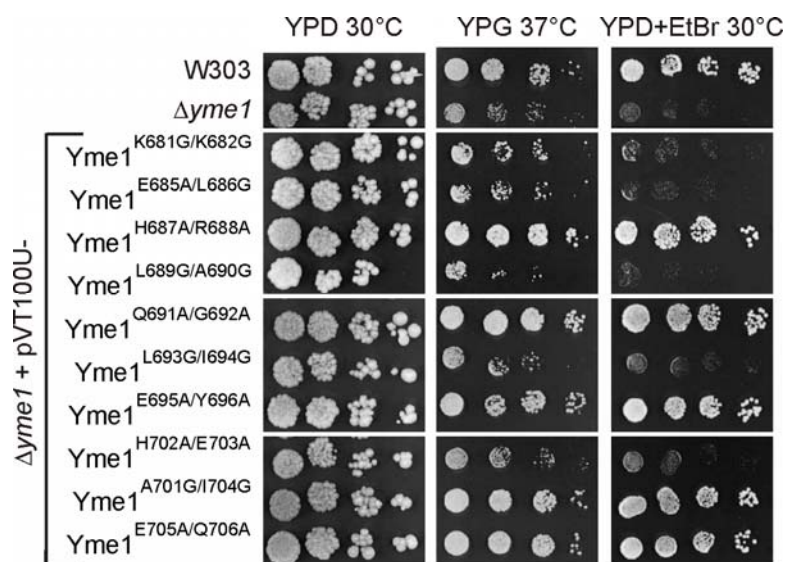


Figure 3.2 *In vivo* activity of CH-mutant variants of the *i*-AAA protease Yme1. $\Delta yme1$ cells expressing different CH-mutant variants of Yme1 are grown on YPD medium, YPD medium containing EtBr (25 μ g/ml) and YPG medium at elevated temperature for two or five days, respectively. The isogenic wild type and $\Delta yme1$ cells served as controls.

Expression of the wild type variant of Yme1 (Fig. 3.5) fully complemented the *YME1* deletion. In case of the mutant Yme1 variants predominantly the exchanges to alanine were able to complement $\Delta yme1$ (Yme1^{H687A/R688A}, Yme1^{Q691A/G692A}, Yme1^{E695A/Y696A}, Yme1^{H702A/E703A} and Yme1^{E705A/Q706A}), while the replacements by glycine (Yme1^{K681G/682G}, Yme1^{E685A/L686G}, Yme1^{L689G/A690G}, Yme1^{L693G/I694G} and Yme1^{A701G/I704G}) did not (Fig. 3.2). To exclude that the difference seen for the mutants is only based on the helix stabilizing effect of alanine relative to glycine (Scott et al., 2007), reverse mutation to glycine instead of alanine have been performed for some mutants leading to similar results (data not shown). CH-mutant variants that were capable to complement $\Delta yme1$ referred to mutated amino acids within the helices α -17 and α -18 of Yme1 that are exposed to the outer surface of the complete molecule. In contrast, those CH-mutants that do not complement $\Delta yme1$ represent mutated residues that face the interior of the molecule. As such mutations can result in an impaired complex assembly that interferes with *in vivo* activity, the complex assembly of the Yme1 mutant variants is monitored by BN-PAGE (data not show). Besides Yme1^{E685A/L686G} all Yme1 mutant variants showed an *i*-AAA protease complex, although the complexes of Yme1^{H687A/R688A} and Yme1^{H702A/E703A} run at lower molecular weight. Since Yme1^{H687A/R688A} was active *in vivo* and Yme1^{H702A/E703A} was not, the complexes formed in the respective strains might not represent the same assembly status of the *i*-AAA protease. For Yme1^{K681G/682G}, Yme1^{L689G/A690G} and Yme1^{L693G/I694G} the absence of *in vivo* activity did not result from impaired complex formation of the *i*-AAA protease, and could therefore reflect a loss of function resulting from impaired substrate binding and degradation. All other introduced mutations (Yme1^{Q691A/G692A},

Yme1^{E695A/Y696A}, Yme1^{H702A/E703A} and Yme1^{E705A/Q706A}) did interfere neither with *in vivo* activity nor with complex formation.

3.1.1.2 Cox2 binding to Yme1 CH-mutant variants

To directly monitor the effect of the CH-mutations on the binding of Cox2 co-immunoprecipitation of Yme1 was performed after *in organello* translation of mitochondrial encoded proteins in the presence of ³⁵S-methionine in isolated mitochondria. Under this conditions the binding and degradation of Cox2 was shown to be a CH-dependent process (Graef et al., 2007). The background signal for Cox2 in the negative control (Fig. 3.3; $\Delta yme1$) is due to the hydrophobicity of the protein.

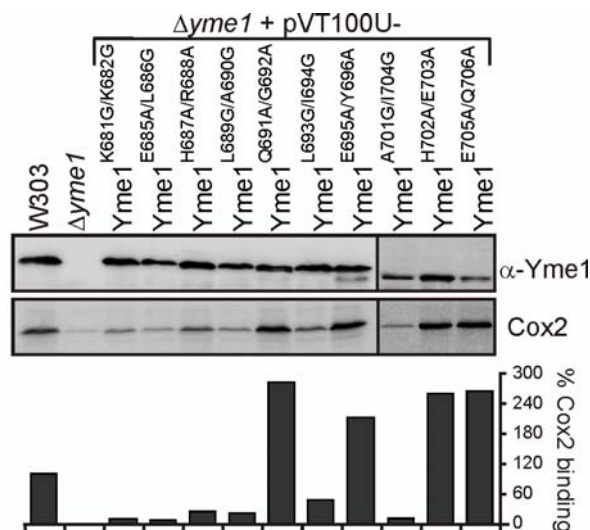


Figure 3.3 Cox2 binding to CH-mutant variants of the *i*-AAA protease. Co-immunoprecipitation of Yme1 from isolated mitochondria. After *in organello* translation of mitochondrial encoded proteins in the presence of ³⁵S-methionin the samples were incubated at 37°C for 5 min. Then co-immunoprecipitation was performed with α -Yme1, precipitates were analysed for Yme1 (immunodetection) and Cox2 (autoradiography). Mitochondria were derived from $\Delta yme1$ cells expressing CH-mutant variants of Yme1. Mitochondria from isogenic wild type and $\Delta yme1$ served as controls. The relative percentage of Cox2 binding was normalised to the amount of Yme1 precipitated. The amount precipitated in the wild type was set to 100%.

For the majority of the CH-mutant variants of Yme1 the binding to Cox2 was decreased, whereas for some mutants the capacity of binding was even increased when compared to wild type (W303, Fig. 3.3). In line with its lack of *in vivo* activity, Yme1^{E685A/L686G} did not show binding of Cox2. The two mutants that showed a lower molecular weight complex of the *i*-AAA protease (Yme1^{H687A/R688A} and Yme1^{A701G/I704G}) are reduced in their binding of Cox2, so the *i*-AAA protease complex formed is likely not fully functional. The fact that Yme1^{H687A/R688A} restores $\Delta yme1$ is arguing against a complete loss of function of this mutant. For the

mutants that assembled into an *i*-AAA protease complex, but did not show a complementation of $\Delta yme1$ (Yme1^{K681G/682G}, Yme1^{L689G/A690G} and Yme1^{L693G/I694G}) no binding of Cox2 was seen. Thus, the alteration of *in vivo* activity correlates with a loss of substrate binding under CH-dependent conditions, but not with a defect of complex assembly. This stresses the role of substrate binding for the *in vivo* activity of the *i*-AAA protease. The mutations that were not affected in complex formation and *in vivo* complementation of $\Delta yme1$ (Yme1^{Q691A/G692A}, Yme1^{E695A/Y696A}, Yme1^{H702A/E703A} and Yme1^{E705A/Q706A}) showed even an increased binding to Cox2 in regard to CH-dependent degradation. As those mutations were introduced at the surface, relative to the complete *i*-AAA protease molecule, a direct effect of the mutation on the binding of substrates was expected. What kind of effect was achieved depends most likely on the mutation that was introduced. These experiments did not identify distinct areas or residues within the CH-region that are required for substrate binding of Yme1. It is therefore conceivable that the complete CH-region structure rather a specific amino acid residues play a role in substrate engagement by the *i*-AAA protease.

3.1.1.3 Degradation of Cox2 in $\Delta sco1 \Delta yme1$ harbouring CH-mutant variants of Yme1

Interfering with the assembly of Cox2 into the COX complex leads to CH-dependent degradation of Cox2 (Graef et al., 2007). Here, a $\Delta sco1$ background was used to render Cox2 degradation CH-dependent. Sco1 is, together with Cox17, responsible for the insertion of copper into the Cox2 molecule prior to its assembly into the COX complex (Cobine et al., 2006; Herrmann and Funes, 2005). As copper binding is impaired in $\Delta sco1$, Cox2 does not assemble and is degraded by the *i*-AAA protease in a CH-dependent manner. Thus, the ability of CH-mutant variants of Yme1 to degrade Cox2 in a $\Delta sco1$ background directly reflects their proteolytic activity, as expression of wild type Yme1 in a $\Delta sco1 \Delta yme1$ background produces a Cox2 pattern similar to that of $\Delta sco1$ (Fig. 3.6).

In general, binding is a prerequisite for degradation. Hence no degradation of Cox2 was found for the CH-mutant variants of Yme1 that did not bind Cox2 (Yme1^{K681G/682G}, Yme1^{E685A/L686G}, Yme1^{H687A/R688A}, Yme1^{L689G/A690G}, Yme1^{L693G/I694G} and Yme1^{A701G/I704G}). Similarly, most mutants that bound Cox2 also showed its degradation (Yme1^{Q691A/G692A}, Yme1^{E695A/Y696A}, Yme1^{H702A/E703A} and Yme1^{E705A/Q706A}). Amino acids required for binding and degradation within the CH-region are facing the interior of the *i*-AAA protease molecule. It therefore appears that mutations interfering with the orientation of the CH-region relative to the rest of the *i*-AAA protease molecule produce Yme1 variants that have lost the ability to bind and degrade substrates. In contrast, mutations which affect the surface exposed residues of the CH-

region do not hinder substrate binding and degradation. This again points to a requirement of the structural integrity and orientation of the Yme1 CH-region in substrate binding and degradation. Two mutants that behaved differently were Yme1^{H687A/R688A} and Yme1^{Q691A/G692A}. Yme1^{H687A/R688A} showed *in vivo* activity although a lower molecular weight complex of the *ι*-AAA protease was formed, CH-dependent binding was reduced and no degradation of Cox2 was evident. So, Yme1^{H687A/R688A} has proteolytic activity although CH-dependent degradation of Cox2 is impaired. The Yme1^{Q691A/G692A} mutation binds Cox2 but does not degrade it. This points to a function of the CH-region of Yme1 beyond substrate binding.

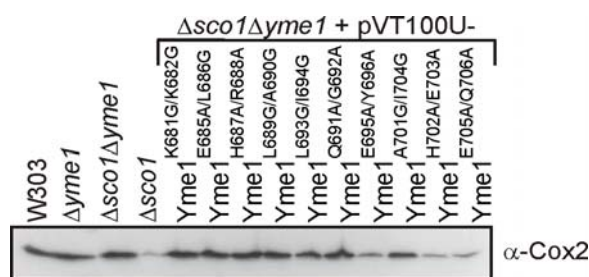


Figure 3.4 Cox2 degradation by CH-mutant variants of the *ι*-AAA protease. Steady state level of Cox2 in $\Delta sco1\Delta yme1$ cells expressing CH-mutant variants of Yme1. Total cellular extracts were separated by SDS-PAGE, followed by immunological detection of Cox2. CH-mutant variants were expressed in $\Delta sco1\Delta yme1$ cells. The isogenic wild type, $\Delta yme1$, $\Delta sco1$ and $\Delta sco1\Delta yme1$ served as controls. Equal loading was assessed via staining of the western blots with ponceau S prior to immunodetection (data not shown).

Taken together these findings highlight the importance of both, the α -17 and α -18 helices of the CH-region in substrate binding and degradation by the *ι*-AAA protease Yme1. Generally, the structural arrangement of helices α -17 and α -18 and their orientation relative to the rest of the *ι*-AAA protease complex appears to be important as mutations interfering with them lead to a loss of substrate binding and degradation. In addition, the surface exposed area from Yme1⁶⁹¹ to Yme1⁶⁸⁸ is important for the transfer of bound substrate to the site of degradation, the proteolytic cavity.

3.1.2 Effects of C-terminal truncations of the CH-region of Yme1 on substrate degradation and complex formation of the *ι*-AAA protease

By introducing subsequent C-terminal deletions into the Yme1 protein the impact of the single helices within the CH-region of Yme1 and of the region following the CH-region was addressed. The truncations were produced by mutating Yme1⁷⁰⁹, Yme1⁶⁹⁸, Yme1⁶⁸¹ and

Yme1⁶⁵¹ to stop residues/codons, generating Yme1^{Δ709-747} (lacking the C-terminal part of Yme1 following the CH region), Yme1^{Δ698-747} (lacking helix α -18), Yme1^{Δ681-747} (lacking helix α -17) and Yme1^{Δ651-747} (lacking the CH-region). The analysis of the region following the CH-region of Yme1 was included here to examine a potential regulatory role of this region on substrate binding to the CH-region. According to the crystal structure of the related FtsH protein from *T. thermophilus* (Suno et al., 2006) this region is resolved as a flexible tail that might regulate substrate binding to the α -17 and α -18 helices within the CH-region of Yme1 (Suno et al., 2006). In other available crystal structures this region is not defined, making it likely to be a flexible element.

Here, the *in vivo* activity of C-terminal truncated Yme1 proteins was determined, as this activity is an indication for their proteolytic function. Further, the requirement of the single helices for substrate degradation was examined. As the degradation is depending on a functionally assembled *i*-AAA protease complex, the status of the hexameric structure of the *i*-AAA protease complex was assessed by native gelelectrophoresis.

3.1.2.1 *In vivo* activity of C-terminal truncation mutants of Yme1

Complementation of $\Delta yme1$ phenotypes was tested by growth on YDP, YDP containing EtBr (25 μ g/ml) and YPG. Growth of $\Delta yme1$ cells expressing the Yme1 C-terminal truncation mutants Yme1^{Δ709-747}, Yme1^{Δ698-747}, Yme1^{Δ681-747} and Yme1^{Δ651-747} was compared to growth of $\Delta yme1$ cells expressing the wild type Yme1.

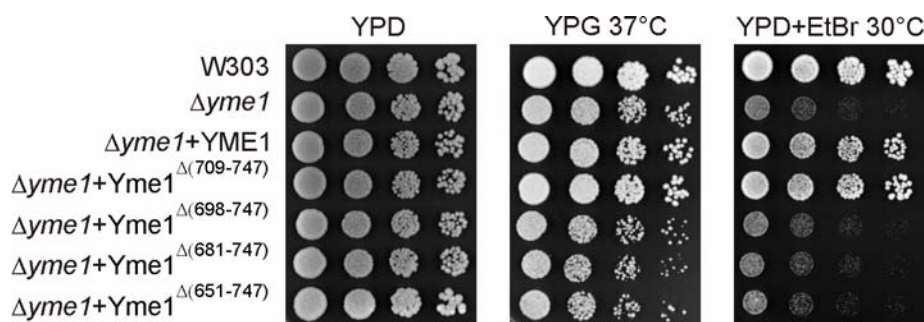


Figure 3.5 *In vivo* activity of C-terminal truncation mutants of the *i*-AAA protease Yme1. $\Delta yme1$ cells expressing Yme1^{Δ709-747}, Yme1^{Δ698-747}, Yme1^{Δ681-747} and Yme1^{Δ651-747} were grown on YPD medium, YPD medium containing EtBr (25 μ g/ml) and YPG medium at elevated temperature for two or five days, respectively. The isogenic wild type, $\Delta yme1$ and $\Delta yme1$ cells expressing Yme1 served as controls.

All of the Yme1 C-terminal truncation mutants disturbing the helices of the CH-region showed a drastic reduction of *in vivo* activity of the corresponding Yme1 protein (Fig. 3.5). This is in line with the impact of mutations within both the α -17 and α -18 region of the CH-

region of Yme1 on the complementation of $\Delta yme1$ phenotypes (Fig. 3.2). There, mutants that did not show complementation of $\Delta yme1$ turned out to be impaired in substrate binding, and hence do not show CH-dependent proteolytic activity. In contrast, the C-terminal truncation mutant lacking only the C-terminal part of Yme1 that is following the CH-region (Yme1 $^{\Delta 709-747}$) showed no apparent effect on *in vivo* activity. Therefore, it is not clear from this result if the region following the CH-region of Yme1 has an impact on substrate binding by the CH-region. These results emphasise the essential role of the CH-region for Yme1 function and also point to a minor relevance of the C-terminal region following the CH-region.

3.1.2.2 Degradation of Cox2 in $\Delta sco1\Delta yme1$ and $\Delta imp1\Delta yme1$ harbouring C-terminal truncation mutants of Yme1

Monitoring the CH-dependent degradation of Cox2 reveals the importance of the deleted amino acids for Cox2 binding and/or degradation. In addition to the already introduced $\Delta sco1\Delta yme1$ mutants, $\Delta imp1\Delta yme1$ mutants were employed. Both mutations impair Cox2 assembly and render Cox2 degradation CH-dependent, but *IMP1* deletion affects Cox processing that occurs within a Sco1 preceding step of Cox2 assembly (Herrmann and Funes, 2005). Imp1 is, together with Imp2 and Som1, part of the mitochondrial inner membrane peptidase complex (IMP) that processes the N-terminal part of Cox2 prior to the insertion of copper by Sco1 (Jan et al., 2000). Therefore, the assembly of Cox2 into the COX complex is disturbed in $\Delta imp1$ cells.

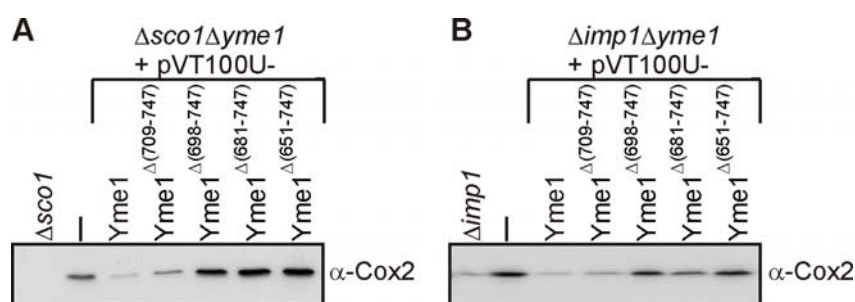


Figure 3.6 Cox2 degradation by C-terminal deletion mutants of the *i*-AAA protease Yme1. (A) Steady state level of Cox2 in $\Delta sco1\Delta yme1$ background. Total cellular extracts were separated by SDS-PAGE, followed by immunological detection of Cox2. Yme1 $^{\Delta 709-747}$, Yme1 $^{\Delta 698-747}$, Yme1 $^{\Delta 681-747}$ and Yme1 $^{\Delta 651-747}$ were expressed in $\Delta sco1\Delta yme1$ cells. $\Delta sco1$ and $\Delta sco1\Delta yme1$ served as controls. **(B)** Similar conditions as in (A). Here the C-terminal deletion mutants were expressed in a $\Delta imp1\Delta yme1$ background. Respectively, $\Delta imp1$ and $\Delta imp1\Delta yme1$ served as controls. Equal loading was assessed via staining of the western blots with ponceau S prior to immunodetection (data not shown).

Consistent with the *in vivo* activity of the C-terminally truncated Yme1 variants only Yme1^{Δ709-74} was able to degrade Cox2 as wild type Yme1 (Fig. 3.6). An even enhanced proteolysis by Yme1^{Δ709-74} could have argued for a restrictive role of this element in substrate binding by the CH-region of Yme1. As degradation of Cox2 by Yme1^{Δ709-74} is, if anything, reduced, such a mode is not obvious by comparison of steady state degradation levels. All the C-terminal truncation mutations lacking any helix of the CH-region were unable to degrade Cox2 (Fig. 3.6). Therefore, either none of the helices within the CH-region of Yme1 is dispensable for substrate binding and subsequent degradation or changes to the structure of the CH-region lead to a destabilisation of the whole protease complex and thereby abolish the existence of a functional *ρ*-AAA protease.

3.1.2.3 Complex formation of C-terminally truncated Yme1 mutants

Complex assembly of the *ρ*-AAA protease is a prerequisite for its function and consistently, no *in vivo* activity is evident in Yme1 mutants that lack a functional *ρ*-AAA protease complex. The high-molecular weight complex of the *ρ*-AAA protease has a molecular mass larger than 850 MDa (Leonhard et al., 1996). Factors known to influence the complex formation of the *ρ*-AAA protease are the two previously described co-factors Mgr1 and Mgr3 (Dunn et al., 2006; Dunn et al., 2008). Deletions of *MGR1* or *MGR3* reduce this mass of the remaining Yme1 complex.

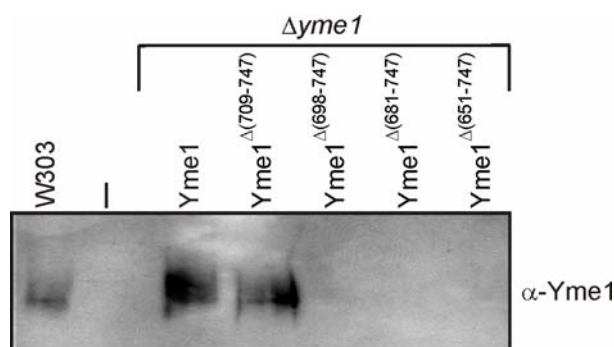


Figure 3.7 Assembly of the *ρ*-AAA protease complex in C-terminally truncated Yme1 mutants. Analysis of the *ρ*-AAA protease complex by BN-PAGE. Cellular membrane fraction from 10 OD₆₀₀ units of $\Delta yme1$ cells expressing Yme1, Yme1^{Δ709-747}, Yme1^{Δ698-747}, Yme1^{Δ681-747} or Yme1^{Δ651-747} were solubilised in 0,5% (w/v) DDM. The soluble extracts were analysed by BN-PAGE, western blot and subsequent immunological detection of Yme1. Soluble extracts from isogenic wild type and $\Delta yme1$ served as controls.

To assess the effect of C-terminal truncations of the Yme1 protein on the assembly of an *ρ*-AAA protease complex, cellular membrane samples of $\Delta yme1$ cells expressing either wild type Yme1 or the four C-terminal truncations of Yme1 (Yme1^{Δ709-747}, Yme1^{Δ698-747}, Yme1^{Δ681-}

⁷⁴⁷ and Yme1^{Δ651-747}) were separated by BN-PAGE (3-11%). Cellular membranes from W303 and $\Delta yme1$ were prepared in parallel for control. Immunological detection of Yme1 revealed an absence of the \hat{i} AAA protease complex in all C-terminal truncations of helices of the CH-region. Consequently their loss of *in vivo* activity and of the ability to degrade Cox2 originates from their incompetence to assemble into a high molecular weight \hat{i} AAA protease complex. Conversely, the impaired substrate degradation of the CH-mutant variants of the α -17 and α -18 helices of Yme1 was based on a lack of substrate binding (Fig. 3.3). The Yme1^{Δ709-747} mutant assembled like wild type Yme1. Taken together, the truncation of the C-terminal part of Yme1 following the CH-region of Yme1 does not have any apparent effect on the function of Yme1, whereas any deletion of the helices of the CH-region of Yme1 abolishes the function of Yme1 by destabilisation of the entire complex. This also implicates a function of the CH-region in complex formation and/or stabilisation.

3.2 Identification of binding partners of the *i*-AAA protease Yme1

Currently only three native substrates, Cox2 (Leonhard et al., 1996; Nakai et al., 1995; Pearce and Sherman, 1995; Weber et al., 1996), Nde1 (Augustin et al., 2005) and Phb1/2 (Kambacheld et al., 2005), as well as two interaction partners, namely Mgr1 (Dunn et al., 2006) and Mgr3 (Dunn et al., 2008), have been identified for the *i*-AAA protease in yeast. However, the pleiotropic phenotypes associated with an *YME1* deletion cannot be explained by the loss of interaction with or the impaired degradation of any of these proteins. Hence, the identification and characterisation of potential interaction partners and novel substrate proteins is needed for a better understanding of the functions of the evolutionary conserved *i*-AAA protease Yme1 in mitochondria. So far, phenotypes associated with the deletion of *YME1* point to a function in mitochondrial protein quality control (Thorsness et al., 1993; Weber et al., 1996), in survival of cells depleted of mtDNA (Thorsness and Fox, 1993), in longevity (Francis et al., 2007; Palermo et al., 2007; Wang et al., 2008) and in mitochondrial morphogenesis (Campbell and Thorsness, 1998). In order to identify physically interacting proteins two Yme1 variants were constructed that harbour an N- or C-terminal hexahistidine tag. Further, a proteolytic inactive variant of Yme1 carrying a mutation in the conserved HEXGH metal binding motif (E541Q) in the proteolytic domain of the *i*-AAA protease (Leonhard et al., 1996; Weber et al., 1996) was used to accumulate proteolytic substrates at the *i*-AAA protease complex. The substrate trap function is adapted from analogous purifications of substrates with a proteolytically inactive *m*-AAA protease variant (Nolden et al., 2005). To reduce possible protein contaminations from non-mitochondrial compartments, cellular fractions enriched for mitochondria served as starting material for affinity purification.

3.2.1 Maturation of the *i*-AAA protease subunits Yme1 from different species

Yme1 harbours a classical N-terminal import sequence that is processed upon mitochondrial import generating mature Yme1 (Leonhard et al., 1996). However, Yme1 processing has not been analysed in detail and neither the processing enzyme nor the N-terminal cleavage site are specified. In order to apply an N-terminal tag to the mature form of the Yme1 proteins, the determination of the cleavage site is required.

3.2.1.1 *In vivo* processing of Yme1 in mutants of different processing peptidases

Specific processing peptidases are present within the different subcompartments of mitochondria (for review see (Koppen and Langer, 2007)). At least three different standard mitochondrial processing peptidases exist in yeast. In the intermembrane space, the membrane embedded mitochondrial inner membrane peptidase (IMP) is built up by Imp1, Imp2 and Som1 subunits (Jan et al., 2000). Here, only a possible involvement of Imp1 in the processing of Yme1 was tested, as Imp1 and Imp2 are known to occupy different substrate specificity. A deletion of *IMP2* was not included in the analysis. As the cleaved N-terminal part of Yme1 resides in the matrix a similar localisation of the peptidase in charge is expected. The mitochondrial matrix processing peptidase (MPP) (Hawlitshchek et al., 1988; Yang et al., 1988) and the mitochondrial intermediate peptidase (MIP) (Kalousek et al., 1988) are located in the mitochondrial matrix. The heterodimer of MPP is composed of α -MPP and β -MPP subunits that are represented in yeast by the proteins Mas2 and Mas1, respectively (Yang et al., 1988). MPP is the major processing peptidase of mitochondria (Gakh et al., 2002). MIP consists of Oct1 subunits and is responsible for the removal of eight amino acids (Isaya et al., 1994). Besides those three processing peptidases, the mitochondrial rhomboid protease Pcp1 (Esser et al., 2002; Herlan et al., 2003), the *m*-AAA protease (Yta10/Yta12) (Esser et al., 2002; Nolden et al., 2005) and the metallopeptidase Atp23 (Osman et al., 2007; Zeng et al., 2007) have been shown to mediate the processing of specific precursor proteins. Although no function in protein processing has been assigned so far, deletion strains of the yeast Lon protease Pim1 (Suzuki et al., 1994; Van Dyck et al., 1994; Wagner et al., 1994), and the inner membrane protease Oma1, that is executing overlapping function with the *m*-AAA protease (Käser et al., 2003), were included in the analysis. In an initial experiment the presence of the Yme1 precursor was assessed in the absence of these peptidases under steady state conditions by immunoblotting (Fig. 3.8). Since MPP function is essential for cell survival, a temperature sensitive allele of Mas1 (*mas1^{ts}*) was employed (Yaffe et al., 1985).

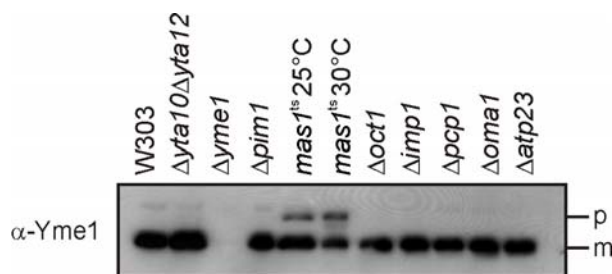


Figure 3.8 *In vivo* processing of Yme1. Steady state level of Yme1 in extracts of $\Delta yta10\Delta yta12$, $\Delta pim1$, $\Delta oct1$, $\Delta imp1$, $\Delta pcp1$, $\Delta oma1$ and $\Delta atp23$ cells. For $mas1^{ts}$ cell extracts were analysed after growth at permissive or restrictive temperature. The protein samples are analysed by SDS-PAGE, western blot and subsequent immunological detection of Yme1 (α -Yme1 directed against amino acids 55-65). Samples from isogenic wild type and $\Delta yme1$ serve as controls.

Only the $mas1^{ts}$ mutant showed an accumulation of an Yme1 specific higher molecular weight form, likely corresponding to the precursor of Yme1 in western blot analysis of whole cell extracts. This form already appeared at permissive temperature, suggesting that processing of the Yme1 precursor form strictly depends on the presence of a functional MPP. The MPP protease has distinct recognition and cleavage motifs (Gakh et al., 2002) allowing the identification of the respective sequence in the *i*-AAA protease Yme1.

3.2.1.2 Processing of *in vitro* translated ^{35}S - radiolabelled Yme1 orthologs by purified MPP

An *in vitro* assay for the processing of ^{35}S -radiolabelled polypeptides by purified MPP peptidase has been established (Luciano et al., 1997). In order to purify the peptidase, simultaneous expression of α -MPP and β -MPP subunits in *E. coli* and subsequent affinity purification of the assembled soluble MPP complex mediated by a hexahistidine tag were performed.

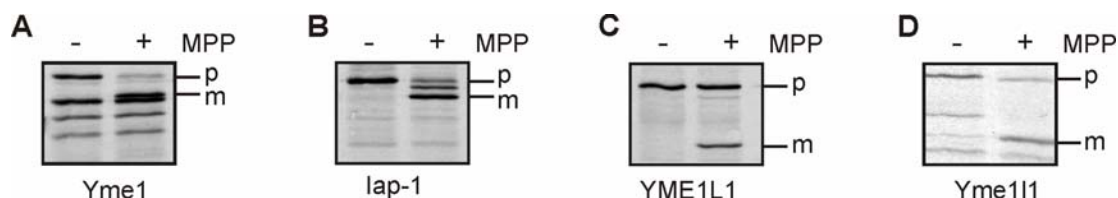


Figure 3.9 *In vitro* processing of ^{35}S -radiolabelled Yme1 orthologs. Processing of ^{35}S -radiolabelled Yme1 in the presence of purified MPP peptidase. Radiolabelled precursors of (A) Yme1, (B) *N. crassa* Iap-1, (C) human YME1L1 and (D) mouse Yme111 were derived from reticulocyte lysate based on *in vitro* translation in the presence of ^{35}S methionine. 10% of radiolabelled precursor protein was incubated with (+) or without (-) purified MPP (24,4 μg) at 30°C for 20 min and analysed by autoradiography after SDS-PAGE and western blotting.

Consistent with the *in vivo* analysis, Yme1 was processed by purified MPP (Fig. 3.9A). Further, Yme1 orthologs from *N. crassa* (Iap-1), *H. sapiens* (YME1L1) and *M. musculus* (Yme1l1) were cleaved by purified MPP *in vitro* supporting a conserved mechanism of Yme1 processing (Leonhard et al., 1996; Luciano et al., 1997; Shah et al., 2000; Weber et al., 1996).

3.2.1.3 *In vivo* activity of N-terminally tagged *i*-AAA protease

Distinct recognition and cleavage motifs have been identified for the MPP peptidase, referred to as R-2 motif and R-3 motif (Gakh et al., 2002). Examination of the Yme1 sequence revealed an R-3 motif (K⁴³FYRFY↓SEKN⁵²). Accordingly, a hexahistidine tag was inserted after the residues E⁵⁰ by site directed mutagenesis.

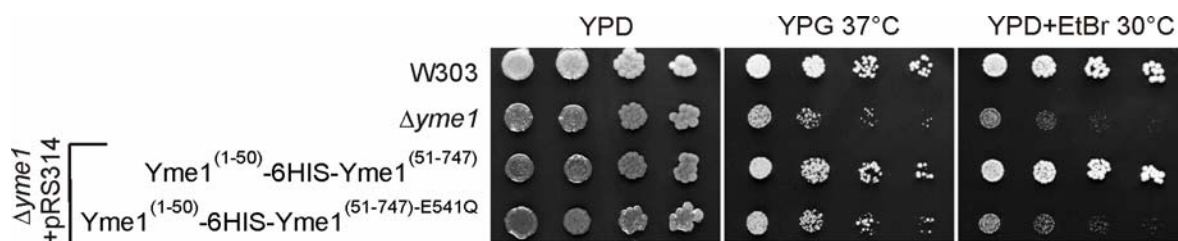


Figure 3.10 *In vivo* activity of N-terminally tagged Yme1. $\Delta yme1$ cells expressing Yme1⁽¹⁻⁵⁰⁾-6HIS-Yme1⁽⁵¹⁻⁷⁴⁷⁾ or Yme1⁽¹⁻⁵⁰⁾-6HIS-Yme1⁽⁵¹⁻⁷⁴⁷⁾-E541Q are grown on YPD medium, YPD medium containing EtBr (25μg/ml) and YPG medium at elevated temperature for two or five days, respectively. The isogenic wild type and $\Delta yme1$ served as controls.

The complementation of $\Delta yme1$ with the N-terminally tagged Yme1 proteins (Yme1⁽¹⁻⁵⁰⁾-6HIS-Yme1⁽⁵¹⁻⁷⁴⁷⁾) permits growth rates comparable to wild type levels (Fig. 3.10). Thus, the N-terminal insertion of a hexahistidine tag does not interfere with the *in vivo* activity of the *i*-AAA protease. Consistently, no complementation of $\Delta yme1$ is achieved by expression of a proteolytic inactive Yme1 variant, Yme1⁽¹⁻⁵⁰⁾-6HIS-Yme1⁽⁵¹⁻⁷⁴⁷⁾-E541Q (Leonhard et al., 1996; Weber et al., 1996).

Similar results were obtained for the C-terminally hexahistidine tagged Yme1 variants (data not shown). Hence, introduced hexahistidine tags do not interfere with *in vivo* activity of Yme1 and can therefore be employed for co-purification of substrate proteins of the *i*-AAA protease.

3.2.2 Affinity purification of a proteolytically inactive variant of Yme1

Co-purification of potential substrate proteins together with the $\hat{\nu}$ AAA protease was accomplished by proteolytic inactive Yme1 variants, Yme1^{E541Q}, harbouring either a C-terminal or N-terminal hexahistidine tag for affinity purification. The use of hexahistidine tags inserted at either side of the $\hat{\nu}$ AAA protease, and therefore at either side of the inner mitochondrial membrane, originated from two aspects. First, a possible absence of substrate binding to the $\hat{\nu}$ AAA protease due to interference with the tag is bypassed. Secondly, the C-terminal tag is inserted close to the CH-region of Yme1 that is known to be important for substrate binding (Graef et al., 2007), so an influence of the tag on the substrate binding to this region is possible. As maintenance of the native status of the $\hat{\nu}$ AAA protease is a prerequisite for efficient co-purification of substrates, the complex status of the different Yme1 variants under the solubilisation conditions used for purification was examined by gel filtration experiments (data not shown) and proved to be intact. The purification of Yme1 was performed with mitochondria isolated from $\Delta yme1$ cells expressing Yme1^{E541Q}, Yme1^{E541Q}-6HIS or Yme1⁽¹⁻⁵⁰⁾-6HIS-Yme1⁽⁵¹⁻⁷⁴⁷⁾-E541Q grown on lactate medium. Mitochondrial extracts were produced by mild solubilisation with 0,5% (w/v) DDM at a protein concentration of 2,5 mg/ml (C-terminal 6HIS) or 4 mg/ml (N-terminal 6HIS). Hexahistidine tagged Yme1 variants were purified by NiNTA affinity chromatography. The resulting elution fractions (350 mM imidazol) were precipitated with TCA, separated by SDS-PAGE and stained with colloidal coomassie (Neuhoff et al., 1990). Prominent bands within the hexahistidine tagged samples were cut out and subjected to peptide mass fingerprint (PMF) analysis for identification of the respective proteins.

The high background present in all purifications probably reflects unspecific binding of hydrophobic or histidine-rich proteins under the used mild purification conditions. The purification procedure allows strong enrichment of both tagged Yme1 variants, Yme1^{E541Q}-6HIS and Yme1⁽¹⁻⁵⁰⁾-6HIS-Yme1⁽⁵¹⁻⁷⁴⁷⁾-E541Q (Fig. 3.11). Proteins co-purified with the hexahistidine tagged $\hat{\nu}$ AAA protease are identified by comparison of the Yme1^{E541Q} elution pattern with the pattern of elution fractions from hexahistidine tagged Yme1 proteins.

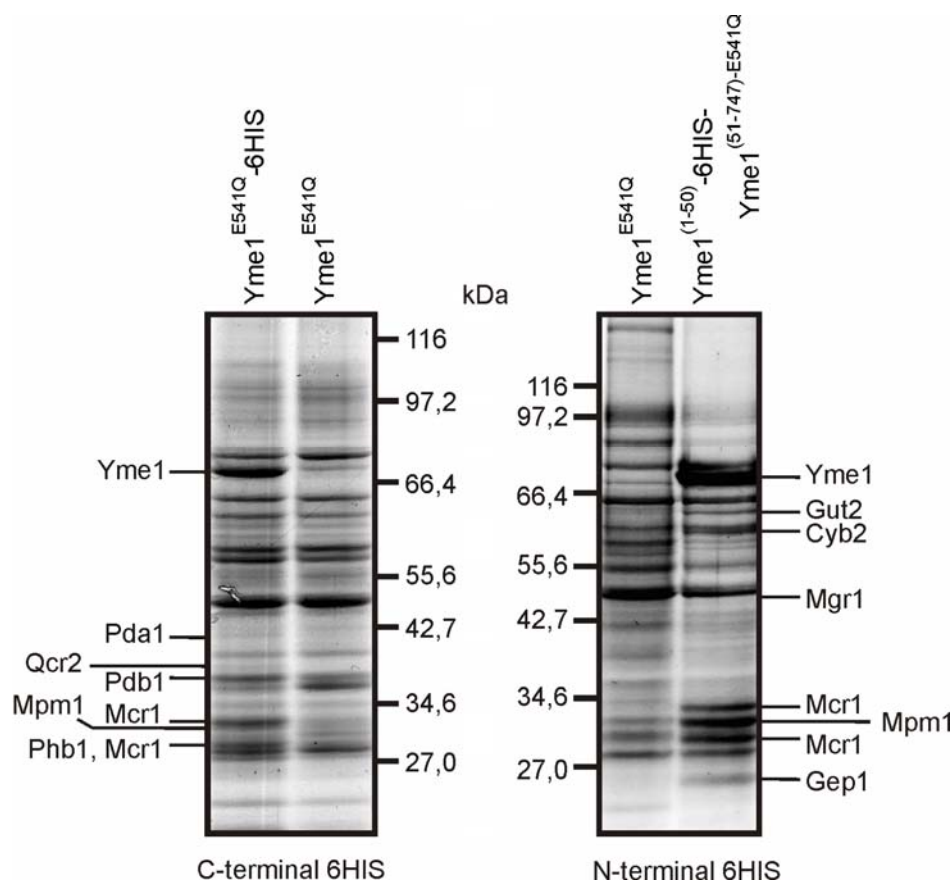


Figure 3.11 Affinity purification of C-terminally and N-terminally tagged *i*-AAA protease. Mitochondria isolated from $\Delta yme1$ cells expressing either Yme1^{E541Q}, Yme1^{E541Q}-6HIS or Yme1⁽¹⁻⁵⁰⁾-6HIS-Yme1⁽⁵¹⁻⁷⁴⁷⁾-E541Q grown on lactate medium were solubilised with 0,5% (w/v) DDM. Yme1 is purified from mitochondrial extracts using NiNTA affinity chromatography. Subsequent washing and elution with 350 mM imidazol are followed by TCA precipitation of the pooled elution fractions. The resulting protein samples are separated by SDS-PAGE and stained with colloidal coomassie. The indicated proteins were identified by peptide mass fingerprint (PMF).

The co-purification of Phb1 and Mgr1 (Fig 3.11) was consistent with known physical interactions of Yme1 demonstrating the proof of principle (Dunn et al., 2006; Graef et al., 2007). Mpm1 and the two forms of Mcr1 are co-purified with either variant of hexahistidine tagged Yme1. Mpm1 (mitochondrial peculiar membrane protein) is a mitochondrial membrane protein of unknown function (Inadome et al., 2001). *MCR1* encodes for the two isoforms of the mitochondrial NADH-cytochrome *b5* reductase (Hahne et al., 1994) and has been linked to ergosterol biosynthesis (Lamb et al., 1999) and to reduction of D-erythroascorbyl free radicals (Lee et al., 2001); just recently the long form (34kDa) of Mcr1 is demonstrated to be localised to mitochondria in a TOM (translocase of the outer membrane) -independent insertion mechanism (Meineke et al., 2008). Gep1, Gut2 and Cyb2 are only co-purified with Yme1⁽¹⁻⁵⁰⁾-6HIS-Yme1⁽⁵¹⁻⁷⁴⁷⁾-E541Q. Gep1 (genetic interaction prohibitin 1) is genetically linked to prohibitins and regulates phosphatidylethanolamine (PE)

levels and mitochondrial morphology (Osman et al., 2009). Gut2 is the mitochondrial glycerol-3-phosphate dehydrogenase important for the utilisation of glycerol under aerobic conditions (Rijken et al., 2007). Furthermore, Gut2 and Cyb2 are components of the glycerol-3-phosphate shuttle which balances the redox state between NAD and NADH under aerobic conditions (Grandier-Vazeille et al., 2001). The inter membrane space protein Cyb2 (Cytochrome b2) is generally required for lactate utilisation (Guiard, 1985).

Strikingly, Mcr1, Gut2 and Cyb2 are all substrates of the IMP peptidase. Together with the known physical interaction of Yme1 and Cox2, which is also an IMP substrate (Herrmann and Funes, 2005), all known substrates of the catalytic IMP subunit Imp1 show physical interaction with the \hat{A} AAA protease Yme1. Since Yme1 is not a substrate of Imp1 (Chapter 3.2.1.1), the interaction of Yme1 with the Imp1 substrates is unlikely to be not mediated by Imp1 itself. Interestingly, all additionally co-purified proteins of Yme1^{E514Q}-6HIS reside within the mitochondrial matrix. Qcr2 is one of the membrane bound core subunits of the ubiquinol cytochrome *c* reductase complex that is part of the mitochondrial inner membrane electron transport chain (Oudshoorn et al., 1987). The proteins Pda1 and Pdb1 built up the E1 subunit of the pyruvate dehydrogenase (PDH) complex which catalyses the direct oxidative decarboxylation of pyruvate to acetyl-CoA (Miran et al., 1993; Steensma et al., 1990). The physical interaction of Yme1 with Pda1, Pdb1, Gut2 and Cyb2 suggests a function of Yme1 in mitochondrial energy metabolism.

In following experiments the physical interactions of Yme1 with the Mcr1, Mpm1, Gep1, Qcr2, Pda1 and Pdb1 are further analysed and possible functions of these interactions are examined.

3.2.3 Co-immunoprecipitation of Yme1 from strains harbouring HA-tagged versions of Yme1-interacting proteins

In order to confirm the physical interaction of Yme1 with the initially identified Yme1-interacting proteins co-immunoprecipitation experiments were conducted. Conditions for co-immunoprecipitations were essentially the same as the conditions applied for the affinity purification of Yme1, besides the fact that mainly cellular membrane fractions served as starting material. With the immunoprecipitation an enrichment of proteins that bind to a specific antibody is achieved. Depending on the conditions applied, co-purification of interaction partners is possible. Here, co-immunoprecipitations were performed for Yme1 and the HA epitope. Respectively, initially identified interaction partners (Mcr1, Mpm1, Gep1, Qcr2, Pda1 and Pdb1) were tagged with three C-terminal HA epitopes for western blot analysis and/or purification.

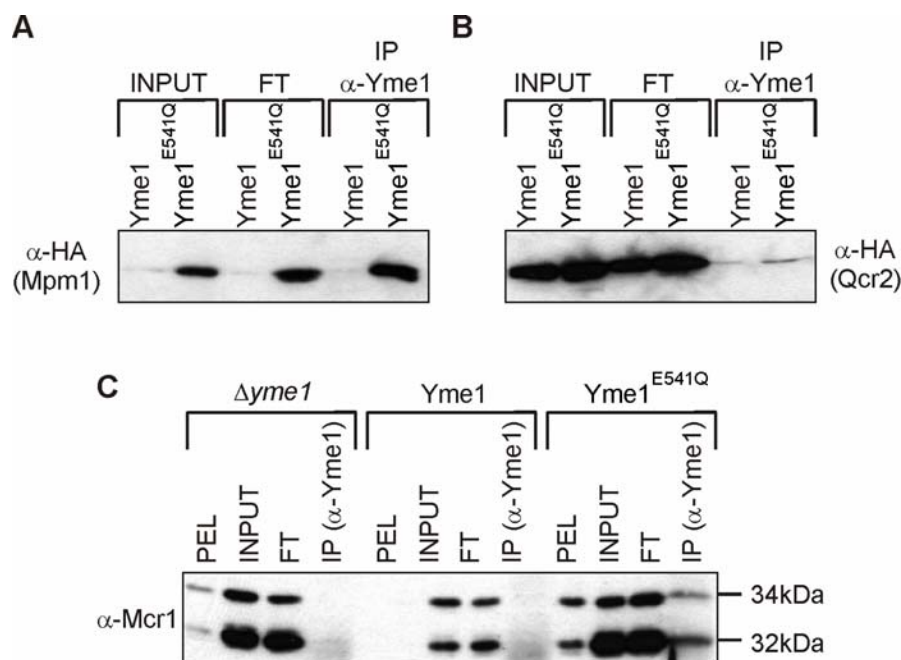


Figure 3.12 Co-immunoprecipitation of Yme1. (A+B) Cellular membranes are isolated from $\Delta yme1$ cells expressing plasmid encoded Yme1 or Yme1^{E541Q} harbouring an HA tagged variant of either Mpm1 (A) or Qcr2 (B), respectively. After solubilisation with 0,5% (w/v) DDM, co-immunoprecipitation was conducted with α -Yme1 coupled to protein A sepharose beads. 1% of input and flow through (FT) and the complete precipitation (Yme1 or Yme1^{E541Q}) sample were subjected to SDS-PAGE and western blot. The presence of Mpm1 and Qcr2 was examined by immunological detection using an α -HA antibody. (C) Mitochondria isolated from $\Delta yme1$ and $\Delta yme1$ cells expressing plasmid encoded Yme1 or Yme1^{E541Q} were solubilised with 0,5% (w/v) DDM prior to co-immunoprecipitation with α -Yme1 coupled to protein A sepharose beads. 1% of the insoluble fraction (PEL), input and flow through (FT) were loaded next to the complete precipitation sample (IP) on SDS-PAGE. The presence of Mcr1 is tested by immunological detection using α -Mcr1 after western blot analysis.

First indications about the nature of interaction between Yme1 and the co-purified interaction partner were achieved by simultaneous co-immunoprecipitation of Yme1 and the proteolytic inactive variant Yme1^{E541Q}. Co-immunoprecipitations of Yme1 from strains harbouring either Mpm1-HA or Qcr2-HA confirmed the interaction of Yme1 with both proteins (Fig. 3.12). The interaction of Yme1 with Qcr2 was weak and represented only \sim 0,2% of the protein. These inefficient co-precipitations could indicate transient or dynamic interactions. For Mpm1, not only a co-precipitation with Yme1 was evident, there was also a clear difference of Mpm1 abundance depending on the presence of either Yme1 or Yme1^{E541Q} in all samples monitored (Fig. 3.12A). Expression of the proteolytic inactive variant Yme1^{E541Q} greatly enhances the steady state level of Mpm1, suggesting that the proteolytic function of Yme1 determines Mpm1 levels. Similarly, an accumulation of both forms of Mcr1 was obvious in mitochondria derived from $\Delta yme1$ and $\Delta yme1$ expressing Yme1^{E541Q} compared to Mcr1 levels in Yme1 expressing cells (Fig. 3.12C). Here, also the co-precipitation of both forms of Mcr1 with Yme1 was restricted to Yme1^{E541Q}, i.e. Mcr1 showed only a stable

interaction with the proteolytic inactive form of Yme1. Increased steady state levels and binding to the proteolytic inactive variant of Yme1 strongly suggest that Mcr1 and Mpm1 are novel substrate proteins of the \hat{A} AAA protease Yme1.

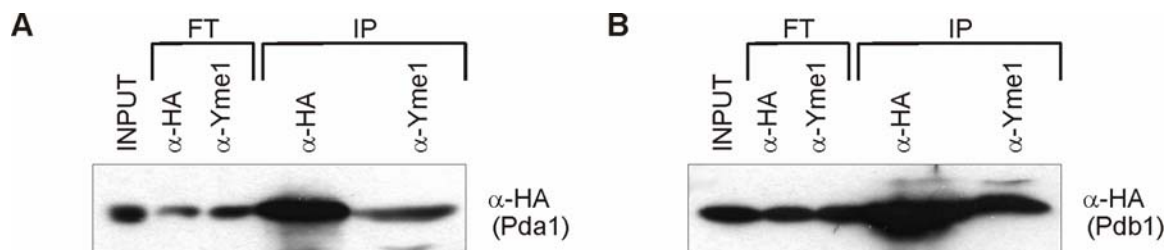


Figure 3.13 Co-immunoprecipitation of Yme1 and Pda1-HA/Pdb1-HA. Cellular membranes were isolated from W303 cells harbouring HA tagged variants of either Pda1 (A) or Pdb1 (B). After solubilisation with 0,5% (w/v) DDM co-immunoprecipitation was achieved with α -Yme1 or α -HA coupled to protein A sepharose beads. 1% of input and flow throughs (FT) and the complete precipitation samples (IP) were subjected to SDS-PAGE and western blot. The presence of Pda1 and Pdb was examined by immunological detection using α -HA.

Both, Pda1 and Pdb1 were co-precipitated with Yme1 (Fig. 3.13). The level of co-precipitation was not influenced by the proteolytic status of Yme1, and no co-precipitation was possible from $\Delta yme1$ cellular membrane extracts (data not shown). Roughly 1% of total Pda1 (Fig. 3.13A) and 2% of total Pdb1 (Fig. 3.13B) (relative to 1% of total input) bound to Yme1. Since only a subfraction of the proteins interacts with Yme1 and the interaction is not influenced by the proteolytic status of the \hat{A} AAA protease, the interaction might reflect a transient or labile structural interplay of Yme1 on Pda1 and Pdb1. An additional higher molecular weight form of Pdb1 can be co-precipitated with Yme1 that might represent the precursor form of Pdb1. As an import function of Yme1 has been proposed (Rainey et al., 2006), Yme1 might contribute to the import of Pdb1 precursor. Finally, the major form of Pdb1 interacting with Yme1 is the mature form. An interaction of Gep1 with Yme1 could not be confirmed by co-immunoprecipitation (data not shown). As a result of the low abundance of Gep1, an interaction with Yme1 might not be detectable by co-immunoprecipitation.

The physical interaction of the initially identified Yme1-interacting proteins could be verified for all candidates but Gep1 by co-precipitation with the \hat{A} AAA protease. However, the amount of protein interacting with Yme1 is low compared to the amount of protein present in the input sample (here only 1% of total). This could be expected as binding of Cox2 and Phb1, known substrates of Yme1, occurs with low affinity (Graef et al., 2007). Thus, Yme1 either interacts only with a subfraction of those proteins or the interaction with Yme1 is transient. It is conceivable further that the interaction of a protein with Yme1 leads to its subsequent degradation.

3.2.4 Correlation of $\Delta yme1$ phenotypes to the phenotypes of Yme1-interacting proteins

To investigate whether a loss of Yme1 function can be correlated to the function of Yme1-interacting proteins, the growth phenotypes of a $\Delta yme1$ strain were compared to phenotypes of deletions of genes encoding for the identified Yme1-interacting proteins.

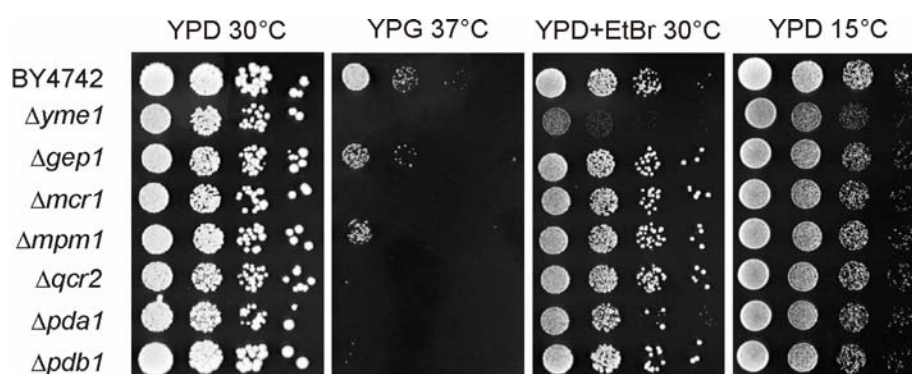


Figure 3.14 Growth phenotypes of deletions of Yme1-interacting proteins. $\Delta gep1$, $\Delta mcr1$, $\Delta mpm1$, $\Delta qcr2$, $\Delta pda1$ and $\Delta pdb1$ cells were grown on YPD medium at 30°C or 15°C, on YPD medium containing EtBr (25 $\mu\text{g/ml}$) and on YPG medium at elevated temperature for two or five days, respectively. The isogenic wild type and $\Delta yme1$ served as controls.

None of the deletion mutants of Yme1-interacting proteins showed retarded growth on YPD medium at 15°C. Similarly, their growth on YPD medium containing EtBr could not be distinguished from wild type (Fig. 3.14). Only for the $\Delta pda1$ strain growth on YPD containing EtBr was mildly reduced, albeit not to the level of $\Delta yme1$. In contrary, a $\Delta pda1$ strain has even been reported to form petite positive colonies implying the tendency to lose mtDNA (Wenzel et al., 1992). Since $\Delta pda1$ shows only a mild phenotype on YPD containing EtBr strain specific differences have to be considered. The growth of most of the tested deletion mutants was effected on a non-fermentable carbon source at elevated temperature (YPG 37°C). Strain harbouring $GEP1$ or $MPM1$ deletions were just slightly affected, whereas $\Delta mcr1$, $\Delta qcr2$, $\Delta pda1$ and $\Delta pdb1$ deletion strains showed no growth. While a mild phenotype of $GEP1$ deletion on YPG at 37°C has already been reported (Osman et al., 2009), no such phenotype is attributed to the $\Delta mpm1$ deletion strain. As Qcr2 is a core component of complex III of the respiratory chain, the loss of growth for the $\Delta qcr2$ deletion strain could be expected on a non-fermentable carbon source and is consistent with published data (di Rago et al., 1997). Growth defects on non-fermentable carbon source at elevated temperature have not been reported for the $\Delta mcr1$, $\Delta pda1$ and $\Delta pdb1$ deletion strains and cannot be reconciled with described functions of these proteins. Mcr1 has not been linked to a function

during respiration. However, since Mcr1 has been identified as a NADH reductase, such a function is conceivable. Pda1 and Pdb1 affect steps in energy production that are rather connected to the presence of oxygen and the absence of respiration, and reactions of pyruvate during fermentation are linked to the pyruvate decarboxylase (Pronk et al., 1996). Nevertheless, analysis of Pda1 expression did not provide evidence for its repression during growth in the presence of ethanol (Wenzel et al., 1993).

The phenotypes of gene deletions of Yme1-interacting proteins differ from the phenotypes displayed by $\Delta yme1$. Hence, the pleiotropic phenotypes of $\Delta yme1$ cannot be attributed to a changed or absent function of one of the identified Yme1-interacting proteins in the absence of Yme1.

3.2.5 Effects of the *i*-AAA protease on Yme1-interacting proteins

Different impacts of the *i*-AAA protease on the interaction between Yme1 and Yme1-interacting proteins were analysed here. Initially, the influence of the presence and absence of Yme1 on the steady state levels of Yme1-interacting proteins was examined. Then, the possible role of Yme1 during import and/or biogenesis of these proteins was addressed. In addition, the Yme1 dependent degradation of the probable substrates Mpm1 and Mcr1 was monitored.

3.2.5.1 Steady state levels of Yme1-interacting proteins in the presence or absence of Yme1

The comparison of the steady state levels of Yme1-interacting proteins in wild type and $\Delta yme1$ cells can indicate whether these proteins are proteolytic substrates or structural interaction partners of the *i*-AAA protease. For example, an increased steady state level in the absence of Yme1 is consistent with a lack of turnover of a substrate protein and can also be observed for other identified substrates (Francis et al., 2007; Pearce and Sherman, 1995). On the other hand, missing structural support in the absence of the *i*-AAA protease can cause destabilisation of the Yme1-interacting protein and can lead to subsequent degradation, resulting in a decreased steady state level. Here, the steady state levels of HA-tagged Yme1-interacting protein variants were analysed in whole cell extracts.

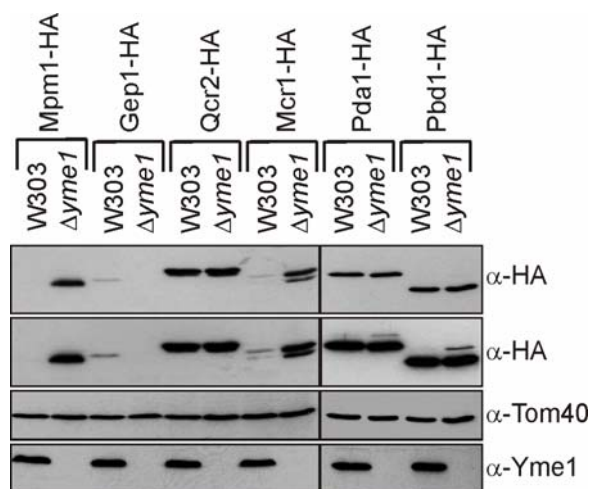


Figure 3.15 Expression levels of Mpm1, Gep1, Qcr2, Mcr1, Pda1 and Pdb1 in wild type and $\Delta yme1$ strains. Gep1, Mcr1, Mpm1, Qcr2, Pda1 and Pdb1 are harbouring a genomic C-terminal HA-tag in W303-wild type and $\Delta yme1$ background. Total protein extracts from 3 OD₆₀₀ units cells grown on YPD were separated by SDS-PAGE. Subsequently western blotting and immunological detection using α -HA, α -Tom40 and α -Yme1 were performed.

The protein level of mature Qcr2, Pda1, and Pdb1 was not changed by the deletion of *YME1* (Fig. 3.15). Interestingly, the precursor of Pda1 and Pdb1 accumulated in a $\Delta yme1$ background. This might point to a role of Yme1 in efficient import or processing of these two matrix proteins, consistent with the reported requirement of Yme1 for protein import into the intermembrane space (Rainey et al., 2006). A negative effect of *YME1* deletion was detected for the steady state level of Gep1-HA (Fig. 3.15). The Gep1 protein which is low abundant in wild type background was not detectable in a $\Delta yme1$ strain, although the genomic insertion of the HA-tag was verified (data not shown). Therefore, the presence of Yme1 is important for the continuance of Gep1 pointing to a structural interaction of both proteins or to a function of Yme1 in the biogenesis of Gep1. Mpm1 and Mcr1 responded to a deletion of *YME1* with increased protein levels (Fig. 3.15). This accumulation and enhanced binding of the proteins to the proteolytic inactive variant of Yme1 support the idea that Mpm1 and Mcr1 are novel substrates of the *i*-AAA protease Yme1.

3.2.5.2 *In organello* import of *in vitro* translated Mcr1, Mpm1, Gep1 and Qcr2 into isolated wild type and $\Delta yme1$ mitochondria

As a function for Yme1 in import has been described (Rainey et al., 2006), the impact of an *YME1* deletion on import and biogenesis of the Yme1-interacting proteins is tested. For this purpose, ³⁵S-radiolabelled precursors of Mcr1, Mpm1, Gep1 and Qcr2 are imported into mitochondria isolated from wild type and $\Delta yme1$ cells, respectively.

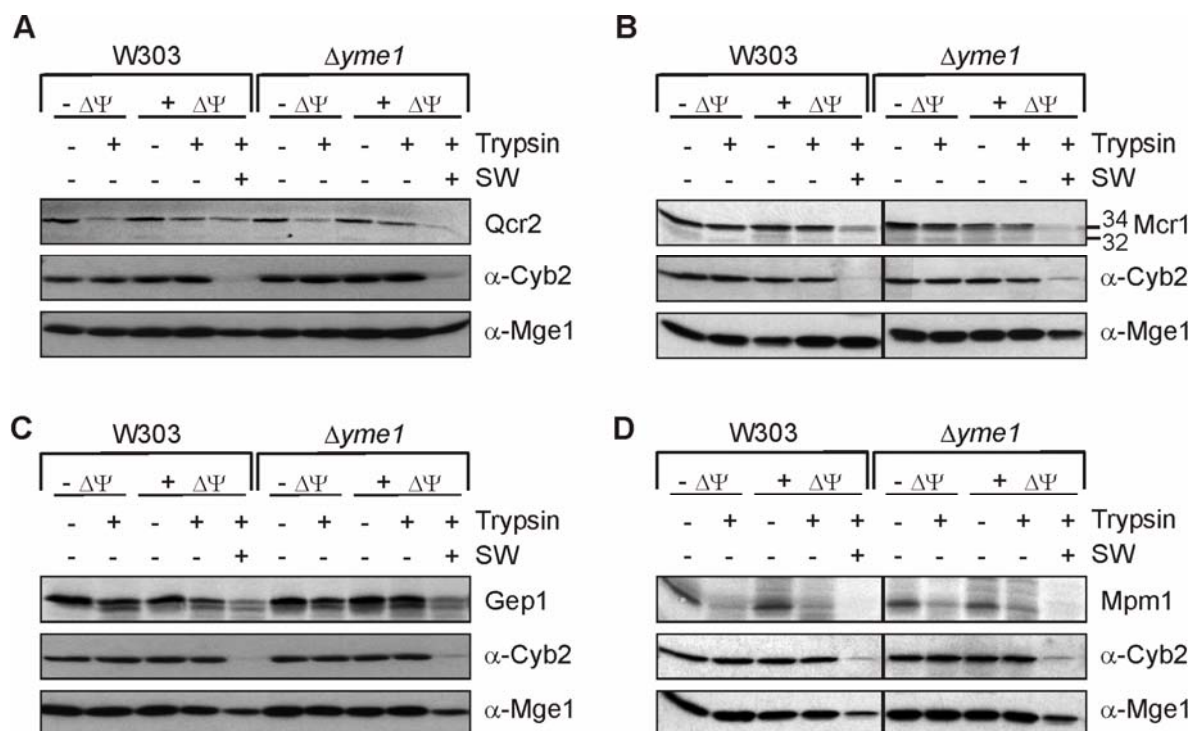


Figure 3.16 *In organello* import of ^{35}S -radiolabelled Mcr1, Mpm1, Gep1 and Qcr2 into mitochondria isolated from wild type and $\Delta yme1$ strains. ^{35}S -radiolabelled precursor proteins of (A) Qcr2, (B) Mcr1 (34 and 32kDa forms), (C) Gep1 and (D) Mpm1 were imported into isolated mitochondria of wild type and $\Delta yme1$. Imports were done in the presence (+ $\Delta\psi$) and absence (- $\Delta\psi$) of membrane potential (valinomycin, 10 $\mu\text{g/ml}$). Non imported proteins were digested by trypsin (20 $\mu\text{g/ml}$) treatment. Localisation of the imported protein was addressed by generation of mitoplasts by osmotic swelling (SW) in combination with trypsin treatment. After import and subsequent treatments isolated mitochondria or mitoplasts were subjected to SDS-PAGE and western blot and analysed by autoradiography. Immunological detection of Cyb2 and Mge1 was performed with α -Cyb2 and α -Mge1 antibodies.

The integrity of the mitochondria was controlled by the marker proteins Cyb2 (intermembrane space) and Mge1 (matrix space). In intact mitochondria Cyb2 and Mge1 are insensitive to trypsin treatment. Disruption of the outer mitochondrial membrane by osmotic shock, however, renders intermembrane space proteins like Cyb2 trypsin sensitive. Since the inner membrane stays intact, the matrix protein Mge1 should not be affected by the combination of osmotic shock and trypsin treatment.

The import of Qcr2 shows the dependence of efficient import on the membrane potential typical for a matrix protein (Fig. 3.16A). Unexpectedly, no lower molecular weight band corresponding to the mature protein is detectable in wild type or $\Delta yme1$ mitochondria. Further, Qcr2 displays a higher sensitivity to trypsin treatment upon osmotic shock in $\Delta yme1$ mitochondria, pointing to a reduced import efficiency or impaired submitochondrial sorting of Qcr2 in $\Delta yme1$ mitochondria. However, a decrease in import of Qcr2 in $\Delta yme1$ is not reflected by a change in the steady state level in the absence of Yme1 (Fig. 3.15).

The import of Mcr1 and its processing to the smaller 32 kDa form of the protein was not affected by the absence of Yme1 (Fig. 3.16B). Gep1 has been identified as an intermembrane space protein (Osman et al., 2009). Here, the import and biogenesis of Gep1 was proven to be not influenced by the absence of Yme1 (Fig. 3.16C). The *in organello* import of Mpm1 was very inefficient in wild type and $\Delta yme1$ mitochondria (Fig. 3.16D). The low level of trypsin resistant Mpm1 is imported independently of $\Delta\psi$ and Yme1, and is localised to either the intermembrane space or inner mitochondrial membrane. Thus, mitochondrial import of ^{35}S -radiolabelled precursor proteins of Mcr1, Mpm1 and Gep1 is approximately equal in mitochondria isolated from W303-wild type or $\Delta yme1$. In case of Qcr2, the import efficiency or submitochondrial sorting is reduced in the absence of Yme1, but not abolished. If Qcr2 import and sorting is requiring a high mitochondrial membrane potential ($\Delta\psi$), the lowered import efficiency of Qcr2 can be explained by the reduced $\Delta\psi$ of $\Delta yme1$ mitochondria (Kominsky et al., 2002; Nakai et al., 1995; Thorsness and Fox, 1993). Therefore, Yme1 is not essential for the import of any of the Yme1-interacting proteins, although this function could have explained, and might still do so for Qcr2, the transient binding of these proteins to the *i*-AAA protease.

3.2.5.3 *i*-AAA protease dependent degradation of Mcr1, Mpm1 and Phb1

Previous experiments showed accumulation of Mcr1 and Mpm1 steady state levels in the absence of Yme1. In addition, the binding of Mcr1 and Mpm1 to the *i*-AAA protease is greatly enhanced by proteolytic inactivation of the protease. Mcr1 and Mpm1 may therefore represent substrates of the *i*-AAA protease. Here, the Yme1 dependent degradation of Mcr1 and Mpm1 is monitored.

Within the *in organello* import chase experiments, the simultaneous import and chase of the known Yme1 substrate Phb1 was used as an internal control (Graef et al., 2007). Indeed, Phb1 is degraded in wild type (W303) mitochondria whereas it is stabilised in $\Delta yme1$ mitochondria (Fig. 3.17A). Conversely, no degradation of Mcr1 (either forms: 32 and 34 kDa) and Mpm1 can be detected after import and chase in wild type mitochondria. Since the difference in degradation within wild type compared to $\Delta yme1$ provides the evidence for Yme1 to be the protease in charge, and no such difference can be seen due to the lack of degradation in wild type, no conclusion on the relation of Yme1 to Mgr1 and Mpm1 is possible.

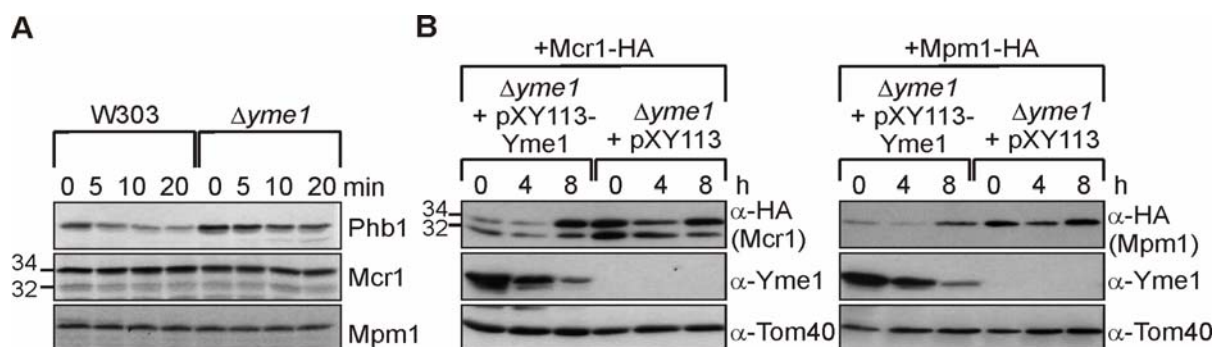


Figure 3.17 Analysis of a Yme1-dependent degradation of Mcr1, Mpm1 and Phb1.

(A) ^{35}S -radiolabelled precursor proteins of Phb1, Mcr1 and Mpm1 were imported into mitochondria isolated from wild type and $\Delta yme1$ cells. Imports were performed in the presence of membrane potential and non imported proteins were digested by trypsin (50 $\mu\text{g}/\text{ml}$) treatment. After incubation of the samples for 0, 5, 10 and 20 min at 37°C isolated mitochondria were subjected to SDS-PAGE and western blot. Signals of ^{35}S -radiolabelled proteins were obtained by autoradiography. **(B)** $\Delta yme1$ cells harbouring HA-tagged Mcr1 or Mpm1 and plasmid-derived expression of Yme1 under a GAL-promoter were grown on SD-Gal over night. Then cultures were shifted to YDP and 10 OD_{600} units cells were taken after 0, 4 and 8 h. Prepared cellular membranes were separated on SDS-PAGE and analysed after western blot by immunological detection using α -HA, α -Yme1 and α -Tom40 antibodies.

Therefore, as an additional attempt the *in vivo* downregulation of Yme1 was used, where the galactose inducible expression of Yme1 (pYX113-Yme1) can be shut off by a switch to glucose. An advantage of this method is the possible analysis of long-termed adaptations that are not encountered by the *in vitro* assay. As depletion of pre-existing Yme1 proteins has to be considered different time points after shift from galactose to glucose were analysed. $\Delta yme1$ cells harbouring a genomically HA-tagged Mcr1 or Mpm1, respectively, containing either pYX113-Yme1 or pYX113, were grown over night in selective medium containing galactose (1% (w/v)). Then cells were shifted to rich medium containing glucose (2% (w/v)); samples were taken at 0, 4 and 8 h after carbon source shift. A gradual depletion of Yme1 occurs during the time course of the experiment (Fig. 3.17B). Interestingly, the depletion of Yme1 correlated with a significant accumulation of Mcr1 and Mpm1 (Fig. 3.17B). Furthermore, a somewhat different response of the two different isoforms of Mcr1 (short - 32 kDa and long - 34 kDa form) to downregulation of Yme1 was noticed. Although a compensatory upregulation of these proteins in the absence of Yme1 cannot be excluded, increased steady state levels and, more importantly, increased binding to the proteolytic inactive variant of Yme1 suggest a Yme1 function for the degradation of Mcr1 and Mpm1.

3.2.5.4 *In organello* import of *in vitro* translated Pda1 and Pdb1 into isolated wild type and $\Delta yme1$ mitochondria

In $\Delta yme1$ cells expressing Pda1-HA or Pdb1-HA, respectively, a slight accumulation of the precursor forms of the two proteins is visible. Since a role of Yme1 in import has been proposed (Rainey et al., 2006), the import of these two proteins is analysed in the absence of Yme1. To detect also the minor alterations of import in the absence of Yme1, different steps within the process of import of Pda1 and Pdb1 were monitored.

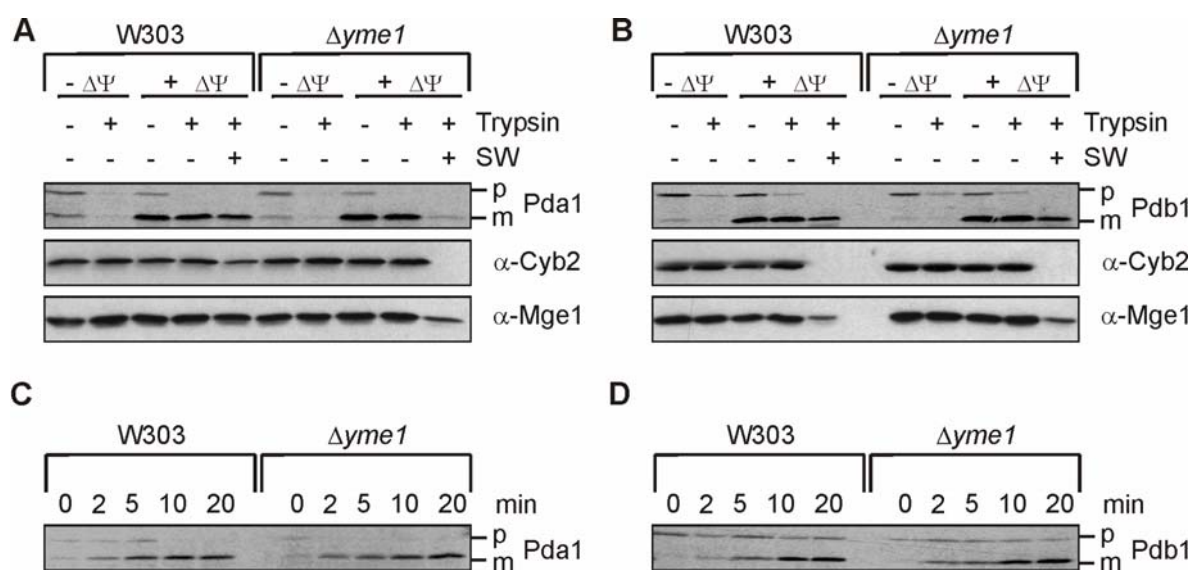


Figure 3.18 *In organello* import of ^{35}S -radiolabelled Pda1 and Pdb1 into mitochondria derived from wild type and $\Delta yme1$ strains. **(A+B)** ^{35}S -radiolabelled precursor proteins of Pda1 and Pdb1 were imported into mitochondria isolated from wild type and $\Delta yme1$ cells. Imports were performed in the presence (+ $\Delta\psi$) and absence (- $\Delta\psi$) of membrane potential (valinomycin, 10 $\mu\text{g/ml}$). Non imported proteins were digested with trypsin (20 $\mu\text{g/ml}$). Localisation of the imported protein was addressed by generation of mitoplasts via osmotic swelling (SW) in combination with trypsin treatment. After import and subsequent treatments isolated mitochondria were subjected to SDS-PAGE and western blot. Signals of ^{35}S -radiolabelled proteins were obtained by autoradiography. Immunological detection of Cyb2 and Mge1 was performed using $\alpha\text{-Cyb2}$ and $\alpha\text{-Mge1}$. **(C+D)** Import of ^{35}S -radiolabelled precursor proteins of Pda1 and Pdb1 was stopped by depletion of $\Delta\psi$ (valinomycin) after 0, 2, 5, 10 and 20 min of import. Non imported proteins were digested by trypsin (20 $\mu\text{g/ml}$) treatment. Samples are subjected to SDS-PAGE and western-blot. Signals of ^{35}S -radiolabelled proteins were obtained by autoradiography. Immunological detection was performed with $\alpha\text{-Cyb2}$ and $\alpha\text{-Mge1}$ antibodies. p indicates precursor, m the mature form of the protein.

Import of Pda1 and Pdb1 in mitochondria isolated from wild type and $\Delta yme1$ cells revealed no difference for the import or maturation of Pda1 and Pdb1 (Fig. 3.18A+B). According to the accumulation of the precursor under steady state levels in the absence of Yme1, an effect of Yme1 on the import of both proteins would have been expected, keeping in mind that the maturation is not abolished in the absence of Yme1 but possibly only reduced or

slowed down. This aspect is addressed by analysis of different import steps (Fig. 3.18C+D). Also in this analysis no apparent effect of the absence of Yme1 on the import of Pda1 and Pdb1 is detected. Hence, the accumulation of Pda1 and Pdb1 precursor forms under steady state levels in the absence of Yme1 has a different origin. The precursor of Pdb1 shows an intermembrane space localisation, as it is depleted in mitoplast samples; therefore Yme1 could possibly act on non imported Pdb1 fulfilling a clearance function in import. As Yme1 apparently interacts with the mature form of Pda1 and Pdb1, additional functions of Yme1 affecting the mature forms of Pda1 and Pdb1 have to exist.

3.2.6 Variations in expression of Yme1-interacting proteins and their influence on $\Delta yme1$

Changes in protein level of the Yme1-interacting proteins may influence the function of Yme1. For example, overexpression of proteins that show an increased steady state level upon depletion of Yme1 might also confer an increased fitness to a wild type strain, as expression of the proteins has an overall beneficial effect for the cell. Conversely, the overexpression could also be toxic, as a feedback mechanism that is induced upon depletion of Yme1 is not active in the presence of the protein. Therefore, it could be valuable to compare the consequences of alterations in the amount of Yme1-interacting proteins in wild type and $\Delta yme1$ cells. This is of particular interest for those Yme1-interacting proteins whose steady state level is changed upon depletion of Yme1.

3.2.6.1 Effects of Gep1 overexpression in wild type and $\Delta yme1$ cells

In the absence of Yme1 the steady state level of Gep1 is strongly reduced (Chapter 3.2.5.1). It is therefore conceivable that Gep1 interacts with Yme1 and is degraded in the absence of Yme1. Furthermore, overexpression of Gep1 is found to be toxic in wild type cells (Osman et al., 2009), indicating that tight regulation of Gep1 levels has to occur in the cell and a role of Yme1 in this process is conceivable. Therefore, the possible increased toxicity of overexpressed Gep1 in the absence of Yme1 was analysed.

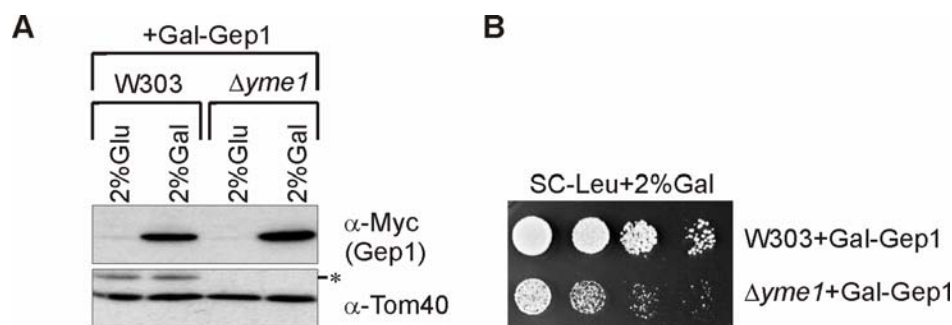


Figure 3.19 Overexpression of Gep1 in wild type and $\Delta yme1$ cells. (A) Wild type and $\Delta yme1$ cells harbouring YEplac181-GAL-Gep1-myc were grown in rich medium containing either 2% (w/v) galactose or glucose for 4 h. Cellular membranes were prepared and immunological detection of Gep1 was performed using α -Myc after SDS-PAGE and western blot. Equal loading was addressed using α -Tom40 and α -Yme1 antibodies (*- signal refers to a degradation band of Yme1). (B) Wild type and $\Delta yme1$ cells harbouring YEplac181-GAL-Gep1-myc were grown on synthetic medium lacking leucine and containing galactose (2% (w/v)) for 3 days. Under similar conditions growth of wild type and $\Delta yme1$ cells without overexpression of Gep1 was comparable (date not shown).

Generally, an overexpression of Gep1-myc can be induced by growth on medium containing galactose as a carbon source. Possible differences due to unequal loading are addressed by immunological detection of Tom40 and Yme1 (Fig. 3.19A). Overexpression of Gep1 has a toxic effect on wild type cells (Osman et al., 2009) that was much more pronounced in $\Delta yme1$ cells (Fig. 3.19.B). This increased toxicity of Gep1 in the absence of Yme1 is consistent with the reduced steady state levels of Gep1 under the same conditions, if higher amounts of Gep1 would possibly be toxic in a $\Delta yme1$ background. Whether alterations of Gep1 in the absence of Yme1 refer to a lack of regulation of Gep1 by the *i*-AAA protease or if they solely reflect a destabilisation in the absence of a structural interaction partner remains elusive. Nevertheless, the strong effect of Gep1 overexpression in $\Delta yme1$ cells underlines the functional link between the two proteins.

3.2.6.2 Overexpression of Mcr1 in wild type and $\Delta yme1$

Accumulation of Mcr1 in $\Delta yme1$ may result from the lack of degradation by Yme1 or maybe is required to mask some of the defect caused by deletion of *YME1*. Alternatively, higher Mcr1 levels could also be responsible for some of the $\Delta yme1$ phenotypes. Therefore, the effect of overexpression of Mcr1 on the growth of wild type and $\Delta yme1$ cells (Thorsness and Fox, 1993; Thorsness et al., 1993; Weber et al., 1995) was examined.

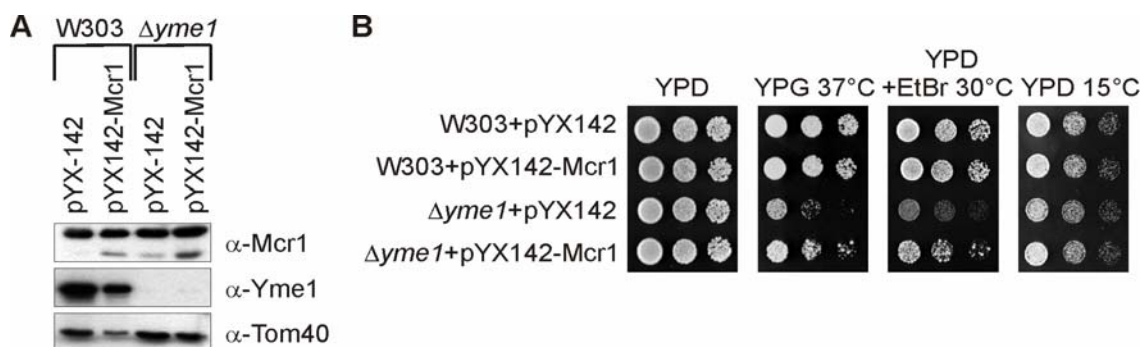


Figure 3.20 Overexpression of Mcr1 in wild type and $\Delta yme1$ cells. (A) Wild type and $\Delta yme1$ cells harbouring pYX142 or pYX142-Mcr1 were grown over night in rich medium containing 2% (w/v) glucose. Cellular membranes were prepared and immunological detection of Mcr1 was performed using α -Mcr1 after SDS-PAGE and western blot. Equal loading was assessed using α -Tom40 and α -Yme1 antibodies. (B) Wild type and $\Delta yme1$ cells harbouring pYX142 or pYX142-Mcr1 were grown on YPD at 15°C and 30°C, on YPD medium containing EtBr (25 μ g/ml) and on YPG medium at 37°C for three or five days.

To exclude an influence of the conferred leucine autotrophy, wild type and $\Delta yme1$ cells harbouring pXY142 are included in the analysis. Overexpression of Mcr1 compared to the endogenous protein level (pXY142) was modest in cellular membrane extracts of wild type and $\Delta yme1$. The induction of Mcr1 is more prominent in wild type than in $\Delta yme1$ cells (Fig. 3.20A). On the *in vivo* level no apparent effect of Mcr1 overexpression on growth of wild type cells was observed (Fig. 3.20B). Therefore, elevated Mcr1 protein levels in $\Delta yme1$ cells are not responsible for the phenotypes associated with the loss of *YME1*. Surprisingly, a beneficial effect of Mcr1 overexpression on $\Delta yme1$ growth is evident, although the overall protein amount of Mcr1 is not drastically changed by the modest overexpression of Mcr1. This partial restoration of $\Delta yme1$ growth by overexpression of Mcr1 points to a backup function of Mcr1 for some of the defects caused by the deletion of the *f*-AAA protease.

3.2.7 Effects of $\Delta yme1$ on cellular ergosterol levels

A possible role of Yme1 in cellular ergosterol distribution is suggested through the interaction of Yme1 with Mcr1 which is involved in ergosterol biosynthesis (Lamb et al., 1999) and by the abolished uptake of sterol in $\Delta yme1$ mutants grown under anaerobic conditions (Reiner et al., 2006). In general, ergosterol is most prominent in the plasma membrane (Zinser et al., 1991) and in yeast only some steps of the ergosterol biosynthesis are linked to mitochondria (Daum et al., 1998; Parks and Casey, 1995). Different aspects of the ergosterol biosynthesis and distribution are addressed by various methods. First, the effect of nystatin on growth is monitored. Nystatin is an antifungal drug that is binding to ergosterol within the plasma membrane and thereby leads to a disruption of the membrane and subsequent cell

death (Woods, 1971). Second, ergosterol levels in lipid samples from whole wild type and $\Delta yme1$ cells are compared to lipid levels in intracellular membrane fractions.

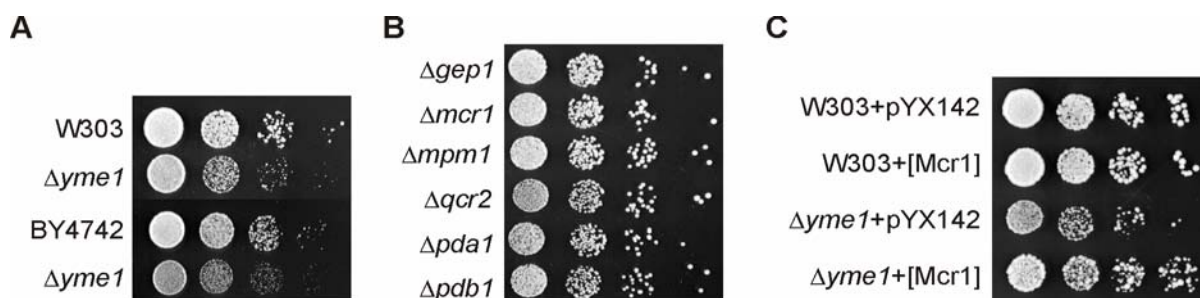


Figure 3.21 Growth phenotypes on YDP medium containing nystatin. (A) Wild type growth (W303 or BY4742) was compared to growth of $\Delta yme1$ cells on YPD containing 50 U/ml nystatin after three days of incubation. **(B)** Growth of Yme1-interactor deletion strains on YPD containing nystatin. $\Delta gep1$, $\Delta mcr1$, $\Delta mpm1$, $\Delta qcr2$, $\Delta pda1$ and $\Delta pdb1$ cells were grown on YPD medium containing nystatin (50 U/ml) for three days. **(C)** Effect of Mcr1 overexpression [Mcr1] on the nystatin phenotype of $\Delta yme1$. W303 and $\Delta yme1$ cells harbouring pYX142 or pYX142-Mcr1 were grown on YPD containing nystatin (50 U/ml) for three days.

When compared to wild type cells (W303 or BY47432) the growth of $\Delta yme1$ cells is reduced on full medium containing nystatin (50 U/ml) in both backgrounds tested (Fig. 3.21). This suggests that the amount of ergosterol within the plasma membrane of $\Delta yme1$ cells is increased. This is unexpected as Yme1 is a mitochondrial protein and yeast mitochondria are not directly involved in ergosterol distribution (Czabany et al., 2007; Sullivan et al., 2006) and biogenesis of ergosterol is predominantly taking place in the ER (Parks and Casey, 1995). Nevertheless, ergosterol is present in the inner mitochondrial membrane (Voelker, 2004; Zinser and Daum, 1995). As the influence of Yme1 on the Yme1-interacting proteins or *vice versa* is analysed here, growth defects of Yme1-interacting protein deletion strains in the presence of nystatin were assessed. However, none of the tested deletion strains of Yme1-interacting proteins ($\Delta gep1$, $\Delta mcr1$, $\Delta mpm1$, $\Delta qcr2$, $\Delta pda1$ and $\Delta pdb1$) showed reduced growth in the presence of nystatin. Similarly, overexpression of Mcr1 partially restored the growth defect observed for $\Delta yme1$ cells in the presence of nystatin, pointing to a general effect by which Mcr1 obviates the growth defects of $\Delta yme1$ cells.

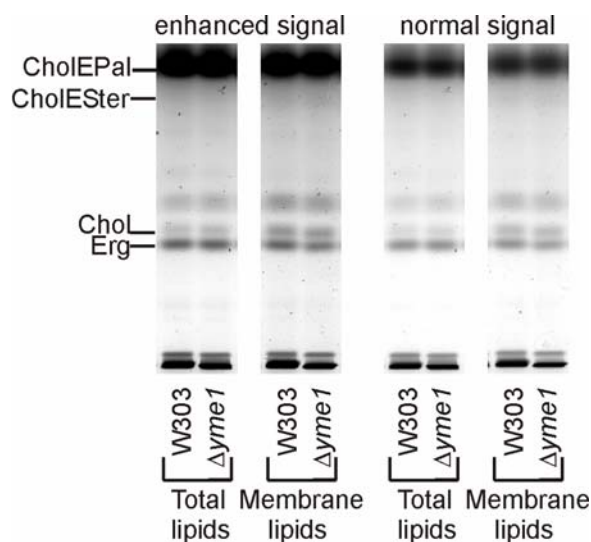


Figure 3.22 Ergosterol levels in total lipids and membrane lipid samples of wild type and $\Delta yme1$ cells. Lipids were isolated from total cell samples and intracellular membrane samples originating from the same culture of wild type and $\Delta yme1$ cells. After determination of phospholipid levels of the samples 5 nmol lipids were dissolved by thin layer chromatography (solvent phase: hexane:ethylacetate (3:1)). Standards for determination of the single bands dissolved were ergosterol (Erg), cholesterol (Chol), cholesterylsterate (CholESTer) and cholesterylpalmitate (CholEPal).

When ergosterol levels of total lipid and membrane lipid samples isolated from wild type and $\Delta yme1$ cells were compared, no obvious difference was visible. Therefore, no conclusion about unequal ergosterol levels in different cellular fractions/subfractions of wild type and $\Delta yme1$ cells is possible by the thin layer chromatography approach utilised here.

3.3 Analysis of genetic interactions of the *i*-AAA protease Yme1

The absence of the conserved *i*-AAA protease Yme1 is associated with a number of phenotypes in yeast. However, the molecular mechanism underlying these pleiotropic phenotypes is far from being understood. In order to identify processes that become essential in the absence of Yme1, a systematic genetic array (SGA) (Tong et al., 2001) was utilised. A deletion of *YME1* is combined with a collection of individual non essential gene deletions associated with mitochondrial function (see attachment). The resulting double deletion strains that fail to grow reflect a synthetic lethal genetic interaction of *YME1* and the respective deleted gene. Hence, according proteins of both genes are involved in related processes. Genetic interactors were listed and assigned to distinct functional classes. Furthermore, high copy suppressors of some synthetic lethal growth phenotypes were determined by application of a high copy suppressor screening to define new functions of the *i*-AAA protease.

3.3.1 Analysis of genetic interactions of $\Delta yme1$ with a deletion library of assorted mitochondrial proteins

The systematic genetic array (SGA) (Tong et al., 2001) was performed to gain new insights into processes that become essential in the absence of Yme1. The genetic interaction of an *YME1* deletion was tested only for an assorted deletion library of non essential mitochondrial proteins that exhibit a general importance within the organelle or could have overlapping functions with the *i*-AAA protease. Altogether 96 gene deletions were tested for a loss of viability upon deletion of *YME1* (see attachment). Within this library gene deletions of the two *m*-AAA protease subunits Yta10 and Yta12 as well as deletion of their regulatory complex partners Phb1 and Phb2 (Steglich et al., 1999) represent established synthetic lethal interactions of the *i*-AAA protease (Lemaire et al., 2000; Leonhard et al., 2000; Osman et al., 2009) and serve as internal controls for assays (Tab. 3.1). 34 synthetic lethal interaction of *YME1* were initially determined. Of these interactions only the synthetic lethal interactions of a *TAZ1* deletion with an *YME1* deletion was not verified by tetrad analysis. The designated synthetic lethality of the *YME1* deletion together with deletion of *MDM10*, *MDM31*, *PSD1* and *CRD1* displayed a milder phenotype in the tetrad analysis and were therefore considered as synthetic sick. The remaining 29 initially identified synthetic lethal interactions were verified by tetrad dissection (Tab. 3.1).

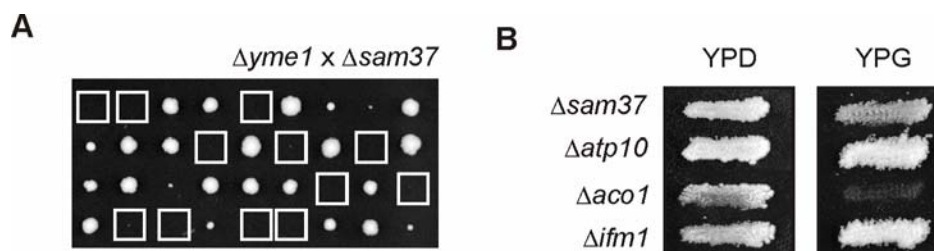


Figure 3.23 Verification of the synthetic lethal interaction of *YME1* and *SAM37*. Verification of the synthetic lethality of $\Delta yme1$ with Δxy exemplified by $\Delta yme1 \Delta sam37$. **(A)** Tetrad dissection of $\Delta yme1 \Delta sam37$ grown on YPD for five days. Distribution of wild type and deletion alleles was attributed by subsequent growth analysis on YPD containing either G418 (250 $\mu\text{g}/\text{ml}$) or NAT (100 $\mu\text{g}/\text{ml}$) for three days. **(B)** Single deletions of the assorted library of non essential mitochondrial proteins were grown on YPD or YPG for three or five days, respectively.

In general, growth of a $\Delta yme1$ strain depends on the presence of mtDNA (Thorsness and Fox, 1993). Therefore, one possible explanation for the synthetic lethality of the combined deletion of *YME1* and a gene *XY* may originate from a loss of mtDNA induced by the *XY* deletion. The potentially induced loss of mtDNA in the absence of a gene, that otherwise proved synthetic lethal interaction with *YME1*, was examined by the ability of the respective single mutants to grow on non-fermentable carbon source. This is based on the fact that components of the respiratory chain are encoded by the mtDNA. Hence, growth a on non-fermentable carbon source requires the presence of mtDNA, and lack of mtDNA should result in an inability to grow on a non-fermentable carbon source. Of the 34 initially identified interacting library mutants 13 respective single mutants did not grow on non-fermentable carbon source pointing to the loss of mtDNA (Tab. 3.1) that would explain the synthetic lethality in the absence of *YME1*. However, additional effects contributing to the synthetic lethal interaction of *Yme1* and those deletions that show a depletion of mtDNA cannot be completely/entirely excluded. Thus, of originally 34 identified synthetic lethal interactors of *Yme1*, 18 synthetic lethal interactions remained indefinable at this point.

Finally, all synthetic lethal interactions are grouped into five functional classes, based on known protein functions of the corresponding interacting gene: Mitochondrial morphology, peptidases/processing, lipids, unknown and diverse (Tab. 3.1).

	Gene	ORF	SL	Loc.	YPG	
Mitochondrial morphology	<i>MMM1</i>	<i>YLL006w</i>		IM/OM		
	<i>MDM10</i>	<i>YAL010c</i>		OM		
	<i>MDM31</i>	<i>YHR194w</i>		IM		
	<i>MDM32</i>	<i>YOR147w</i>		IM		
	<i>MDM38</i>	<i>YOL027c</i>		IM		
	<i>FZO1</i>	<i>YBR179c</i>		OM		
	<i>MGM1</i>	<i>YOR211c</i>		IM		
Peptidases/Processing	<i>ATP23</i>	<i>YNR020c</i>		IMS		
	<i>PCP1</i>	<i>YGR101w</i>		IMS		
	<i>PIM1</i>	<i>YBL022c</i>		M		
	<i>OMA1</i>	<i>YKR087c</i>		IM		
	<i>OCT1</i>	<i>YKL134c</i>		M		
	<i>IMP1</i>	<i>YMR150c</i>		IM		
	<i>YTA10*</i>	<i>YER017c</i>		IM		
	<i>YTA12*</i>	<i>YMR089c</i>		IM		
	<i>PHB1*</i>	<i>YGR132c</i>		IM		
	<i>PHB2*</i>	<i>YGR231c</i>		IM		
	Lipids	<i>PSD1</i>	<i>YNL169c</i>		IM	
		<i>CRD1</i>	<i>YDL142c</i>		IM	
<i>UPS1</i>		<i>YLR193c</i>		IMS		
<i>GEP4</i>		<i>YHR100c</i>		-		
Unknown		<i>GEP8</i>	<i>YER093c-a</i>		-	
		<i>YLR091w</i>	<i>YLR091w</i>		-	
		<i>YKR016w</i>	<i>YKR016w</i>		-	
Diverse		<i>GEP3</i>	<i>YOR205c</i>		M	
		<i>QRI5</i>	<i>YLR204w</i>		IM	
		<i>HMI1</i>	<i>YOL095c</i>		IM/M	
	<i>SAM37</i>	<i>YMR060c</i>		OM		
	<i>ATP10</i>	<i>YLR393w</i>		IM		
	<i>ACO1</i>	<i>YLR304c</i>		M		
	<i>IFM1</i>	<i>YOL023w</i>		M		
	<i>COX11</i>	<i>YPL132w</i>		IM		

Table 3.1 Synthetic lethal interaction with the *i*-AAA protease. Evaluation of synthetic lethal interactions found by SGA. Double deletions are verified by tetrad dissection: **SL**-synthetic lethality (dark - synthetic lethal, medium - synthetic sick). Intramitochondrial localisation: **Loc.** (OM - outer membrane, IMS - intermembrane space, IM - inner membrane, M - Matrix, "-" - unknown). Growth of single mutant on YPG: **YPG** (dark – growth, light - no growth). * known synthetic lethal interactions of the *i*-AAA protease (Lemaire et al., 2000; Leonhard et al., 2000; Osman et al., 2009).

Two major groups of genes known to affect mitochondrial morphology or to harbour peptidase activity show synthetic lethality with $\Delta yme1$. For the first group *MMM1*, *MDM10*, *MDM12*, *MDM31*, *MDM32* and *MDM38* show genetic interaction with *YME1* and are, except for *MDM38*, shown to genetically interact with each other (Dimmer et al., 2005). The other major class of synthetic lethal interactions of *YME1* consists of proteins that have either by themselves peptidase function or are involved in the regulation of peptidase function (Koppen and Langer, 2007; Steglich et al., 1999). Substrate overlapping functions are likely to be responsible for some of the synthetic lethal interactions in this group (Lemaire et al., 2000; Leonhard et al., 2000), since *Yme1* is also a peptidase. Further, lipid related genes are

synthetic lethal or sick with *YME1*. In addition, three undescribed genes and some genes involved in diverse processes are found to be synthetic lethal with *YME1*. Of all assigned groups some genes are already implicated to be synthetic lethality with prohibitins, described synthetic lethal interactors of *YME1* (Tab. 3.1; e.g. *HMI1*) (Steglich et al., 1999). The genetic interactions of prohibitins have in turn been correlated with alterations in mitochondrial phospholipids levels (Osman et al., 2009). Hence, these synthetic lethal interactions point to a role of Yme1 in lipid metabolism. This is underlined by the just recently identified deregulated phospholipid levels in $\Delta yme1$ cells (Nebauer et al., 2007).

To gain further insights into new processes that involve the function of the *f*-AAA protease, selected candidates showing synthetic lethal intereraction with Yme1 were analysed in more detail.

3.3.1.1 Phenotypic analysis of $\Delta yme1$ synthetic lethal interactors

Another way to correlate the function of two genes is a comparison of single deletion phenotypes, as deletion of genes involved in similar or overlapping processes are likely to exhibit same phenotypes. Therefore, phenotypes associated with the loss of *YME1* (Thorsness and Fox, 1993; Thorsness et al., 1993; Weber et al., 1995) (see Chapter 3.2.7) were analysed for single deletion strains of selected candidates that show synthetic lethal interaction with the *f*-AAA protease. Here the single deletions $\Delta cox11$, $\Delta imp1$, $\Delta mdm38$, $\Delta ups1$ and $\Delta gep8$ were monitored and compared to $\Delta yme1$ phenotypes.

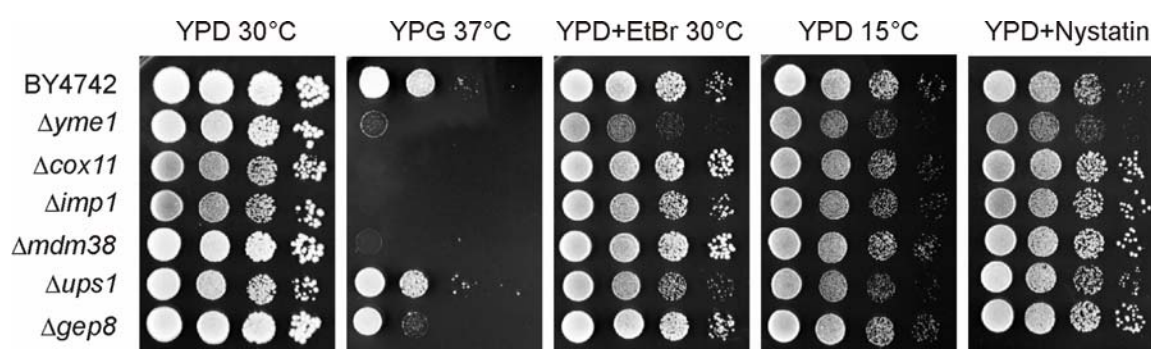


Figure 3.24 Correlation of $\Delta yme1$ growth phenotypes with phenotypes of $\Delta cox11$, $\Delta imp1$, $\Delta mdm38$, $\Delta ups1$ and $\Delta gep8$. $\Delta cox11$, $\Delta imp1$, $\Delta mdm38$, $\Delta ups1$ and $\Delta gep8$ cells were grown on YPD 30°C or 15°C, on YPG at 37°C, on YPD containing EtBr (25 μ g/ml) or nystatin (50 U/ml) for two to five days respectively. Wild type and $\Delta yme1$ served as controls.

Except for a retarded growth on non-fermentable carbon source at elevated temperature, $\Delta gep8$ and $\Delta mdm38$ cells do not resemble any of the $\Delta yme1$ phenotypes (Fig. 3.24). For $\Delta ups1$ some slight effect can be seen on the growth on YPD medium containing either EtBr or nystatin and at decreased temperature. As a growth phenotype of $\Delta ups1$ on YPD at 30°C

is known (Sesaki et al., 2006), a correlation of this phenotype with the reduced growth under the related conditions tested cannot be excluded, especially as $\Delta ups1$ shows no reduction of growth on non-fermentable carbon source at elevated temperature. For $\Delta imp1$ and $\Delta cox11$ only a lack of growth on the non-fermentable carbon source at elevated temperature is apparent. Since both proteins are involved in the complex assembly of the respiratory chain such a phenotype is expected and will not correlate with the effect of an *YME1* deletion. Therefore, none of the single deletions ($\Delta cox11$, $\Delta imp1$, $\Delta mdm38$, $\Delta ups1$ and $\Delta gep8$) resemble the phenotypes associated with $\Delta yme1$. This, however, does not completely exclude a function of both genetic interactors in a similar pathway.

3.3.2 High copy suppressor screening for synthetic lethal interactors of Yme1

High copy suppressors were applied for some of the synthetic lethal interactions, namely double deletions of *YME1* together with *COX11*, *IMP1*, *MDM38*, *UPS1* and *GEP8*. The mitochondrially localised proteins encoded by these genes are related to different functions within the organelle. Cox11 is, together with Cox17, required for copper delivery to Cox1 (Hiser et al., 2000). Imp1 is already introduced as one of the subunits of the IMP complex responsible for protein processing within the inter membrane space (Jan et al., 2000). The functions reported for Mdm38 are somewhat controversial. Its first characterisation links Mdm38 to mitochondrial morphology defects (Dimmer et al., 2002); additionally roles in K^+/H^+ exchange within mitochondrial membrane vesicles (Froschauer et al., 2005) and in export of the mitochondrial protein (Frazier et al., 2006) are described. Ups1 is required for processing and sorting of Mgm1 (Sesaki et al., 2006) and its deletion has just lately been related to aberrant cardiolipin (CL) levels (Osman et al., 2009). For the just recently entitled protein Gep8 no distinct function has been assigned so far (Osman et al., 2009).

Since combination of $\Delta yme1$ with any mutation leading to the loss of mtDNA results in synthetic lethality corresponding single deletions ($\Delta cox11$, $\Delta imp1$, $\Delta mdm38$, $\Delta ups1$ and $\Delta gep8$) of the six double deletions analysed by high copy suppressor screening are examined for the presence of mtDNA by growth on non-fermentable carbon source. However, none of the single mutants show loss of mtDNA (Tab. 3.1) as those mutants unable to grow on non-fermentable carbon source ($\Delta cox11$ and $\Delta imp1$) show a role in complex assembly of the respiratory chain.

Because all haploid double deletions by themselves are lethal (Fig. 3.25), viable strains expressing Yme1 from pVT100U-Yme1 are created by tetrad dissection.

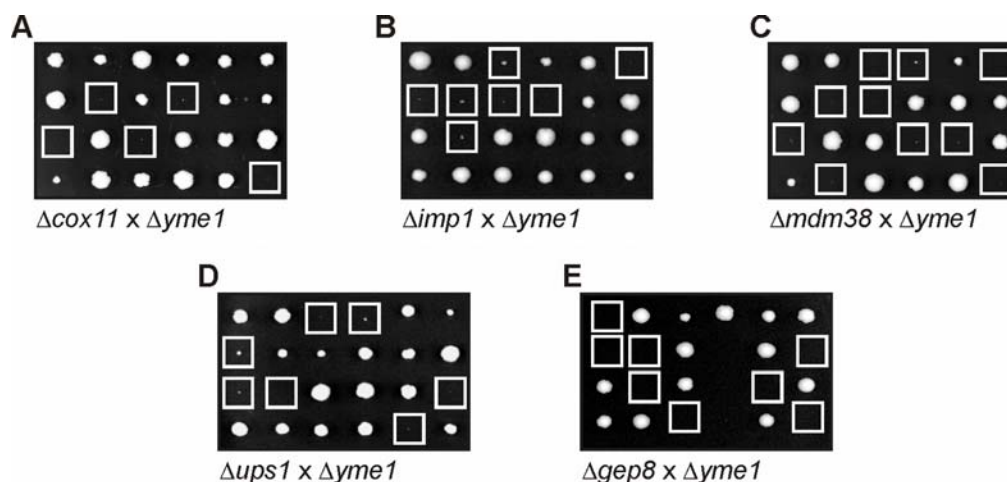


Figure 3.25 Verification of the synthetic lethality of $\Delta yme1\Delta cox11$, $\Delta yme1\Delta imp1$, $\Delta yme1\Delta mdm38$, $\Delta yme1\Delta ups1$ and $\Delta yme1\Delta gep8$. Tetrads of diploid double deletions of (A) $\Delta yme1\Delta cox11$, (B) $\Delta yme1\Delta imp1$, (C) $\Delta yme1\Delta mdm38$, (D) $\Delta yme1\Delta ups1$ and (E) $\Delta yme1\Delta gep8$ were dissected and synthetic lethality was verified for the haploid double deletions (squares). Respective haploid double deletion strains harbouring pVT100U-Yme1 were created by the same procedure.

All haploid double deletion strains harbouring the pVT100U-Yme1, were transformed with a yeast genomic library cloned into Yep13 (Daignan-Fornier et al., 1994). Subsequent selection on medium lacking leucine was followed by growth on medium without leucine and additionally containing 5'FOA (1 mg/mg) for counter selection of the pVT100U-Yme1. Growth of remaining colonies could then be attributed to the suppression of genomic fragments within the Yep13 plasmid as both the presence of the uracil resistance of pVT100U-Yme1 and the haploid double deletion alone lead to a lethal phenotype. Through further analysis of the genomic fragment from Yep13 library plasmids suppressing the lethality of the haploid double deletions, the gene responsible for the suppression was identified. Finally, single genes were cloned and the suppressive effects of the single gene expressed under its endogenous promoter were tested. Comparison of the known functions of the three genetically interconnected genes might then explain the synthetic lethality of the haploid double deletion strains $\Delta yme1\Delta cox11$, $\Delta yme1\Delta imp1$, $\Delta yme1\Delta mdm38$, $\Delta yme1\Delta ups1$ and $\Delta yme1\Delta gep8$. Furthermore, the suppression of the single mutation of $\Delta yme1$, was determined.

3.3.2.1 Identification of genes suppressing the synthetic lethality of $\Delta yme1\Delta imp1$

Genes suppressing the synthetic lethality of $\Delta yme1\Delta imp1$ were identified after isolation of Yep13 library plasmids from $\Delta yme1\Delta imp1$ cells depleted of pVT100U-Yme1. Sequencing of

the respective Yep13 library plasmids identified the following open reading frame combinations: *PGK1*; *CRP6 + YLR218c*; *PET54 + HSV2*; *MIC14 + RAD28*. After cloning of individual genes into YEplac181 and transformation of the generated plasmids, suppression of $\Delta yme1\Delta imp1$ was tested for *PGK1*, *YLR218c*, *PET54* and *MIC14*.

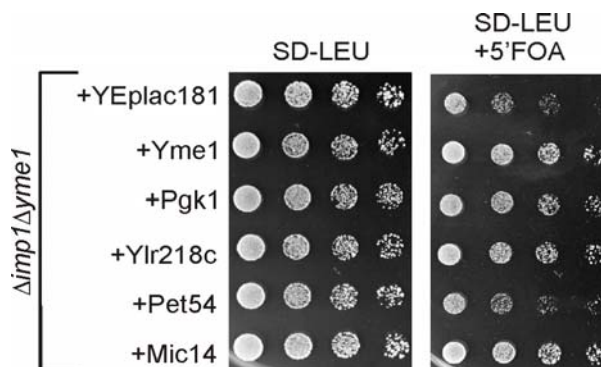


Figure 3.26 Suppression of $\Delta yme1\Delta imp1$ synthetic lethality by expression of suppressor. $\Delta yme1\Delta imp1$ cells harbouring either the empty plasmid (YEplac181) or the same plasmid containing Pgc1, Ylr218c, Pet54 or Mic14 were either grown on synthetic media containing 2% (w/v) glucose and lacking leucine (SD-LEU) or on synthetic media containing 2% (w/v) glucose, lacking leucine (SD-LEU) supplied with 5'FOA (1 mg/ml) for three or five days respectively. As a control $\Delta yme1\Delta imp1$ cells harbouring YEp13-Yme1 were included.

The setup for the suppression test of the single genes is essentially the same as the one used for the identification of the Yep13 library construct suppressing $\Delta yme1\Delta imp1$. Only here the growth of colonies without counter selection for the pVT100U-Yme1 plasmid (SD-LEU) was compared to those cells counter selected for the pVT100U-Yme1 (SD-LEU+5'FOA) (Fig. 3.26). Remaining growth of the negative control is based on residual growth of the cells that were only shifted to medium containing 5'FOA at this point. A suppression of the $\Delta yme1\Delta imp1$ associated growth defects could be observed upon expression of Pgc1, Ylr218c, Mic14 and the positive control Yme1. However, such an effect was not evident for Pet54. Pgc1 (3-phosphoglycerate-kinase) is a key enzyme in glycolysis and gluconeogenesis (Blake and Rice, 1981; Hitzeman et al., 1980). Cells deleted for *YLR218c* lack growth on non-fermentable carbon source and exhibit a glycogen storage defect (Wilson et al., 2002). Mic14 has been identified as one of the proteins that are depending on the Mia import pathway for their mitochondrial localisation (Gabriel et al., 2007), however no function has been assigned to Mic14.

In conclusion, the known functions of the identified suppressors cannot be immediately linked to functions of Imp1 or Yme1, respectively.

3.3.2.2 Suppression of $\Delta yme1$ phenotypes by suppressors of $\Delta yme1\Delta imp1$

In order to understand whether the identified suppressor alleviates growth impairment of the $\Delta yme1\Delta imp1$ double mutant by suppression of the $\Delta yme1$ associated dysfunctions, YEplac181 plasmids containing suppressor genes were transformed into $\Delta yme1$. Then growth of the resulting $\Delta yme1$ strain harbouring YEplac181, Yep13-Yme1, YEplac181-Pgk1, YEplac181-Ylr218c, YEplac181-Pet54 and YEplac181-Mic14 was examined.

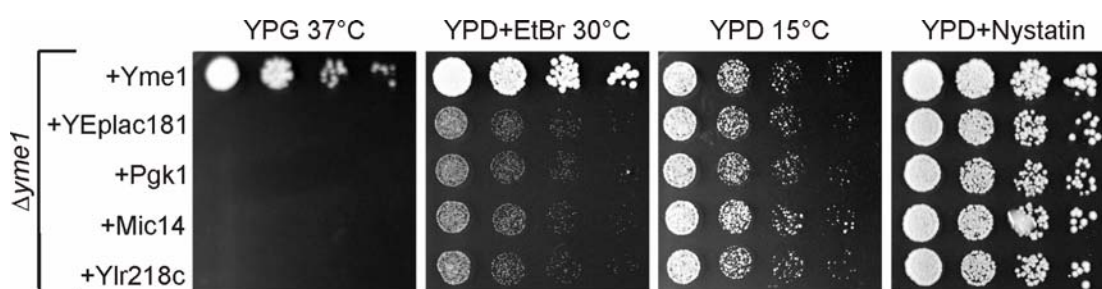


Figure 3.27 Suppression of $\Delta yme1$ phenotypes by suppressors of the $\Delta yme1\Delta imp1$ double deletion. $\Delta yme1$ cells harbouring YEplac181 containing Pgk1, Ylr218c, Pet54 or Mic14 were grown on YPD 15°C, on YPG at 37°C, on YPD containing EtBr (25 $\mu\text{g}/\text{ml}$) or nystatin (50 U/ml) for two to five days respectively. $\Delta yme1$ harbouring the empty vector (YEplac181) and $\Delta yme1$ served as controls.

The expression of the identified suppressors of the $\Delta yme1\Delta imp1$ double mutant did not suppress any of the tested growth defects of the $\Delta yme1$ strain (Fig. 3.27). Therefore, a suppression of the $\Delta yme1\Delta imp1$ double deletion is not caused by the suppression of $\Delta yme1$ associated defects. Whether the suppression of Pgk1, Ylr218c and Mic14 restores only defects of a $\Delta yme1\Delta imp1$ double deletion or the defects caused by a $\Delta imp1$ single deletion remains to be examined.

4 Discussion

4.1 Role of the CH-region of the *i*-AAA protease Yme1 in substrate binding

Substrate recognition and binding are crucial events during substrate degradation by a protease. This is also true for the highly conserved mitochondrial *i*-AAA protease, a membrane embedded ATP-dependent metallopeptidase composed of Yme1 subunits. Two autonomous substrate binding regions have been identified for the *i*-AAA protease Yme1, the NH-and the CH-region. The NH-region is essential for the proteolytic function of the *i*-AAA protease, as mutagenesis of this region abolishes degradation of all tested substrates (Graef and Langer, 2006). Replacement of the yeast CH-region by an orthologous sequence reduces the *in vivo* activity of the *i*-AAA protease and its deletion alters the assembly of a functional *i*-AAA protease complex (Graef et al., 2007). Only degradation of some substrates depends on the CH-region of the *i*-AAA protease and their CH-dependent degradation is shown to be also influenced by the NH-region. However, substrates can bind independently to either of the two regions (Graef et al., 2007). Other substrates are degraded in a CH-independent manner, solely requiring recognition by the NH-region. The parameters that determine CH-dependent or CH-independent degradation of a substrate are not understood so far. Two properties that potentially ascertain the CH-dependence of a substrate are its folding state and its association with the membrane.

In order to understand the underlying molecular mechanisms in substrate engagement of the CH-region the importance of distinct residues or certain areas within the CH-region of Yme1 on substrate binding and degradation is assessed by mutational analysis.

4.1.1 Initial substrate binding by the CH-region of the *i*-AAA protease Yme1

The CH-region of the *i*-AAA protease Yme1 is composed of three helices, the α -16, α -17 and α -18 helix based on the crystal structures of the homologous FtsH protease from *T. maritima* (Bieniossek et al., 2006). All three helices are exposed at the apical and lateral side of the proteolytic domain of the *i*-AAA protease. However, the CH-region does not represent the C-terminal end of Yme1, but 38 amino acids that follow the CH-region comprise the exact C-terminal end of Yme1. These residues are only resolved in the crystal structure of *T. thermophilus* (Suno et al., 2006) (Fig. 4.1), where they reside within the cleft of the U-like

structure that is built up by the α -17 and α -18 helices of Yme1. This relative orientation to the CH-region points to a regulatory function of the flexible element separating substrate and the α -17 and α -18 helices. Deletion of this region, however, has no detectable influence on the proteolytic activity of the *i*-AAA protease (Fig. 3.6). The region is thus not essential for substrate degradation by the *i*-AAA protease Yme1. Consistently, *in vitro* experiments show binding of substrates to the purified CH-region lacking the C-terminal extension (Graef et al., 2007). Further, these amino acids within this C-terminal region do not show a high degree of similarity when compared to homologous proteins of Yme1 in higher eukaryotes (Tab. 1.1). Although the C-terminal region of Yme1 is not essential for proteolytic activity, a negative regulatory mode for substrate binding to the CH-region cannot be completely ruled out by this analysis.

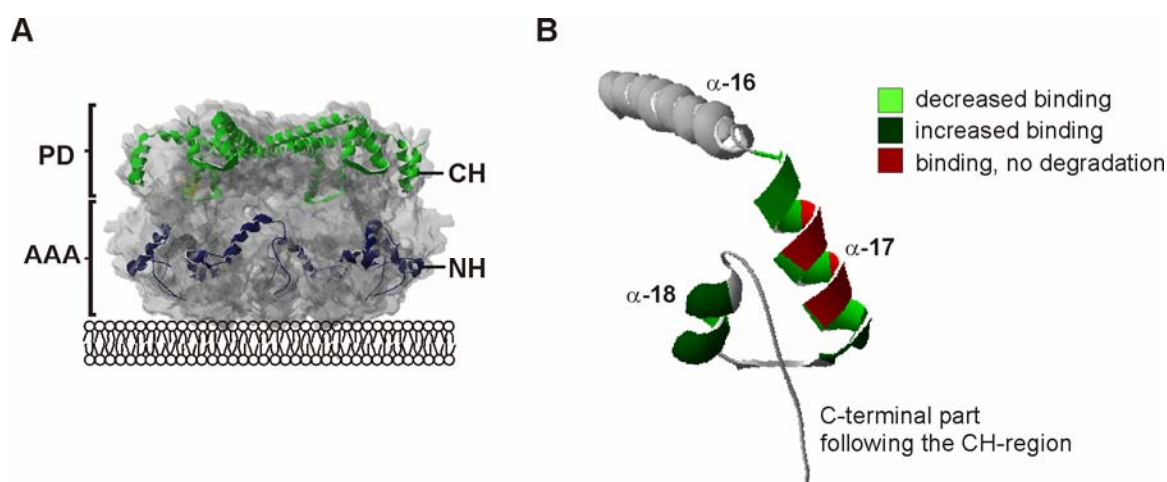


Figure 4.1 Mutations within the CH-region of the *i*-AAA protease Yme1. (A) Initial substrate binding sites of the *i*-AAA protease. NH- (N-terminal helices) and CH- (C-terminal helices) substrate binding regions of the *i*-AAA protease form a lattice-like structure at the surface of the predicted proteolytic cylinder of AAA proteases. (B) Effect of mutations in the CH-region of the *i*-AAA protease Yme1. Mutation of amino acids leading to loss of substrate binding is indicated with light green, enhanced substrate binding with dark green. Amino acids involved in substrate binding, but when mutated impaired in degradation are highlighted in red. The corresponding structures within the crystal structure of the related AAA protease FtsH from *T. thermophilus* are shown (Suno et al., 2006).

Analysis of pair wise mutations introduced into the helices α -17 and α -18 of Yme1 revealed a loss of substrate binding for those residues that might influence the overall fold of the CH-region. In this respect, mutation of residues predicted to face the interior of the *i*-AAA protease complex did not prevent the binding of Cox2 (Fig. 3.3) and its subsequent degradation (Fig. 3.4). In contrast, mutation of residues localised to the surface of the protease enabled efficient, even increased, binding of Cox2 to the protease which was able to degrade Cox2 in a wild type like manner. However, the mutational analysis did not reveal

surface exposed amino acids required for initial substrate binding. Only amino acids facing the interior of the \hat{i} -AAA protease were affected in their ability to bind Cox2. This points to an essential structural integrity of the α -17 and α -18 helices for substrate binding consistent with the role of the complete CH-region in substrate binding. Hence, arranging the CH-region onto the \hat{i} -AAA protease complex might result in more efficient binding of substrate. One should keep in mind that any structural information is based on crystal structures of bacterial FtsH proteases (Bieniossek et al., 2006; Suno et al., 2006).

4.1.2 CH-dependent degradation of substrates by the \hat{i} -AAA protease Yme1

Within the analysis of CH-mutant variants of Yme1 two mutations were identified (Yme1^{H687A/R688A} and Yme1^{Q691A/G692A}) that showed binding (Yme1^{H687A/R688A} only decreased) and impaired degradation of the substrate protein Cox2 (Fig. 3.3 and Fig. 3.4). Nevertheless, both mutants showed normal respiratory growth (Fig. 3.1), demonstrating proteolytic activity of the mutant \hat{i} -AAA protease (Leonhard et al., 1996; Weber et al., 1996). Further, the restoration of proteolytic activity is also achieved by the lower molecular weight complex found for the assembled \hat{i} -AAA protease complex of the Yme1^{H687A/R688A} mutant. The identification of mutants that are able to bind but not to degrade a CH-dependent proteolytic substrate raises the possibility that the CH-region is relevant for transfer of the substrate to the proteolytic site of the \hat{i} -AAA protease. This transfer of substrates from the CH-region is currently not understood. However, different models of substrate entry pathways exist for membrane embedded AAA proteases (Graef et al., 2008). Soluble AAA⁺-proteases mediate substrate engagement through the central pore of the AAA⁺ domain (Sauer et al., 2004). AAA proteases harbour a membrane adjacent AAA domain that complicates internalisation and transfer of substrate to the proteolytic chamber.

The 'threading model' proposed entry of substrates to the proteolytic cavity through an opening between the membrane and the membrane adjacent surface of the AAA domain, leading to translocation through the central pore loops (Graef et al., 2008) (Fig. 4.2). This model is more suitable for membrane inserted proteins, as soluble substrate proteins cannot easily reach the central pore lying in close proximity to the membrane surface. Consistently, such a degradation mode rather accounts for substrates that bind to the NH-region of the protease.

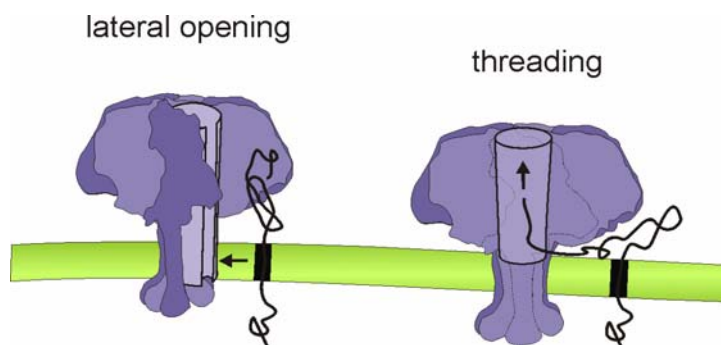


Figure 4.2 Alternative substrate entry pathways of the *i*-AAA protease Yme1. *Lateral opening model:* The substrate enters the proteolytic cavity after lateral opening of the protease ring. Subsequently, it is transferred to the proteolytic center via vectorial transport, while the protease ring rearranges its closed conformation. *Threading model:* The substrate reaches the central pore through an opening between the membrane and the membrane adjacent site of the AAA domain. It can then enter the proteolytic cavity through the central pore. The figure is adapted from (Graef et al., 2008).

In this regard, an epistatic analysis proved a mechanism where substrates first bind to the NH-region before they are transferred to the central pore loops for internalisation into the proteolytic chamber (Graef and Langer, 2006). Also a mode of action with initial substrate binding to the CH-region and subsequent transfer of the substrate to the NH-region is conceivable. In this scenario, the mutated CH-region would impair the transfer of substrate from the CH- to the NH-region. Within the structure of the CH-region the respective mutated residues are facing the surface of the molecule and are most likely important for direct substrate contact. Moreover, these CH-region residues do partially align with the NH-region of the *i*-AAA protease. Thus, a block of substrate transfer from CH to NH in these Yme1 CH-mutant variants is possible.

The second model for substrate entry into the proteolytic cavity suggests a lateral opening of the protease ring that is followed by vectorial transport of the substrate to the proteolytic chamber. Rearrangement of the protease ring leads to subsequent closure of the hexameric ring structure of the *i*-AAA protease (Graef et al., 2008) (Fig. 4.2). Such a mechanism has already been demonstrated for the double-stranded-DNA packaging motor of the bacteriophage ϕ 29 (Moffitt et al., 2009). Accordingly, mutations in the CH-region which interfere with the degradation of the bound substrate would affect opening or closing of the protease ring. As the mutated residues are facing the surface of the *i*-AAA protease, their involvement in a process that requires intramolecular communication seems unlikely. Moreover, a complete inactivation of the protease would be expected when such a mechanism is impaired. On the contrary, the *i*-AAA protease of both Yme1 CH-mutant variants showed proteolytic activity, as both mutants were able to complement known $\Delta yme1$ phenotypes. Thus, the lateral opening model is not appealing for the *i*-AAA protease,

based on results found for the two mutants Yme1^{H687A/R688A} and Yme1^{Q691A/G692A}. However, although the two mutated amino acids might not have a role within the opening and closing process, a function of both in the vectorial transport of the substrate while the ring structure is opened is still possible.

Generally, the intriguing characteristics of the two Yme1 CH-mutations, Yme1^{H687A/R688A} and Yme1^{Q691A/G692A}, that separate the processes of substrate binding and degradation but maintain proteolytic activity of the $\dot{\iota}$ -AAA protease suggest the existence of different pathways of CH-dependent substrate degradation by the $\dot{\iota}$ -AAA protease Yme1.

4.1.3 Structural importance of the CH-region of Yme1

Analysis of successive deletions of C-terminal parts of the $\dot{\iota}$ -AAA protease revealed a destabilisation of the $\dot{\iota}$ -AAA protease complex in mutants lacking any of the three helices that build up the CH-region. A complete deletion of the CH-region results in the formation of a complex with an apparent molecular weight of 200 kDa (Graef et al., 2007). The functional complex has a molecular mass larger than 850 kDa (Leonhard et al., 1996). The analysis of successive deletion of the CH-region refined the structural role of the CH-region to the single helices of the region. Hence, the single helices of the CH-region are not only important as a functional element, but have a potential function in organisation and stabilisation of the $\dot{\iota}$ -AAA protease complex.

Taken together, two new functions of the three helices of the $\dot{\iota}$ -AAA protease CH-region could be identified. First, the CH-region is involved in substrates transfer from the CH-region to the proteolytic site. Second, the integrity of the CH-region is required for the stability of the $\dot{\iota}$ -AAA protease complex.

4.2 Processing of the $\dot{\iota}$ -AAA protease Yme1

In order to identify the mitochondrial peptidase responsible for the maturation of Yme1, yeast cells lacking different mitochondrial peptidases were tested for the accumulation of the precursor form of Yme1. Only for cells harbouring a temperature sensitive allele of *MAS1* the precursor form of Yme1 was appearing (Fig. 3.8). *MAS1* encodes for the major mitochondrial processing peptidase MPP which resides in the matrix of mitochondria (Gakh et al., 2002; Leonhard et al., 1996).

In vitro processing assays verified the cleavage of S³⁵-radiolabeled Yme1 precursor by purified MPP. Furthermore, the processing of three Yme1 orthologs from *N. crassa* (Iap-1), *H. sapiens* (YME1L1) and *M. musculus* (Yme1l1) was addressed in the *in vitro* assay. All

three orthologs of Yme1 show processing by purified MPP (Fig. 3.9). As distinct recognition and cleavage motifs are assigned for MPP (Gakh et al., 2002), sequence analysis of all four Yme1 orthologs revealed the existence of putative R2- or R3-motifs (Tab. 4.1).

Yme1 ortholog	MPP motif
Yme1	K ⁴³ FYRFY↓SEKN ⁵²
Iap-1	L ¹² FRRSF↓SALM ²¹ N ²⁹ TLRSM↓STHQ ³⁸ Q ³⁸ PGRIP↓SFFR ⁴⁷
YME1L1	R ¹⁵⁷ TRRLQ↓STSE ¹⁶⁶
Yme1l1	K ⁸⁶ DKRVS↓SCWH ⁹⁵ S ¹¹⁶ TLRSS↓SLYR ¹²⁵

Table 4.1 Sequence alignment of MPP processing sites in different Yme1 orthologs. The R2-motif of MPP is composed of xRx↓x(S/x), whereas the R3-motif of MPP has a slightly different arrangement: xRx(Y/x)↓(S/A/x)x. Respective sequence motifs of Yme1 and its orthologs from *N. crassa* (Iap-1), *H. sapiens* (YME1L1) and *M. musculus* (Yme1l1) are depicted here.

One predicted MPP cleavage site is present in the sequence of Yme1 and YME1L1. Similarly, only one lower molecular weight form appeared for S³⁵-radiolabeled Yme1 and YME1L1 after processing with purified MPP (Fig. 3.9). In contrast, Iap-1 and Yme1l1 harbour more than one predicted MPP cleavage site in their N-terminal region. Consistently, two lower molecular weight species were produced upon MPP cleavage of S³⁵-radiolabeled Iap-1. If both forms represent the *in vivo* form of Iap-1 cannot be concluded from this approach. Cleavage of Yme1l1, however, only generated one lower molecular weight form. The size difference between the precursor and the mature form of Yme1l1 suggests that mature Yme1l1 is generated by processing at the second MPP cleavage site (Fig. 4.3). To determine whether the lower molecular weight forms generated by MPP cleavage of either of the Yme1 orthologs represent the *in vivo* maturation of these proteins, additional analysis are awaited. Whether the lower molecular weight form of Yme1 indeed represents the mature form of the *i*-AAA protease was addressed analysing processing of an N-terminally tagged Yme1 variant. The integration of six histidines, inserted after Yme1^{E50}, did not interfere with the *in vivo* activity of the *i*-AAA protease and the hexahistidine tag was still present after maturation of Yme1, as affinity purification of this Yme1 variant was possible (Fig. 3.11). Further, the molecular size of the N-terminally tagged Yme1 variant in cell extracts was comparable to the mature form and not to the precursor form of Yme1 (data not shown). Therefore, the

consensus motif for MPP cleavage depicted in Fig. 4.3 represents the MPP cleavage site of Yme1.

4.3 Novel interaction partners of the *i*-AAA protease Yme1

Affinity purification of proteolytically inactive Yme1 allowed the identification of eight novel interaction partners of the *i*-AAA protease of which six have been analysed in more detail (Fig. 4.3). Co-purification of the known proteolytic substrate Phb1 (Graef et al., 2007) and the known interaction partner Mgr1 (Dunn et al., 2006) proved the general eligibility of the approach.

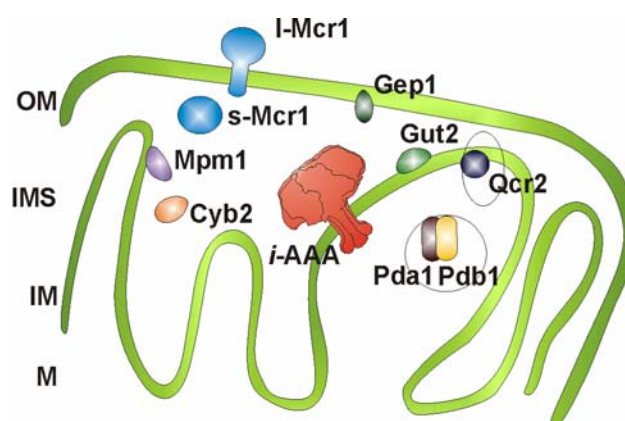


Figure 4.3 Relative localisation of Yme1-interacting proteins. Substrates identified by affinity purification of the *i*-AAA protease Yme1. In the matrix space Qcr2 was identified which is part of complex III of the respiratory chain (circle). Further, Pda1 and Pdb1 showed interaction with Yme1. These two proteins build up the E1 subunit of the pyruvate dehydrogenase complex (circle). Gut2 is localised to the inner mitochondrial membrane and is required for glycerol utilisation. Mpm1, for which no function is assigned, also localises to the inner mitochondrial membrane. Cyb2 and the short form (s) of Mcr1 represent soluble intermembrane space proteins. Cyb2 is reported to have a role in lactate utilisation. The long form (l) of Mcr1 resides in the outer mitochondrial membrane. Both forms are involved in ergosterol biogenesis and reduction of D-erythroascorbyl free radical. OM, outer mitochondrial membrane; IMS, intermembrane space; IM, inner mitochondrial membrane; M, matrix; circles, protein is part of a larger complex.

Qcr2 and the two assembly partners Pda1 and Pdb1 are new interaction partners of Yme1 localised to the mitochondrial matrix. In the intermembrane space, Mpm1, Gep1, Gut2, Cyb2 and the short form of Mcr1 were identified as novel interaction partners of the *i*-AAA protease. Furthermore, the long form of Mcr1 localised to the outer mitochondrial membrane was found to interact with the *i*-AAA protease.

Interestingly, three of the intermembrane space interaction partners (Cyb2, Gut2 and Mcr1) and the previously identified *i*-AAA protease substrate Cox2 (Graef et al., 2007) are

processed by the IMP peptidase. Even more intriguing these four proteins constitute the known set of substrates for the catalytic subunit Imp1 (Esser et al., 2004). However, no physical interaction of the \hat{i} -AAA protease and Imp1 or one of the other subunits of the IMP peptidase (Imp2 or Som1) could be identified. Imp1 was further excluded to be the peptidase responsible for processing of Yme1, as described in Chapter 4.2. However, *YME1* and *IMP1* show a synthetic lethal genetic interaction (Tab. 3.1), suggesting an overlapping function of both proteins in related processes. One probable reason for the interaction of the \hat{i} -AAA protease with substrates of the IMP peptidase could be a clearance function by which accumulated precursor proteins are removed. However, no peptides corresponding to the N-terminal targeting sequence were identified by PMF analysis of co-purified Cyb2 and Gut2 (data not shown). Although this does not exclude that Yme1 interacts with the precursor form of those proteins, a more prominent interaction with the mature form of those two proteins points to a different role of the \hat{i} -AAA protease. As those two proteins were not analysed in more detail, no final conclusion is possible. The other six interactions were analysed by co-immunoprecipitation. Although all other interactions of Yme1 with Yme1-interacting proteins could be verified, the interaction of Yme1 and Gep1 was not detected in this assay. In this case, the low abundance of Gep1 together with an only transient interaction with Yme1 may explain why no interaction is detectable. Moreover, a potential role of the Yme1-interaction partners as assembly partners of the \hat{i} -AAA protease was analysed (data not shown). However, no alterations of the \hat{i} -AAA protease complex were observed in the absence of any of the six Yme1-interacting proteins. Subsequently, the nature of interaction between the Yme1-interacting proteins and the \hat{i} -AAA protease was addressed, and a possible functional link of Yme1 and the newly identified interaction partners was analysed.

4.3.1 Possible function of the \hat{i} -AAA protease Yme1 in sorting and assembly of the mitochondrial proteins Qcr2, Pda1 and Pdb1

Three novel interaction partners of the \hat{i} -AAA protease localised to the matrix site of mitochondria are Qcr2, Pda1 and Pdb1. These interaction partners were exclusively identified with the Yme1 variant harbouring the hexahistidine tag at the C-terminus (Fig. 3.11). Possibly, an interaction of these three proteins occurs with that part of the N-terminal domain of the \hat{i} -AAA protease that is localised to the matrix. In line with this, the steady state levels of these proteins were not altered in the absence of Yme1 (Fig. 3.15). This supports the idea that these proteins do not represent proteolytic substrates of the \hat{i} -AAA

protease. Similarly, no or only a slightly increased co-precipitation efficiency of these proteins was detected when co-immunoprecipitations of proteolytically inactive Yme1^{E541Q} and Yme1 were compared. Thus, the proteolytic activity of the *̑*-AAA protease has no impact on these interaction partners, pointing to a role of Yme1 during import of the three proteins. Especially for Pda1 and Pdb1 such a function could be possible as both proteins showed a slight Yme1 dependent accumulation of their precursor form (Fig. 3.15) which was precipitated together with Yme1 (Fig. 3.13). In general, such an import function of the *̑*-AAA protease has been described for the import of the heterologously expressed mammalian PNPase (Rainey et al., 2006). However, the absence of Yme1 had no apparent effect on the import of Pda1 and Pdb1 (Fig. 3.18). In contrast, Qcr2 was less efficiently imported into isolated mitochondria of $\Delta yme1$ cells compared to wild type. This may reflect a specific effect of Yme1 on Qcr2 or may be an indirect consequence of a deletion of *YME1*. $\Delta yme1$ cells conduct reduced activities of the respiratory chain and the F₁F₀-ATPase and thereby possess a reduced membrane potential across the inner mitochondrial membrane (Kominsky et al., 2002; Nakai et al., 1995; Thorsness and Fox, 1993). As import of Qcr2 is depending on the membrane potential, the reduction of the membrane potential in $\Delta yme1$ mitochondria might also reduce the import efficiency of Qcr2. Alternatively, the sorting and assembly of Qcr2 could be impaired in the absence of the *̑*-AAA protease. However, such a function has not been shown for the *̑*-AAA protease so far. The sorting or assembly process of Qcr2 could further be influenced by its phosphorylation as it is proposed for the assembly of the ATP synthase (Reinders et al., 2007). Phosphorylation is also described for Pda1, but not for Pdb1. Phosphorylation of Pda1 and Qcr2 could potentially affect their interaction with the *̑*-AAA protease.

The significance of the interaction of Yme1 with either of the three matrix proteins remains unclear at this point. As deletion of *YME1* does not influence the abundance of these proteins, phenotypes monitored in the absence of Yme1 cannot be explained by the loss or accumulation of these proteins. However, whether the interaction between Yme1 and these proteins is required for either function is not clear yet. The attempt to correlate the $\Delta yme1$ associated phenotypes with the loss of either of these proteins did not provide insights into the functional relevance of the interaction of Yme1 and Qcr2, as well as the interaction of Yme1 with Pda1 and Pdb1. Thus, the nature of interaction between the *̑*-AAA protease and Qcr2, Pda1 and Pdb1 remains to be established.

The identification of Qcr2, Pda1 and Pdb1 as new interaction partners of the *̑*-AAA protease suggests the existence of alternative functions of Yme1 in addition to proteolytic quality control. As all three interaction partners are involved in energy metabolism it is appealing to speculate on a regulatory function of the *̑*-AAA proteins that modulates certain steps of the

energy metabolism within mitochondria. Furthermore, the identification of Pgc1, a key enzyme in glycolysis and gluconeogenesis, as a suppressor of the $\Delta yme1\Delta imp1$ synthetic lethality suggests a reduced cellular energy status in the absence of Yme1. In this line, depletion of the \dot{i} -AAA protease was shown to induce the expression of genes responsible for energy metabolism and the biogenesis of the respiratory chain (Arnold et al., 2006), further supporting the idea of a function of the \dot{i} -AAA protease in cellular energy metabolism.

4.3.2 New substrates of the \dot{i} -AAA protease: Mpm1 and Mcr1

Mcr1 and Mpm1 represent proteolytic substrates of the \dot{i} -AAA protease as indicated by their increased steady state level in the absence of Yme1 (Fig. 3.15). Co-precipitation of the two proteins was only evident when the proteolytic inactive variant of Yme1 was used (Fig. 3.12). Therefore, the stability of the two interaction partners and the role of Yme1 in degradation of Mcr1 and Mpm1 was addressed by import chase experiments. However, no degradation of any of the two interaction partners was obvious after import into mitochondria isolated from wild type and the import chase in $\Delta yme1$ mitochondria was comparable (Fig. 3.17). Therefore, no conclusion about the role of the \dot{i} -AAA protease in degradation of newly imported Mcr1 and Mpm1 was possible. Hence, an additional assay using an *in vivo* downregulation approach of Yme1 was applied. Here, an accumulation of the two proteins correlated with decreasing levels of Yme1 (Fig. 3.17). An increased transcription of both proteins in $\Delta yme1$ cells is not responsible for increased abundance of the proteins in the absence of the \dot{i} -AAA protease (Arnold et al., 2006), suggesting a role of the \dot{i} -AAA protease in the degradation of the two novel substrate proteins Mcr1 and Mpm1. As both proteins are not degraded under the same conditions employed for already known substrate proteins, the nature of interaction and degradation might be different. In contrast to Mcr1 and Mpm1, no accumulation is evident for the already known substrates Phb1 and Cox2 in a $\Delta yme1$ background (Graef et al., 2007), where additional factors are needed to provoke degradation. Furthermore, Phb1 and Cox2 were predominantly degraded by the \dot{i} -AAA protease in a largely unfolded or unassembled conformation. On the contrary, the two novel substrates Mcr1 and Mpm1 might not need unfolding for their degradation by Yme1. Since the \dot{i} -AAA protease is a representative of the ATP-dependent AAA protease family for which an 'unfoldase' activity has been reported (Martin et al., 2008) an unfolded protein conformation is probably not strictly required for recognition and part of the general quality control function of the \dot{i} -AAA protease. Thus, the new substrates Mcr1 and Mpm1 might be degraded in a regulatory manner by the \dot{i} -AAA protease adjusting the protein levels to cellular requirements. In addition to the regulation of Mcr1 and Mpm1 levels by proteolysis,

the *i*-AAA protease could also restrict their mitochondrial abundance by a regulation of their import and/or maturation. As Mcr1 and Mpm1 show different import pathways this aspect will be discussed separately for each protein.

Another interesting aspect of the identification of new substrates of the *i*-AAA protease is their functional integration into the already known pleiotropic phenotypes of $\Delta yme1$ cells. Mcr1 is described as an NADH cytochrome *b5* reductase that is present in two different isoforms within mitochondria (Hahne et al., 1994). Processing of Mcr1 is achieved by the IMP1 processing peptidase. Recently, an alternative import mechanism for the sorting of the long, 34 kDa form of Mcr1 has been described that does not depend on the TOM complex (Meineke et al., 2008). However, although no key players of this mechanism have been identified so far and Yme1 has a suggested role in mitochondrial protein import (Rainey et al., 2006), an involvement of Yme1 in import of Mcr1 could be excluded (Fig. 3.16). In addition, no impaired processing of the long Mcr1 isoform could be observed in the absence of Yme1. Therefore, regulation of Mcr1 levels likely occurs after import and maturation of the protein. Functionally, Mcr1 is linked to ergosterol biosynthesis and plays a crucial role in the reduction of D-erythroascorbyl free radical in yeast (Lamb et al., 1999; Lee et al., 2001). Whether both isoforms of Mcr1 are important for these processes is unclear. Mammalian NADH cytochrome *b5* reductase is dually localised to the ER and to mitochondria upon N-myristoylation (Colombo et al., 2005). As mammalian NADH cytochrome *b5* reductase does not resemble the signal peptides of yeast Mcr1, a different sorting mechanism can be expected (Tomatsu et al., 1989). Nevertheless, the mammalian ortholog shows localisation to the mitochondria, strengthening the importance of Mcr1 for mitochondrial function. Indeed, $\Delta mcr1$ cells exhibited growth defects on non-fermentable carbon source at elevated temperature (Fig. 3.14), a phenotype that has also been described for $\Delta yme1$ cells. This correlation might point to some related functions of Mcr1 and Yme1. However, deletion of *YME1* leads to an accumulation of Mcr1 that is in striking contrast to $\Delta mcr1$ cells. Therefore, the effect of overexpression of Mcr1 in wild type cells was monitored in parallel. Surprisingly, no effect of Mcr1 overexpression was seen in wild type cells, but in $\Delta yme1$ cells (Fig. 3.20). Here, overexpression of Mcr1 alleviated all $\Delta yme1$ associated phenotypes: impaired growth of $\Delta yme1$ cells on non-fermentable carbon source at elevated temperature, retarded growth on YPD at lower temperature and growth in the absence of mtDNA. It is thus conceivable, that the increased level of Mcr1 in $\Delta yme1$ cells does not plainly recapitulate the lack of degradation, but is actually beneficial for the cell and reduces defects caused by the loss of the *i*-AAA protease. The underlying molecular mechanisms are not clear and need further examination.

The other novel substrate Mpm1 is hardly described yet (Inadome et al., 2001). One name giving feature of the 'mitochondrial peculiar membrane protein 1' (Mpm1) is its co-fractionation with the membrane fraction, although no prominent hydrophobic stretches are present in the sequence of Mpm1. It is further localised in mitochondria in an oligomeric form and no phenotypes have been associated with a deletion of MPM1 so far (Inadome et al., 2001). Also testing the growth conditions of $\Delta yme1$ phenotypes did not reveal strong defects in the absence of Mpm1 (Fig. 3.14). No defect of $\Delta mpm1$ cells was obvious in the absence of mtDNA or on glucose-rich medium at lower temperature. The growth on non-fermentable carbon source at elevated temperature was reduced, albeit not to the level observed for $\Delta yme1$ cells. If anything, the growth of $\Delta mpm1$ on non-fermentable carbon source at elevated temperature was comparable to the deletion of *GEP1*, another newly identified interaction partner. Other features pointing to related functions of these two proteins are the postulated regulation of mitochondrial PE levels by Gep1 that is influencing the membrane composition (Osman et al., 2009) and the association of Mpm1 with detergent resistant membranes or comparable uncharacterized insoluble structures (Inadome et al., 2001). This could suggest a potential function of Mpm1 in either organisation or participation of distinct microdomains of the membrane. Concerning the interaction of Yme1 and Mpm1, no direct correlation of phenotypes associated with their deletion is possible. To further address the nature of interaction between those two proteins, an impairment of Mpm1 import or sorting in the absence of the *f*-AAA protease was analysed (Fig. 3.16). However, import of Mpm1 into mitochondria isolated from $\Delta yme1$ cells was comparable to its import into mitochondria isolated from wild type cells. Thus, the *f*-AAA protease is not important for the import and/or sorting of Mpm1 to the inner mitochondrial membrane, but promotes its degradation.

Taken together, two novel substrates have been identified for the *f*-AAA protease, Mcr1 and Mpm1. Both proteins show direct interaction with Yme1 and are degraded in an Yme1 dependent manner. Unlike for other described substrates, Mcr1 and Mpm1 might represent a new class of *f*-AAA protease substrates. Proteins of this class are not degraded for the purpose of quality control, but in a regulatory manner.

4.3.3 The *f*-AAA protease Yme1 functionally interacts with Gep1

Another newly identified interaction partner of the *f*-AAA protease is Gep1, although no independent verification of Gep1 and the *f*-AAA protease was possible. Gep1 is localised in the intermembrane space of mitochondria. Depletion of *YME1* resulted in a reduced Gep1 steady state level (Fig. 3.12), underlining the functional interaction of the two proteins. A

reduced protein level of Gep1 in the absence of Yme1 could be explained by different scenarios: Yme1 might stabilise Gep1 by direct physical interaction; or Yme1 could be involved in the biogenesis of Gep1.

Yme1 interaction partner	localisation	steady state level in $\Delta yme1$ cells	function
Qcr2	IM/M	not influenced	core subunit of the ubiquinol cytochrome <i>c</i> reductase complex
Pda1/Pdb1	M	not influenced	E1 subunit of the pyruvate dehydrogenase complex
Mcr1 (both isoforms)	OM (long) IMS (short)	increased	required for ergosterol biosynthesis and reduction of D-erythroascorbyl free radical
Mpm1	IMS/IM	increased	unknown
Gep1	IMS/OM	decreased	organisation of mitochondrial phospholipids

Table 4.2 Yme1-interacting proteins. Identified interaction partners of the \bar{F} -AAA protease Yme1. Additional analysis determined Qcr2, Pda1 and Pdb1 as interaction partners whose function might be regulated by the action of the \bar{F} -AAA protease, independent of its proteolytic activity. Mcr1 and Mpm1 represent substrates of the \bar{F} -AAA protease and show increased steady state levels in the absence of the \bar{F} -AAA protease. Furthermore, the \bar{F} -AAA protease functionally interacts with Gep1, whose steady state level is decrease in $\Delta yme1$ cells.

Analysis of the import of Gep1 into mitochondria isolated from $\Delta yme1$ cells, however, did not reveal any role of Yme1 during Gep1 biogenesis (Fig. 3.16). Further, no reduction of Gep1 transcription could be identified in the absence of Yme1 (Arnold et al., 2006), pointing to a regulation of Gep1 expression on protein levels.

Since Gep1 overexpression has been described to elicit toxic effects in wild type cells (Osman et al., 2009) and Gep1 steady state levels were reduced in $\Delta yme1$ cells, a potential increased sensitivity towards Gep1 overexpression in the absence of Yme1 was analysed. Indeed, cells lacking the \bar{F} -AAA protease were more sensitive to Gep1 overexpression (Fig. 3.19). Hence, Yme1 could be responsible for the adjustment of Gep1 levels in mitochondria or a so far unknown Yme1 function can buffer toxic effects of Gep1 overexpression. Whether such a potential regulation is achieved by direct interaction of Yme1 with Gep1 or a different mechanism is not clear. Further, the sensitivity of $\Delta yme1$ cells to Gep1 overexpression strengthens the functional connection of the two proteins.

Moreover, Gep1 has recently been linked to the regulation of mitochondrial PE levels and its overexpression results in a reduction of cardiolipin levels (Osman et al., 2009). The increased

sensitivity towards Gep1 overexpression of $\Delta yme1$ cells suggests a decreased tolerance of $\Delta yme1$ cells to reduction of mitochondrial cardiolipin levels. Therefore, possibly not the accumulation of the Gep1 protein might be toxic, but the induced alteration of the mitochondrial membrane. Similarly, a deletion of *UPS1* in the absence of Yme1 results in a synthetic lethal phenotype. As deletion of *UPS1* also reduces mitochondrial cardiolipin levels, the increased sensitivity of $\Delta yme1$ cells towards Gep1 overexpression does most likely originate from changes in mitochondrial phospholipid levels. The general connection of the *AAA* protease to cellular phospholipids will be discussed later in more detail.

4.4 Genetic interaction of the *AAA* protease Yme1

A synthetic genetic array (SGA) was conducted to identify processes that are essential in the absence of Yme1. Additional analysis of determined synthetic lethal interactions of *YME1* aimed at the identification of suppressors that would link the *AAA* protease to more precise functions. Increasing the knowledge about both, processes involving Yme1 and certain functions of Yme1, is of particular importance, as none of the described pleiotropic phenotypes associated with the deletion of Yme1 are explained by the known functions of the conserved *AAA* protease so far.

4.4.1 Synthetic lethality of the *AAA* protease Yme1 – more than just an consequence of mtDNA loss

An assorted library of 96 mitochondrial genes was tested for a potential synthetic lethal interaction with *YME1*. 34 of these gene deletions were identified to be synthetically sick or lethal with a deletion of *YME1* (Fig. 4.4). For some of these synthetic lethal interactions, the possible origin of lethality could be linked to the loss of mtDNA, as the respective single mutant strains were unable to grow on non-fermentable carbon source, a growth condition that requires the presence of mtDNA. As $\Delta yme1$ cells are not able to tolerate the absence of mtDNA (Thorsness and Fox, 1993), combination of $\Delta yme1$ with a deletion triggering the loss of mtDNA will result in a lethal phenotype. However, the contribution of additional effects to the synthetic lethal interaction of the *AAA* protease and the respective gene inducing mtDNA loss cannot be excluded.

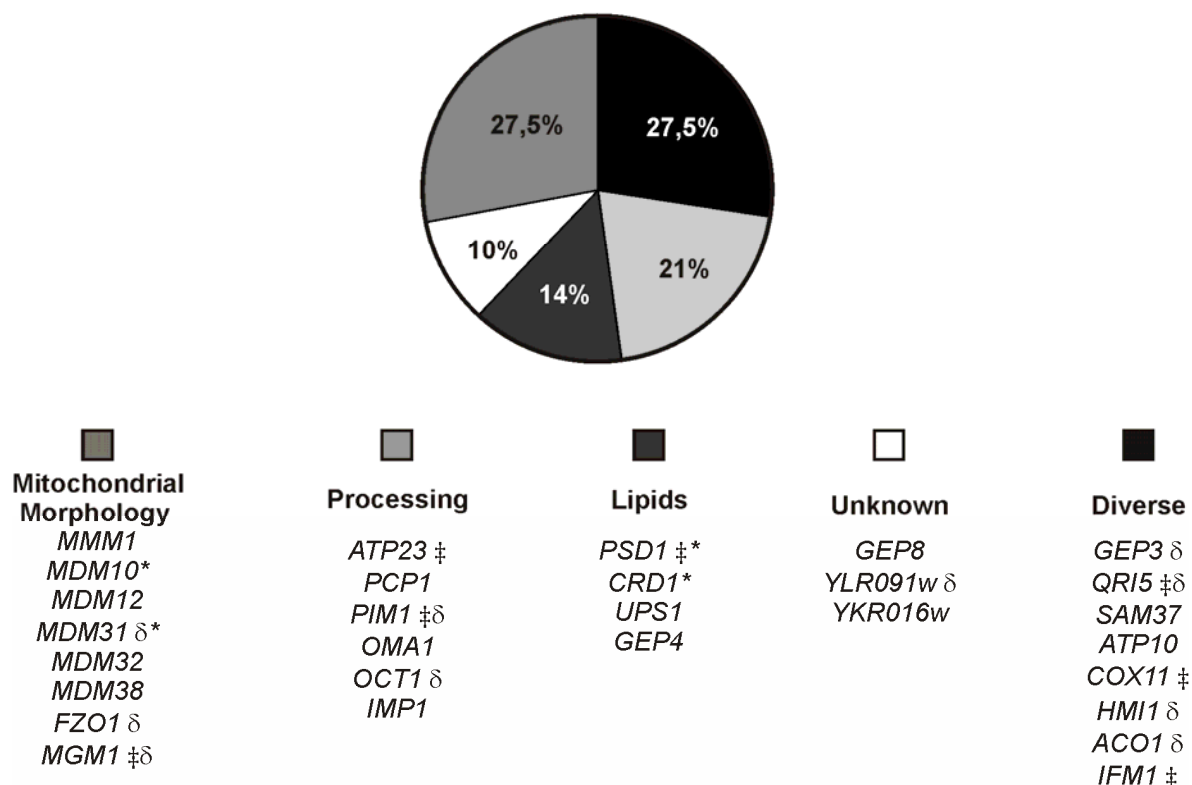


Figure 4.4 Classification of synthetic lethal interactions of *YME1*. Evaluation of synthetic lethal interactions found by SGA. Verified synthetic lethal interactors of the *i*-AAA protease were grouped into functional classes: Mitochondrial morphology, processing, lipids, unknown and diverse. δ , single deletion strain does not grow on non-fermentable carbon source indicating the absence of mtDNA;*, respective deletion strain shows synthetic sick interaction with *YME1*; \ddagger , mRNA upregulated in $\Delta yme1$ (Arnold et al., 2006).

Notably, an upregulation of mRNA in the absence of Yme1 was found for some of the synthetic lethal interactors of the *i*-AAA protease (Arnold et al., 2006), namely *MGM1*, *ATP23*, *PIM1*, *PSD1*, *QRI5*, *COX11* and *IFM1*. This is in line with the compensatory function of the pathways involving these proteins with pathways involving Yme1 and emphasises the action of both proteins in related processes. Consequently, the deletion of *YME1* most likely results in an increased dependence on the synthetically lethal interactor for cellular survival. That such an induced expression was not found for all candidates or only one particular functional class highlights the requirement of *i*-AAA protease function for different processes.

4.4.2 New implications for Yme1 function

As a combined evaluation of all synthetic lethal interactions identified for the *i*-AAA protease is not yet possible, an implication of some potential functions of Yme1 based on the different functional groups classified is performed.

Depletion of Yme1 induces aberrant mitochondrial morphology (Campbell et al., 1994). However, up to date the reason for this defect has not been understood. Only components of the mitochondrial fusion machinery could be identified (Fzo1 and Mgm1) to be synthetic lethal with *YME1*. Moreover, Mgm1 expression is induced in the absence of Yme1 (Arnold et al., 2006) and the mammalian homolog of Yme1 is processing OPA1, the mammalian homolog of Mgm1 (Griparic et al., 2007; Song et al., 2007). Whether these results argue for a function of Yme1 in mitochondrial fusion is not clear yet, as fusion mutants are described to lose mtDNA (Hoppins et al., 2007) and will, hence, be synthetically lethal in combination with the petite negative depletion of the *f*-AAA protease. Further, the combination of mutants that exhibit defects in mitochondrial morphology might lead to the accumulation of severely aberrant mitochondrial structures interfering with cell survival. Such a scenario might be possible for the combination of $\Delta yme1$ with any of the genetically linked deletions of *MMM1*, *MDM10*, *MDM12*, *MDM31* and *MDM32* (Dimmer et al., 2005). For Mmm1, Mdm10 and Mdm12 an additional function in sorting of outer membrane proteins has been described (Bolender et al., 2008). Therefore, the synthetic lethality of these genes and *YME1* may also originate from an accumulation of non imported proteins that impairs mitochondrial activity. No potential overlapping process is described for Mdm38 and Yme1, hence this synthetic lethal interaction is currently being analysed (Fig. 3.24).

The next functional group links the function of the *f*-AAA protease to lipids. Two of the initially identified synthetic lethal interactions proved to be synthetically sick (Psd1 and Crd1). In addition, changes in the phospholipid levels of $\Delta yme1$ cells (Nebauer et al., 2007) also hint at a role of the *f*-AAA protease in lipid biogenesis or distribution. In this respect, the deletions of *MMM1*, *MDM10*, *MDM31* and *MDM32* revealed alteration of PE and/or CL levels (Osman et al., 2009). Therefore, also the synthetic lethal interaction of these genes in combination with $\Delta yme1$ could originate from changes in mitochondrial lipid levels, further pointing to a relevance of Yme1 for lipid metabolism.

Synthetic lethal interactions of *YME1* with components important for processing or degradation of mitochondrial proteins could be identified. This was expected, as one of the basic functions of the *f*-AAA protease is the quality control of mitochondrial membrane proteins and a similar phenotype based on this function has already been described by the synthetic lethal interaction of *YME1* with a deletion of *YTA10* or *YTA12* encoding for either subunit of the *m*-AAA protease (Lemaire et al., 2000; Leonhard et al., 2000; Osman et al., 2009). Moreover, some of the single deletions of these peptidases cause the loss of mtDNA that can also be responsible for the synthetic lethal interaction with *YME1*. Surprisingly, the $\Delta pcp1$ strain used in this screen still harboured mtDNA, although the absence of mtDNA is one of its reported phenotypes (Sesaki et al., 2003). Hence, the synthetic lethality of *PCP1*

and *YME1* is caused by loss of a *Pcp1* function in processes that do not have an influence on mtDNA maintenance. Similarly, different reasons might account for the other identified synthetic lethal interactor of *YME1* referring to the depletion of a protein with mitochondrial peptidase activity.

Furthermore, the *F*-AAA protease could be implicated to have a role in processes which are required for an efficient assembly of the respiratory chain. This is not surprising, as $\Delta yme1$ cells exhibit a reduced membrane potential, and any additional alteration influencing the respiratory chain activity might lead to an elimination of the membrane potential generated across the inner mitochondrial membrane. Nonetheless, not all of the tested components responsible for the assembly of the respiratory chain exhibit a genetic interaction with *YME1*. As deletion of *YME1* only leads to a reduction of mitochondrial membrane potential only a subset of the respiratory chain components might be influenced by the absence of the *F*-AAA protease. In the same line, the loss of respiratory chain assembly factors likely leads to an accumulation of assembly intermediates that could exhibit toxic effects. This effect might be more drastic in the absence of the *F*-AAA protease which has been shown to degrade non assembled Cox2 (Graef et al., 2007). Therefore, the assembly of certain respiratory chain components might be crucial in the absence of *YME1*.

4.4.3 High copy suppressor screen of $\Delta yme1\Delta imp1$

The genetic interaction of *Yme1* and *Imp1* is of particular interest in this context, as all known substrates of *Imp1* have been identified as interaction partners of the *F*-AAA protease earlier (Fig. 3.11). In this line, the already proposed clearance function of *Yme1* for precursor proteins processed by the IMP peptidase could account for the synthetic lethality, as accumulation of immature proteins could impair mitochondrial function. The accomplishment of a high copy suppressor screening of the $\Delta yme1\Delta imp1$ double mutant (Fig. 3.25) might enable the discovery of the origin of the *Yme1* interaction with *Imp1* substrates. Moreover, the approach might ascertain new functions of the *F*-AAA protease independent from the detected physical interactions of *Yme1*. One identified suppressor, *Pgk1*, is a key enzyme of glycolysis and gluconeogenesis acting in the cytosol. Overexpression of *Pgk1* rescues the synthetic lethality of a $\Delta yme1\Delta imp1$ double mutant (Fig. 3.26). This points to an impairment of mitochondrial energy metabolism in $\Delta yme1\Delta imp1$ double mutant cells that can possibly not any longer rely on the function of the respiratory chain, but are depending on an enhanced ATP production by glycolysis. Indeed, already the single mutant of *IMP1* exhibits a petite phenotype and therefore depends on glycolysis for the production of ATP. Recently, a role of *Pgk1* in suppression of apoptotic phenotypes has

been identified in yeast (Mazzoni et al., 2009). There, a similar ATP related effect has been described that accounts for the suppression of apoptosis in the absence of the essential gene *LSM4*. Furthermore, the *i*-AAA protease was also linked to metabolic processes by the identification of two new interaction partners, Pda1 and Pdb1. Hence, a potential role of Yme1 in mitochondrial metabolic processes is likely. However, no suppression of the single deletion mutant of *YME1* could be observed (Fig. 3.27). Thus, additional metabolic defects associated with the petite phenotype of the deletion of *IMP1* exist. Whether Pgk1 suppresses either the single depletion of *IMP1* or only the defects caused in the $\Delta yme1\Delta imp1$ double mutant is not clear yet.

4.5 Impact of the *i*-AAA protease Yme1 on cellular and mitochondrial lipid levels

Two classes of lipids are present in mitochondrial membranes of yeast, glycerophospholipids (phospholipids) and the yeast sterol ergosterol. Both are asymmetrically distributed between the inner and/or outer mitochondrial membrane (Zinser and Daum, 1995). Considering the high protein content of the inner mitochondrial membrane, such an organisation is probably crucial for mitochondrial functions. On the other hand, proteins have to be organised and controlled to ensure mitochondrial function. Therefore, mitochondria might not only rely on an efficient system for protein quality control surveillance, but might additionally depend on a modulatory lipid environment for the maintenance of their function. Similarly, the adjustment of distinct lipid environments can be important for protein quality control. Here, a possible link between lipid homeostasis and the *i*-AAA protease will be discussed.

4.5.1 Depletion of Yme1 changes mitochondrial phospholipid levels

Phospholipids are the dominant lipids in mitochondrial membranes. In contrast to phosphatidylethanolamine (PE) and phosphatidylcholine (PC) which are distributed more or less equally between both mitochondrial membranes, the mitochondria specific polyglycerophospholipid cardiolipin (CL) is predominantly present within the inner mitochondrial membrane. The preferential organisation of different proteins within the inner mitochondrial membrane might be linked to its lipid content. The IMP peptidase, for example, depends on the presence of phosphatidylserine (PS) for its function (Schneider et al., 1991), whereas one of its substrates, Gut2, was shown to require PC for its incorporation

into membranes (Rijken et al., 2007). Furthermore, Psd1 which is required for the conversion of phosphatidylserin (PS) to PE and $\Delta psd1$ cells exhibit growth phenotypes on non-fermentable carbon source, pointing to a role of PE in the organisation or biogenesis of the respiratory chain (Birner et al., 2003; Osman et al., 2009).

Different connections to the mitochondrial phospholipids metabolism have been established for the \hat{i} -AAA protease Yme1. Initially, the level of different phospholipids is reported to be altered upon depletion of Yme1 (Nebauer et al., 2007; Osman et al., 2009). The most prominent effect is the increase in PE levels monitored for $\Delta yme1$. This effect seems to depend on the carbon source. Additionally, a link of the \hat{i} -AAA protease to phospholipids alterations could be identified within the analysis performed here. First, cells are more sensitive to Gep1 overexpression in the absence of Yme1. Second, deletion of *UPS1* in a $\Delta yme1$ background results in a synthetic lethal phenotype. Both conditions, overexpression of Gep1 and deletion of *UPS1*, result in a reduction of CL levels. Therefore, it is tempting to speculate about an increased sensitivity to CL reduction in the absence of the \hat{i} -AAA protease. In that line, a slight increase of CL can be observed upon deletion of *YME1* which might partially counteract the increased sensitivity (Nebauer et al., 2007). A direct effect of CL on Yme1 function might exist, but has not been addressed so far.

Therefore, an impairment of the inner mitochondrial membrane integrity, achieved by lipid alterations, is lethal in the absence of the \hat{i} -AAA protease. Although no exact impact of lipid alterations is described so far, influences on the assembly of proteins into the lipid bilayer leading to their functional impairment are conceivable. In regard to Yme1, an impaired protein processing might lead to precursor accumulation which is toxic in the absence of the \hat{i} -AAA protease.

4.5.2 A potential influence of Yme1 on cellular ergosterol distribution

Ergosterol is present in the inner mitochondrial membrane of yeast mitochondria. However, its function within the organelle has not been established. This is different in mammalian mitochondria where the rate limiting steps of steroidogenesis are conducted within this organelle (Miller, 2007). However, besides this function not much more is known about the relevance of sterols in mitochondrial membranes. Although ergosterol resides predominantly in the plasma membrane, mutants of the ergosterol biogenesis pathway exhibit mitochondrial morphology defects (Altmann and Westermann, 2005). This might either underline the essential membrane material function of ergosterol within the organelle, or

could further point to a role of ergosterol in organisation of mitochondrial membranes which might be important for the function of the mitochondrial fission and fusion machinery.

With respect to the *Yme1* protease, a reduced uptake of ergosterol under anaerobic conditions was reported (Reiner et al., 2006). In general, sterol uptake only becomes essential for a cell under anaerobic conditions, as its synthesis requires molecular oxygen that is usually provided in the form of heme by mitochondria. Under aerobic conditions a phenomenon called 'aerobic sterol exclusion' prevents the uptake of ergosterol from the medium. The phenomenon is thought to depend on the amount of ergosterol present within a cell, especially the plasma membrane. At this point a certain minimal threshold level is reached, uptake of ergosterol becomes possible. In this line, the amount of ergosterol present in the plasma membrane of $\Delta yme1$ cells was monitored, and based on the enhanced sensitivity of $\Delta yme1$ cells to nystatin shown to be increased. Nystatin binds to ergosterols in the plasma membrane resulting in its disruption and cell death. Enhanced sensitivity to nystatin therefore reflects an increased ergosterol content of the plasma membrane. It was somehow surprising that the mitochondrial *Yme1* protease should influence the ergosterol level of the plasma membrane. However, an increased sensitivity of $\Delta yme1$ to nystatin does most likely not account for a general defect of the plasma membrane, as no synthetic lethal effects can be observed upon simultaneous deletion of components of the cell wall. Next, the overall content of ergosterol in the absence of *Yme1* was compared to ergosterol levels in wild type. However, this analysis did not reveal any differences, neither in total lipid samples, nor in lipid samples of crude cellular membranes excluding the plasma membrane. Similarly, no change in ergosterol content could be observed in the absence of *Arv1*, a protein implicated in the intracellular distribution of ergosterol, although accumulation of free ergosterol was observed by immunofluorescence and nystatin sensitivity (Fei et al., 2008; Tinkelenberg et al., 2000). This effect was attributed to the presence of different ergosterol regulatory pathways that can to a certain extent substitute for one another to assure homeostasis of ergosterol levels and cell survival, respectively. Therefore, a more accurate function of the *Yme1* protease in ergosterol distribution remains to be defined in yeast cells, where no protein regulating the organellar ergosterol distribution has been identified so far, making a potential role of *Yme1* in this process highly interesting. In addition, the phenotypes observed for the mitochondrial morphology defect in $\Delta yme1$ and mammalian *STAR*^{-/-} cells show some correlation, as both cells contain swollen mitochondria. In *STAR*^{-/-} cells this effect can be clearly attributed to mitochondrial sterol exclusion (Ishii et al., 2002). Finally, the increased ergosterol in $\Delta yme1$ cells is intriguing, as reduced ergosterol levels are observed in cells depleted of intramitochondrial energy (Hunakova et al., 1997). A similar effect would thus be expected for $\Delta yme1$ cells that also show a reduced activity of the

mitochondrial F_1F_0 -ATPase. Therefore, a more direct effect of the \dot{i} -AAA protease on the cellular or mitochondrial ergosterol level is conceivable.

5 Zusammenfassung

Die *f*-AAA Protease Yme1 ist eine hochkonservierte ATP-abhängige AAA (ATPase Associated with various cellular Activities) Protease, die in der inneren mitochondrialen Membran verankert ist und dort die Qualität der Proteine überwacht; dies ist entscheidend für das Überleben der Zelle. In Hefe ist eine Deletion des *YME1* Gens mit pleiotropen Phänotypen assoziiert. Der molekulare Hintergrund dieser Phänotypen kann jedoch nicht mit den bislang bekannten proteolytischen Substraten und Interaktionspartnern von Yme1 erklärt werden. Deshalb wurden im Rahmen dieser Arbeit verschiedene Ansätze angewandt, um die Funktion der *f*-AAA Protease genauer zu definieren. Zunächst wurden mit Hilfe von Affinitätsaufreinigung einer proteolytisch inaktiven Variante von Yme1, die als Substratfalle dient, acht neue Interaktionspartner aus unterschiedlichen mitochondrialen Subkompartimenten identifiziert. Zweien dieser Interaktionspartner, Mcr1 und Mpm1, wurde eine Rolle als proteolytisches Substrat der *f*-AAA Protease zugewiesen. Für weitere identifizierte Interaktionen sollten andere Funktionen der *f*-AAA Protease verantwortlich sein. Ferner wurde ein „synthetisch genetischer Array“ (SGA) mit 96 nicht-essentiellen mitochondrialen Gendeletionen verwendet, um Prozesse zu untersuchen, welche auf die Funktion der *f*-AAA Protease angewiesen sind. 34 synthetisch letale Interaktionen stellten eine mögliche Verbindung von Yme1 zu neuen Funktionen, wie der mitochondrialen Morphology, der Prozessierung von Proteinen und dem Metabolismus von Lipiden her. Außerdem wurden Suppressoren der synthetisch letalen Interaktion von *IMP1* und *YME1* gesucht. Diese genetische Interaktion ist insofern von besonderem Interesse, da alle bekannten Substrate der katalytischen Untereinheit Imp1 der IMP Prozessierungs-Peptidase als Interaktionspartner der *f*-AAA Protease identifiziert wurden. Dabei wurde ein entscheidendes Enzym der Glykolyse und Glukoneogenese, Pgc1, als Suppressor der $\Delta yme1 \Delta imp1$ Doppelmutante gefunden. Dies deutet auf eine Beeinträchtigung des Energiemetabolismus in diesen Zellen hin.

Darüber hinaus wurden in dieser Arbeit die Bedingungen der Substraterkennung der *f*-AAA Protease mit Hilfe von Mutationsanalysen untersucht. Kürzlich konnte die Existenz von zwei Substratbindestellen der *f*-AAA Protease gezeigt werden: die CH-(C-terminale Helices) und die NH-(N-terminale Helices) Region. Im Gegensatz zur NH-Region wurden bislang keine Untersuchungen zu molekularen Mechanismen der Substratbindung der CH-Region durchgeführt. Hier konnte zusätzlich zur Signifikanz der CH-Region für die Substratbindung und -übermittlung, eine Funktion dieser Region in der Stabilisierung des *f*-AAA Proteasekomplexes identifiziert werden.

Im Rahmen dieser Arbeit wurden neue Substrate und Interaktionspartner der *Yme1* AAA Protease identifiziert, die auf die Existenz weiterer Funktionen von Yme1 hindeuten. Da nur wenige Erkenntnisse über die Funktion der AAA Protease in höheren Eukaryoten vorliegen, wird eine Analyse der Bedeutung der hier erlangten Befunde in Säugern interessant.

6 References

- Abe, F., and Hiraki, T. (2009). Mechanistic role of ergosterol in membrane rigidity and cycloheximide resistance in *Saccharomyces cerevisiae*. *Biochim Biophys Acta* *1788*, 743-752.
- Achleitner, G., Gaigg, B., Krasser, A., Kainersdorfer, E., Kohlwein, S. D., Perktold, A., Zellnig, G., and Daum, G. (1999). Association between the endoplasmic reticulum and mitochondria of yeast facilitates interorganelle transport of phospholipids through membrane contact. *Eur J Biochem* *264*, 545-553.
- Altmann, K., and Westermann, B. (2005). Role of essential genes in mitochondrial morphogenesis in *Saccharomyces cerevisiae*. *Mol Biol Cell* *16*, 5410-5417.
- Ammelburg, M., Frickey, T., and Lupas, A. N. (2006). Classification of AAA+ proteins. *J Struct Biol* *156*, 2-11.
- Arnold, I., Wagner-Ecker, M., Ansorge, W., and Langer, T. (2006). Evidence for a novel mitochondria-to-nucleus signalling pathway in respiring cells lacking *f*AAA protease and the ABC-transporter Mdl1. *Gene* *367*, 74-88.
- Athenstaedt, K., and Daum, G. (1999). Phosphatidic acid, a key intermediate in lipid metabolism. *Eur J Biochem* *266*, 1-16.
- Augustin, S., Nolden, M., Müller, S., Hardt, O., Arnold, I., and Langer, T. (2005). Characterization of peptides released from mitochondria: evidence for constant proteolysis and peptide efflux. *J Biol Chem* *280*, 2691-2699.
- Bauerfeind, M., Esser, K., and Michaelis, G. (1998). The *Saccharomyces cerevisiae* SOM1 gene: heterologous complementation studies, homologues in other organisms, and association of the gene product with the inner mitochondrial membrane. *Mol Gen Genet* *257*, 635-640.
- Baumann, N. A., Sullivan, D. P., Ohvo-Rekila, H., Simonot, C., Pottekat, A., Klaassen, Z., Beh, C. T., and Menon, A. K. (2005). Transport of newly synthesized sterol to the sterol-enriched plasma membrane occurs via nonvesicular equilibration. *Biochemistry* *44*, 5816-5826.
- Beh, C. T., Alfaro, G., Duamel, G., Sullivan, D. P., Kersting, M. C., Dighe, S., Kozminski, K. G., and Menon, A. K. (2009). Yeast oxysterol-binding proteins: sterol transporters or regulators of cell polarization? *Mol Cell Biochem*.
- Behrens, M., Michaelis, G., and Pratje, E. (1991). Mitochondrial inner membrane protease 1 of *Saccharomyces cerevisiae* shows sequence similarity to the *Escherichia coli* leader peptidase. *Mol Gen Genet* *228*, 167-176.
- Bieniossek, C., Schalch, T., Bumann, M., Meister, M., Meier, R., and Baumann, U. (2006). The molecular architecture of the metalloprotease FtsH. *Proc Natl Acad Sci U S A* *103*, 3066-3071.
- Bione, S., D'Adamo, P., Maestrini, E., Gedeon, A. K., Bolhuis, P. A., and Toniolo, D. (1996). A novel X-linked gene, G4.5, is responsible for Barth syndrome. *Nat Genet* *12*, 385-389.
- Birner, R., Burgermeister, M., Schneiter, R., and Daum, G. (2001). Roles of phosphatidylethanolamine and of its several biosynthetic pathways in *Saccharomyces cerevisiae*. *Mol Biol Cell* *12*, 997-1007.
- Birner, R., Nebauer, R., Schneiter, R., and Daum, G. (2003). Synthetic lethal interaction of the mitochondrial phosphatidylethanolamine biosynthetic machinery with the prohibitin complex of *Saccharomyces cerevisiae*. *Mol Biol Cell* *14*, 370-383.
- Blake, C. C., and Rice, D. W. (1981). Phosphoglycerate kinase. *Philos Trans R Soc Lond B Biol Sci* *293*, 93-104.

- Bolender, N., Sickmann, A., Wagner, R., Meisinger, C., and Pfanner, N. (2008). Multiple pathways for sorting mitochondrial precursor proteins. *EMBO Rep* *9*, 42-49.
- Bolon, D. N., Wah, D. A., Hersch, G. L., Baker, T. A., and Sauer, R. T. (2004). Bivalent tethering of SspB to ClpXP is required for efficient substrate delivery: a protein-design study. *Mol Cell* *13*, 443-449.
- Bota, D. A., and Davies, K. J. (2002). Lon protease preferentially degrades oxidized mitochondrial aconitase by an ATP-stimulated mechanism. *Nat Cell Biol* *4*, 674-680.
- Brachmann, C. B., Davies, A., Cost, G. J., Caputo, E., Li, J., Hieter, P., and Boeke, J. D. (1998). Designer deletion strains derived from *Saccharomyces cerevisiae* S288C: a useful set of strains and plasmids for PCR-mediated gene disruption and other applications. *Yeast* *14*, 115-132.
- Brandt, A. (1991). Pulse labeling of yeast cells as a tool to study mitochondrial protein import. *Methods Cell Biol* *34*, 369-376.
- Burri, L., Strahm, Y., Hawkins, C. J., Gentle, I. E., Puryer, M. A., Verhagen, A., Callus, B., Vaux, D., and Lithgow, T. (2005). Mature DIABLO/Smac is produced by the IMP protease complex on the mitochondrial inner membrane. *Mol Biol Cell* *16*, 2926-2933.
- Campbell, C. L., Tanaka, N., White, K. H., and Thorsness, P. E. (1994). Mitochondrial morphological and functional defects in yeast caused by *yme1* are suppressed by mutation of a 26S protease subunit homologue. *Mol Biol Cell* *5*, 899-905.
- Campbell, C. L., and Thorsness, P. E. (1998). Escape of mitochondrial DNA to the nucleus in *yme1* yeast is mediated by vacuolar-dependent turnover of abnormal mitochondrial compartments. *J Cell Sci* *111*, 2455-2464.
- Casari, G., De-Fusco, M., Ciarmatori, S., Zeviani, M., Mora, M., Fernandez, P., DeMichele, G., Filla, A., Coccozza, S., Marconi, R., *et al.* (1998). Spastic paraplegia and OXPHOS impairment caused by mutations in paraplegin, a nuclear-encoded mitochondrial metalloprotease. *Cell* *93*, 973-983.
- Cerneus, D. P., Ueffing, E., Posthuma, G., Strous, G. J., and van der Ende, A. (1993). Detergent insolubility of alkaline phosphatase during biosynthetic transport and endocytosis. Role of cholesterol. *J Biol Chem* *268*, 3150-3155.
- Cervený, K. L., Tamura, Y., Zhang, Z., Jensen, R. E., and Sesaki, H. (2007). Regulation of mitochondrial fusion and division. *Trends Cell Biol* *17*, 563-569.
- Chan, D. C. (2006). Mitochondria: dynamic organelles in disease, aging, and development. *Cell* *125*, 1241-1252.
- Chang, S. C., Heacock, P. N., Clancey, C. J., and Dowhan, W. (1998). The PEL1 gene (renamed PGS1) encodes the phosphatidylglycero-phosphate synthase of *Saccharomyces cerevisiae*. *J Biol Chem* *273*, 9829-9836.
- Chang, S. C., Heacock, P. N., Mileykovskaya, E., Voelker, D. R., and Dowhan, W. (1998). Isolation and characterization of the gene (CLS1) encoding cardiolipin synthase in *Saccharomyces cerevisiae*. *J Biol Chem* *273*, 14933-14941.
- Chelstowska, A., Liu, Z., Jia, Y., Amberg, D., and Butow, R. A. (1999). Signalling between mitochondria and the nucleus regulates the expression of a new D-lactate dehydrogenase activity in yeast. *Yeast* *15*, 1377-1391.
- Chen, X. J., and Clark-Walker, G. D. (1999). Alpha and beta subunits of F1-ATPase are required for survival of petite mutants in *Saccharomyces cerevisiae*. *Mol Gen Genet* *262*, 898-908.

- Chew, A., Rollins, R. A., Sakati, W. R., and Isaya, G. (1996). Mutations in a putative zinc-binding domain inactivate the mitochondrial intermediate peptidase. *Biochem Biophys Res Commun* *226*, 822-829. Order.
- Choi, J. Y., Riekhof, W. R., Wu, W. I., and Voelker, D. R. (2006). Macromolecular assemblies regulate nonvesicular phosphatidylserine traffic in yeast. *Biochem Soc Trans* *34*, 404-408.
- Clancey, C. J., Chang, S. C., and Dowhan, W. (1993). Cloning of a gene (PSD1) encoding phosphatidylserine decarboxylase from *Saccharomyces cerevisiae* by complementation of an *Escherichia coli* mutant. *J Biol Chem* *268*, 24580-24590.
- Claypool, S. M., McCaffery, J. M., and Koehler, C. M. (2006). Mitochondrial mislocalization and altered assembly of a cluster of Barth syndrome mutant tafazzins. *J Cell Biol* *174*, 379-390.
- Cobine, P. A., Pierrel, F., and Winge, D. R. (2006). Copper trafficking to the mitochondrion and assembly of copper metalloenzymes. *Biochim Biophys Acta* *1763*, 759-772.
- Colombo, S., Longhi, R., Alcaro, S., Ortuso, F., Sprocati, T., Flora, A., and Borgese, N. (2005). N-myristoylation determines dual targeting of mammalian NADH-cytochrome b5 reductase to ER and mitochondrial outer membranes by a mechanism of kinetic partitioning. *J Cell Biol* *168*, 735-745.
- Crowley, J. H., Leak, F. W., Jr., Shianna, K. V., Tove, S., and Parks, L. W. (1998). A mutation in a purported regulatory gene affects control of sterol uptake in *Saccharomyces cerevisiae*. *J Bacteriol* *180*, 4177-4183.
- Czabany, T., Athenstaedt, K., and Daum, G. (2007). Synthesis, storage and degradation of neutral lipids in yeast. *Biochim Biophys Acta* *1771*, 299-309.
- Czabany, T., Wagner, A., Zweytick, D., Lohner, K., Leitner, E., Ingolic, E., and Daum, G. (2008). Structural and biochemical properties of lipid particles from the yeast *Saccharomyces cerevisiae*. *J Biol Chem* *283*, 17065-17074.
- Daignan-Fornier, B., Nguyen, C. C., Reisdorf, P., Lemeignan, B., and Bolotin-Fukuhara, M. (1994). MBR1 and MBR3, two related yeast genes that can suppress the growth defect of hap2, hap3 and hap4 mutants. *Mol Gen Genet* *243*, 575-583.
- Dalbey, R. E., Lively, M. O., Bron, S., and van Dijl, J. M. (1997). The chemistry and enzymology of the type I signal peptidase. *Protein Sci* *6*, 1129-1138.
- Daum, G., Lees, N. D., Bard, M., and Dickson, R. (1998). Biochemistry, cell biology and molecular biology of lipids of *Saccharomyces cerevisiae*. *Yeast* *14*, 1471-1510.
- Desautels, M., and Goldberg, A. L. (1982). Liver mitochondria contain an ATP-dependent, vanadate-sensitive pathway for the degradation of proteins. *Proc Natl Acad Sci USA* *79*, 1869-1873.
- Detmer, S. A., and Chan, D. C. (2007). Functions and dysfunctions of mitochondrial dynamics. *Nat Rev Mol Cell Biol* *8*, 870-879.
- di Rago, J. P., Sohm, F., Boccia, C., Dujardin, G., Trumpower, B. L., and Slonimski, P. P. (1997). A point mutation in the mitochondrial cytochrome b gene obviates the requirement for the nuclear encoded core protein 2 subunit in the cytochrome bc1 complex in *Saccharomyces cerevisiae*. *J Biol Chem* *272*, 4699-4704.
- Dimmer, K. S., Fritz, S., Fuchs, F., Messerschmitt, M., Weinbach, N., Neupert, W., and Westermann, B. (2002). Genetic basis of mitochondrial function and morphology in *Saccharomyces cerevisiae*. *Mol Biol Cell* *13*, 847-853.

- Dimmer, K. S., Jakobs, S., Vogel, F., Altmann, K., and Westermann, B. (2005). Mdm31 and Mdm32 are inner membrane proteins required for maintenance of mitochondrial shape and stability of mitochondrial DNA nucleoids in yeast. *J Cell Biol* *168*, 103-115.
- Dunn, C. D., Lee, M. S., Spencer, F. A., and Jensen, R. E. (2006). A genomewide screen for petite-negative yeast strains yields a new subunit of the *i*-AAA protease complex. *Mol Biol Cell* *17*, 213-226.
- Dunn, C. D., Y., T., H., S., and Jensen, R. E. (2008). Mgr3p and Mgr1p are adaptors for the mitochondrial *i*-AAA protease complex. *Mol Biol Cell* *19*, 5387-5397.
- Esser, K., Jan, P. S., Pratje, E., and Michaelis, G. (2004). The mitochondrial IMP peptidase of yeast: functional analysis of domains and identification of Gut2 as a new natural substrate. *Mol Genet Genomics* *271*, 616-626.
- Esser, K., Pratje, E., and Michaelis, G. (1996). SOM 1, a small new gene required for mitochondrial inner membrane peptidase function in *Saccharomyces cerevisiae*. *Mol Gen Genet* *252*, 437-445.
- Esser, K., Tursun, B., Ingenhoven, M., Michaelis, G., and Pratje, E. (2002). A novel two-step mechanism for removal of a mitochondrial signal sequence involves the *m*-AAA complex and the putative rhomboid protease Pcp1. *J Mol Biol* *323*, 835-843.
- Fei, W., Alfaro, G., Muthusamy, B. P., Klaassen, Z., Graham, T. R., Yang, H., and Beh, C. T. (2008). Genome-wide analysis of sterol-lipid storage and trafficking in *Saccharomyces cerevisiae*. *Eukaryot Cell* *7*, 401-414.
- Flynn, J. M., Neher, S. B., Kim, Y. I., Sauer, R. T., and Baker, T. A. (2003). Proteomic discovery of cellular substrates of the ClpXP protease reveals five classes of ClpX-recognition signals. *Mol Cell* *11*, 671-683.
- Folsch, H., Guiard, B., Neupert, W., and Stuart, R. A. (1996). Internal targeting signal of the BCS1 protein: a novel mechanism of import into mitochondria. *Embo J* *15*, 479-487.
- Francis, B. R., White, K. H., and Thorsness, P. E. (2007). Mutations in the Atp1p and Atp3p subunits of yeast ATP synthase differentially affect respiration and fermentation in *Saccharomyces cerevisiae*. *J Bioenerg Biomembr* *39*, 127-144.
- Frazier, A. E., Taylor, R. D., Mick, D. U., Warscheid, B., Stoepel, N., Meyer, H. E., Ryan, M. T., Guiard, B., and Rehling, P. (2006). Mdm38 interacts with ribosomes and is a component of the mitochondrial protein export machinery. *J Cell Biol* *172*, 553-564.
- Freeman, M. (2008). Rhomboid proteases and their biological functions. *Annu Rev Genet* *42*, 191-210.
- Froschauer, E., Nowikovsky, K., and Schweyen, R. J. (2005). Electroneutral K⁺/H⁺ exchange in mitochondrial membrane vesicles involves Yol027/Letm1 proteins. *Biochim Biophys Acta* *1711*, 41-48.
- Gabriel, K., Milenkovic, D., Chacinska, A., Muller, J., Guiard, B., Pfanner, N., and Meisinger, C. (2007). Novel mitochondrial intermembrane space proteins as substrates of the MIA import pathway. *J Mol Biol* *365*, 612-620.
- Gaigg, B., Simbeni, R., Hrastnik, C., Paltauf, F., and Daum, G. (1995). Characterization of a microsomal subfraction associated with mitochondria of the yeast, *Saccharomyces cerevisiae*. Involvement in synthesis and import of phospholipids into mitochondria. *Biochim Biophys Acta* *1234*, 214-220.
- Gakh, O., Cavadini, P., and Isaya, G. (2002). Mitochondrial processing peptidases. *Biochim Biophys Acta* *1592*, 63-77.

- Gencic, S., Schagger, H., and von Jagow, G. (1991). Core I protein of bovine ubiquinol-cytochrome-c reductase; an additional member of the mitochondrial-protein-processing family. Cloning of bovine core I and core II cDNAs and primary structure of the proteins. *Eur J Biochem* *199*, 123-131.
- Gietz, R. D., and Sugino, A. (1988). New yeast-*Escherichia coli* shuttle vectors constructed with *in vitro* mutagenized yeast genes lacking six-base pair restriction sites. *Gene* *74*, 527-534.
- Gietz, R. D., and Woods, R. A. (2002). Transformation of yeast by lithium acetate/single-stranded carrier DNA/polyethylene glycol method. *Methods Enzymol* *350*, 87-96.
- Glaser, E., and Dessi, P. (1999). Integration of the mitochondrial-processing peptidase into the cytochrome bc1 complex in plants. *J Bioenerg Biomembr* *31*, 259-274.
- Goldstein, A. L., and McCusker, J. H. (1999). Three new dominant drug resistance cassettes for gene disruption in *Saccharomyces cerevisiae*. *Yeast* *15*, 1541-1553.
- Gottesman, S. (2003). Proteolysis in bacterial regulatory circuits. *Annu Rev Cell Dev Biol* *19*, 565-587.
- Graef, M., and Langer, T. (2006). Substrate specific consequences of central pore mutations in the β -AAA protease Yme1 on substrate engagement. *J Struct Biol* *151*, 101-108.
- Graef, M., Langer, T., and Engmann, T. (2008). The recognition of substrates by AAA proteases in mitochondria. In: ATP-dependent proteases. ATP-dependent proteases Ed Eva KutejováResearch Signpost, Kerala, India, 179-195.
- Graef, M., Seewald, G., and Langer, T. (2007). Substrate recognition by AAA⁺ ATPases: Distinct substrate binding modes in the ATP-dependent protease Yme1 of the mitochondrial intermembrane space. *Mol Cell Biol* *in press*.
- Grandier-Vazeille, X., Bathany, K., Chaignepain, S., Camougrand, N., Manon, S., and Schmitter, J. M. (2001). Yeast mitochondrial dehydrogenases are associated in a supramolecular complex. *Biochemistry* *40*, 9758-9769.
- Griparic, L., Kanazawa, T., and van der Blik, A. M. (2007). Regulation of the mitochondrial dynamin-like protein Opa1 by proteolytic cleavage. *J Cell Biol* *178*, 757-764.
- Guiard, B. (1985). Structure, expression and regulation of a nuclear gene encoding a mitochondrial protein: the yeast L(+)-lactate cytochrome c oxidoreductase (cytochrome b2). *Embo J* *4*, 3265-3272.
- Guillery, O., Malka, F., Landes, T., Guillou, E., Blackstone, C., Lombes, A., Belenguer, P., Arnoult, D., and Rojo, M. (2008). Metalloprotease-mediated OPA1 processing is modulated by the mitochondrial membrane potential. *Biol Cell* *100*, 315-325.
- Guo, F., Esser, L., Singh, S. K., Maurizi, M. R., and Xia, D. (2002). Crystal structure of the heterodimeric complex of the adaptor, ClpS, with the N-domain of the AAA+ chaperone, ClpA. *J Biol Chem* *277*, 46753-46762.
- Hahne, K., Haucke, V., Ramage, L., and Schatz, G. (1994). Incomplete arrest in the outer membrane sorts NADH-cytochrome b5 reductase to two different submitochondrial compartments. *Cell* *79*, 829-839.
- Halpin, C., Elderfield, P. D., James, H. E., Zimmermann, R., Dunbar, B., and Robinson, C. (1989). The reaction specificities of the thylakoidal processing peptidase and *Escherichia coli* leader peptidase are identical. *EMBO J* *8*, 3917-3921.
- Hamza, I. (2006). Intracellular trafficking of porphyrins. *ACS Chem Biol* *1*, 627-629.
- Hanson, P. I., and Whiteheart, S. W. (2005). AAA+ proteins: have engine, will work. *Nat Rev Mol Cell Biol* *6*, 519-529.

- Hartl, F. U., Ostermann, J., Guiard, B., and Neupert, W. (1987). Successive translocation into and out of the mitochondrial matrix: targeting of proteins to the intermembrane space by a bipartite signal peptide. *Cell* *51*, 1027-1037.
- Hata, S., Nishino, T., Komori, M., and Katsuki, H. (1981). Involvement of cytochrome P-450 in delta 22-desaturation in ergosterol biosynthesis of yeast. *Biochem Biophys Res Commun* *103*, 272-277.
- Hawlitschek, G., Schneider, H., Schmidt, B., Tropschug, M., Hartl, F. U., and Neupert, W. (1988). Mitochondrial protein import: identification of processing peptidase and of PEP, a processing enhancing protein. *Cell* *53*, 795-806.
- Hegde, R., Srinivasula, S. M., Zhang, Z., Wassell, R., Mukattash, R., Cilenti, L., DuBois, G., Lazebnik, Y., Zervos, A. S., Fernandes-Alnemri, T., and Alnemri, E. S. (2002). Identification of Omi/HtrA2 as a mitochondrial apoptotic serine protease that disrupts inhibitor of apoptosis protein-caspase interaction. *J Biol Chem* *277*, 432-438.
- Herlan, M., Vogel, F., Bornhövd, C., Neupert, W., and Reichert, A. S. (2003). Processing of Mgm1 by the rhomboid-type protease Pcp1 is required for maintenance of mitochondrial morphology and of mitochondrial DNA. *J Biol Chem* *278*, 27781-27788.
- Herman, C., Prakash, S., Lu, C. Z., Matouschek, A., and Gross, C. A. (2003). Lack of a robust unfoldase activity confers a unique level of substrate specificity to the universal AAA protease FtsH. *Mol Cell* *11*, 659-669.
- Herrmann, J. M., and Funes, S. (2005). Biogenesis of cytochrome oxidase-sophisticated assembly lines in the mitochondrial inner membrane. *Gene* *354*, 43-52.
- Hinnerwisch, J., Fenton, W. A., Furtak, K. J., Farr, G. W., and Horwich, A. L. (2005). Loops in the central channel of ClpA chaperone mediate protein binding, unfolding, and translocation. *Cell* *121*, 1029-1041.
- Hinnerwisch, J., Reid, B. G., Fenton, W. A., and Horwich, A. L. (2005). Roles of the N-domains of the ClpA unfoldase in binding substrate proteins and in stable complex formation with the ClpP protease. *J Biol Chem* *280*, 40838-40844.
- Hiser, L., Di Valentin, M., Hamer, A. G., and Hosler, J. P. (2000). Cox11p is required for stable formation of the Cu(B) and magnesium centers of cytochrome c oxidase. *J Biol Chem* *275*, 619-623.
- Hishida, T., Han, Y. W., Fujimoto, S., Iwasaki, H., and Shinagawa, H. (2004). Direct evidence that a conserved arginine in RuvB AAA+ ATPase acts as an allosteric effector for the ATPase activity of the adjacent subunit in a hexamer. *Proc Natl Acad Sci U S A* *101*, 9573-9577.
- Hitzeman, R. A., Clarke, L., and Carbon, J. (1980). Isolation and characterization of the yeast 3-phosphoglycerokinase gene (PGK) by an immunological screening technique. *J Biol Chem* *255*, 12073-12080.
- Hoppins, S., Lackner, L., and Nunnari, J. (2007). The machines that divide and fuse mitochondria. *Annu Rev Biochem* *76*, 751-780.
- Hoskins, J. R., Yanagihara, K., Mizuuchi, K., and Wickner, S. (2002). ClpAP and ClpXP degrade proteins with tags located in the interior of the primary sequence. *Proc Natl Acad Sci U S A* *99*, 11037-11042.
- Hunakova, A., Daum, G., and Hapala, I. (1997). Changes in cellular ergosterol distribution in intramitochondrial energy-depleted *Saccharomyces cerevisiae* cells. *Folia Microbiol (Praha)* *42*, 229-231.
- Ikonen, E. (2008). Cellular cholesterol trafficking and compartmentalization. *Nat Rev Mol Cell Biol* *9*, 125-138.

- Inadome, H., Noda, Y., Adachi, H., and Yoda, K. (2001). A novel protein, Mpm1, of the mitochondria of the yeast *Saccharomyces cerevisiae*. *Biosci Biotechnol Biochem* *65*, 2577-2580.
- Isaya, G., Kalousek, F., and Rosenberg, L. E. (1992). Amino-terminal octapeptides function as recognition signals for the mitochondrial intermediate peptidase. *J Biol Chem* *267*, 7904-7910.
- Isaya, G., Miklos, D., and Rollins, R. A. (1994). *MIP1*, a new yeast gene homologous to the rat mitochondrial intermediate peptidase gene, is required for oxidative metabolism in *Saccharomyces cerevisiae*. *Mol Cell Biol* *14*, 5603-5616.
- Ishii, T., Hasegawa, T., Pai, C. I., Yvigi-Ohana, N., Timberg, R., Zhao, L., Majdic, G., Chung, B. C., Orly, J., and Parker, K. L. (2002). The roles of circulating high-density lipoproteins and trophic hormones in the phenotype of knockout mice lacking the steroidogenic acute regulatory protein. *Mol Endocrinol* *16*, 2297-2309.
- Ishikawa, T., Maurizi, M. R., and Steven, A. C. (2004). The N-terminal substrate-binding domain of ClpA unfoldase is highly mobile and extends axially from the distal surface of ClpAP protease. *J Struct Biol* *146*, 180-188.
- Ito, K., and Akiyama, Y. (2005). Cellular functions, mechanism of action, and regulation of FtsH protease. *Ann Rev Microbiol* *59*, 211-231.
- Iyer, L. M., Leipe, D. D., Koonin, E. V., and Aravind, L. (2004). Evolutionary history and higher order classification of AAA+ ATPases. *J Struct Biol* *146*, 11-31.
- Jakovcic, S., Getz, G. S., Rabinowitz, M., Jakob, H., and Swift, H. (1971). Cardiolipin content of wild type and mutant yeasts in relation to mitochondrial function and development. *J Cell Biol* *48*, 490-502.
- Jan, P. S., Esser, K., Pratje, E., and Michaelis, G. (2000). Som1, a third component of the yeast mitochondrial inner membrane protease complex that contains Imp1 and Imp2. *Mol Gen Genet* *263*, 483-491.
- Janke, C., Magiera, M. M., Rathfelder, N., Taxis, C., Reber, S., Maekawa, H., Moreno-Borchart, A., Doenges, G., Schwob, E., Schiebel, E., and Knop, M. (2004). A versatile toolbox for PCR-based tagging of yeast genes: new fluorescent proteins, more markers and promoter substitution cassettes. *Yeast* *21*, 947-962.
- Joshi, A. S., Zhou, J., Gohil, V. M., Chen, S., and Greenberg, M. L. (2008). Cellular functions of cardiolipin in yeast. *Biochim Biophys Acta*.
- Kalousek, F., Hendrick, J. P., and Rosenberg, L. E. (1988). Two mitochondrial matrix proteases act sequentially in the processing of mammalian matrix enzymes. *Proc Natl Acad Sci U S A* *85*, 7536-7540.
- Kambacheld, M., Augustin, S., Tatsuta, T., Muller, S., and Langer, T. (2005). Role of the novel metallopeptidase Mop112 and saccharolysin for the complete degradation of proteins residing in different subcompartments of mitochondria. *J Biol Chem* *280*, 20132-20139.
- Kaput, J., Goltz, S., and Blobel, G. (1982). Nucleotide sequence of the yeast nuclear gene for cytochrome *c* peroxidase precursor. Functional implications of the pre sequence for protein transport into mitochondria. *J Biol Chem* *257*, 15054-15058.
- Karata, K., Inagawa, T., Wilkinson, A. J., Tatsuta, T., and Ogura, T. (1999). Dissecting the role of a conserved motif (the second region of homology) in the AAA family of ATPases. Site-directed mutagenesis of the ATP-dependent protease FtsH. *J Biol Chem* *274*, 26225-26232.
- Käser, M., Kambacheld, M., Kisters-Woike, B., and Langer, T. (2003). Oma1, a novel membrane-bound metallopeptidase in mitochondria with activities overlapping with the *m*-AAA protease. *J Biol Chem* *278*, 46414-46423.

- Keiler, K. C., Waller, P. R., and Sauer, R. T. (1996). Role of a peptide tagging system in degradation of proteins synthesized from damaged messenger RNA. *Science* *271*, 990-993.
- Kenniston, J. A., Baker, T. A., Fernandez, J. M., and Sauer, R. T. (2003). Linkage between ATP consumption and mechanical unfolding during the protein processing reactions of an AAA+ degradation machine. *Cell* *114*, 511-520.
- Kent, C. (1995). Eukaryotic phospholipid biosynthesis. *Annu Rev Biochem* *64*, 315-343.
- Kim, D. Y., and Kim, K. K. (2003). Crystal structure of ClpX molecular chaperone from *Helicobacter pylori*. *J Biol Chem* *278*, 50664-50670.
- Kim, I., Rodriguez-Enriquez, S., and Lemasters, J. J. (2007). Selective degradation of mitochondria by mitophagy. *Arch Biochem Biophys* *462*, 245-253.
- Klanner, C., Prokisch, H., and Langer, T. (2001). MAP-1 and IAP-1, two novel AAA proteases with catalytic sites on opposite membrane surfaces in the mitochondrial inner membrane of *Neurospora crassa*. *Mol Biol Cell* *12*, 2858-2869.
- Kleinhans, F. W., Lees, N. D., Bard, M., Haak, R. A., and Woods, R. A. (1979). ESR determinations of membrane permeability in a yeast sterol mutant. *Chem Phys Lipids* *23*, 143-154.
- Köffel, R., Tiwari, R., Falquet, L., and Schneider, R. (2005). The *Saccharomyces cerevisiae* YLL012/YEH1, YLR020/YEH2, and TGL1 genes encode a novel family of membrane-anchored lipases that are required for sterol ester hydrolysis. *Mol Cell Biol* *25*, 1655-1668.
- Kominsky, D. J., Brownson, M. P., Updike, D. L., and Thorsness, P. E. (2002). Genetic and biochemical basis for viability of yeast lacking mitochondrial genomes. *Genetics* *162*, 1595-1604.
- Koppen, M., and Langer, T. (2007). Protein degradation within mitochondria: versatile activities of AAA proteases and other peptidases. *Crit Rev Biochem Mol Biol* *42*, 221-242.
- Koppen, M., Metodiev, M. D., Casari, G., Rugarli, E. I., and Langer, T. (2007). Variable and Tissue-Specific Subunit Composition of Mitochondrial *m*-AAA Protease Complexes Linked to Hereditary Spastic Paraplegia. *Mol Cell Biol* *27*, 758-767.
- Korbel, D., Wurth, S., Käser, M., and Langer, T. (2004). Membrane protein turnover by the *m*-AAA protease in mitochondria depends on the transmembrane domains of its subunits. *EMBO Rep* *5*, 698-703.
- Kornblatt, J. A., and Rudney, H. (1971). Two forms of acetoacetyl coenzyme A thiolase in yeast. II. Intracellular location and relationship to growth. *J Biol Chem* *246*, 4424-4430.
- Kozak, M. (1987). An analysis of 5'-noncoding sequences from 699 vertebrate messenger RNAs. *Nucleic Acids Res* *15*, 8125-8148.
- Kuchler, K., Daum, G., and Paltauf, F. (1986). Subcellular and submitochondrial localization of phospholipid-synthesizing enzymes in *Saccharomyces cerevisiae*. *J Bacteriol* *165*, 901-910.
- Lamb, D. C., Kelly, D. E., Manning, N. J., Kaderbhai, M. A., and Kelly, S. L. (1999). Biodiversity of the P450 catalytic cycle: yeast cytochrome b5/NADH cytochrome b5 reductase complex efficiently drives the entire sterol 14-demethylation (CYP51) reaction. *FEBS Lett* *462*, 283-288.
- Lämmli, U. K. (1970). Cleavage of structural proteins during the assembly of the head of bacteriophage T4. *Nature* *227*, 680-685.
- Lee, J. S., Huh, W. K., Lee, B. H., Baek, Y. U., Hwang, C. S., Kim, S. T., Kim, Y. R., and Kang, S. O. (2001). Mitochondrial NADH-cytochrome b(5) reductase plays a crucial role in the reduction of D-erythroascorbyl free radical in *Saccharomyces cerevisiae*. *Biochim Biophys Acta* *1527*, 31-38.

- Lees, N. D., Bard, M., Kemple, M. D., Haak, R. A., and Kleinhans, F. W. (1979). ESR determination of membrane order parameter in yeast sterol mutants. *Biochim Biophys Acta* 553, 469-475.
- Lemaire, C., Hamel, P., Velours, J., and Dujardin, G. (2000). Absence of the mitochondrial AAA protease Yme1p restores F₀-ATPase subunit accumulation in an *oxa1* deletion mutant of *Saccharomyces cerevisiae*. *J Biol Chem* 275, 23471-23475.
- Leonhard, K., Guiard, B., Pellechia, G., Tzagoloff, A., Neupert, W., and Langer, T. (2000). Membrane protein degradation by AAA proteases in mitochondria: extraction of substrates from either membrane surface. *Mol Cell* 5, 629-638.
- Leonhard, K., Herrmann, J. M., Stuart, R. A., Mannhaupt, G., Neupert, W., and Langer, T. (1996). AAA proteases with catalytic sites on opposite membrane surfaces comprise a proteolytic system for the ATP-dependent degradation of inner membrane proteins in mitochondria. *EMBO J* 15, 4218-4229.
- Leonhard, K., Stiegler, A., Neupert, W., and Langer, T. (1999). Chaperone-like activity of the AAA domain of the yeast Yme1 AAA protease. *Nature* 398, 348-351.
- Levchenko, I., Seidel, M., Sauer, R. T., and Baker, T. A. (2000). A specificity-enhancing factor for the ClpXP degradation machine. *Science* 289, 2354-2356.
- Lewis, T. A., Taylor, F. R., and Parks, L. W. (1985). Involvement of heme biosynthesis in control of sterol uptake by *Saccharomyces cerevisiae*. *J Bacteriol* 163, 199-207.
- Liang, H., Luo, W., Green, N., and Fang, H. (2004). Cargo sequences are important for Som1p-dependent signal peptide cleavage in yeast mitochondria. *J Biol Chem* 279, 39396-39400.
- Licht, S., and Lee, I. (2008). Resolving individual steps in the operation of ATP-dependent proteolytic molecular machines: from conformational changes to substrate translocation and processivity. *Biochemistry* 47, 3595-3605.
- Lill, R., and Muhlenhoff, U. (2006). Iron-Sulfur Protein Biogenesis in Eukaryotes: Components and Mechanisms. *Annu Rev Cell Dev Biol*.
- Lill, R., and Muhlenhoff, U. (2008). Maturation of iron-sulfur proteins in eukaryotes: mechanisms, connected processes, and diseases. *Annu Rev Biochem* 77, 669-700.
- Lin, M. T., and Beal, M. F. (2006). Mitochondrial dysfunction and oxidative stress in neurodegenerative diseases. *Nature* 443, 787-795.
- Liu, T., Lu, B., Lee, I., Ondrovicova, G., Kutejova, E., and Suzuki, C. K. (2004). DNA and RNA binding by the mitochondrial lon protease is regulated by nucleotide and protein substrate. *J Biol Chem* 279, 13902-13910.
- Lodi, T., and Ferrero, I. (1993). Isolation of the DLD gene of *Saccharomyces cerevisiae* encoding the mitochondrial enzyme D-lactate ferricytochrome c oxidoreductase. *Mol Gen Genet* 238, 315-324.
- Longtine, M. S., McKenzie, A., 3rd, Demarini, D. J., Shah, N. G., Wach, A., Brachat, A., Philippsen, P., and Pringle, J. R. (1998). Additional modules for versatile and economical PCR-based gene deletion and modification in *Saccharomyces cerevisiae*. *Yeast* 14, 953-961.
- Lorenz, R. T., and Parks, L. W. (1991). Involvement of heme components in sterol metabolism of *Saccharomyces cerevisiae*. *Lipids* 26, 598-603.
- Lorenz, R. T., Rodriguez, R. J., Lewis, T. A., and Parks, L. W. (1986). Characteristics of sterol uptake in *Saccharomyces cerevisiae*. *J Bacteriol* 167, 981-985.
- Luciano, P., Geoffroy, S., Brandt, A., Hernandez, J. F., and Geli, V. (1997). Functional cooperation of the mitochondrial processing peptidase subunits. *J Mol Biol* 272, 213-225.

- Luo, W., Fang, H., and Green, N. (2006). Substrate specificity of inner membrane peptidase in yeast mitochondria. *Mol Genet Genomics* *275*, 431-436.
- Lupas, A. N., and Martin, J. (2002). AAA proteins. *Curr Opin Struct Biol* *12*, 746-753.
- Martin, A., Baker, T. A., and Sauer, R. T. (2005). Rebuilt AAA + motors reveal operating principles for ATP-fuelled machines. *Nature* *437*, 1115-1120.
- Martin, A., Baker, T. A., and Sauer, R. T. (2008). Pore loops of the AAA+ ClpX machine grip substrates to drive translocation and unfolding. *Nat Struct Mol Biol* *15*, 1147-1151.
- Martins, L. M., Morrison, A., Klupsch, K., Fedele, V., Moiso, N., Teismann, P., Abuin, A., Grau, E., Geppert, M., Livi, G. P., *et al.* (2004). Neuroprotective role of the Reaper-related serine protease HtrA2/Omi revealed by targeted deletion in mice. *Mol Cell Biol* *24*, 9848-9862.
- Mazzoni, C., Torella, M., Petrera, A., Palermo, V., and Falcone, C. (2009). PGK1, the gene encoding the glycolytic enzyme phosphoglycerate kinase, acts as a multicopy suppressor of apoptotic phenotypes in *S. cerevisiae*. *Yeast* *26*, 31-37.
- McBride, H. M., Neuspiel, M., and Wasiak, S. (2006). Mitochondria: more than just a powerhouse. *Curr Biol* *16*, R551-560.
- McConnell, H. M., and Radhakrishnan, A. (2003). Condensed complexes of cholesterol and phospholipids. *Biochim Biophys Acta* *1610*, 159-173.
- Meineke, B., Engl, G., Kemper, C., Vasiljev-Neumeyer, A., Paulitschke, H., and Rapaport, D. (2008). The outer membrane form of the mitochondrial protein Mcr1 follows a TOM-independent membrane insertion pathway. *FEBS Lett* *582*, 855-860.
- Miller, W. L. (1997). Congenital lipid adrenal hyperplasia: the human gene knockout for the steroidogenic acute regulatory protein. *J Mol Endocrinol* *19*, 227-240.
- Miller, W. L. (2007). StAR search--what we know about how the steroidogenic acute regulatory protein mediates mitochondrial cholesterol import. *Mol Endocrinol* *21*, 589-601.
- Miran, S. G., Lawson, J. E., and Reed, L. J. (1993). Characterization of PDH beta 1, the structural gene for the pyruvate dehydrogenase beta subunit from *Saccharomyces cerevisiae*. *Proc Natl Acad Sci U S A* *90*, 1252-1256.
- Moberg, P., Stahl, A., Bhushan, S., Wright, S. J., Eriksson, A. C., Bruce, B. D., and Glaser, E. (2003). Characterization of a novel zinc metalloprotease involved in degrading targeting peptides in mitochondria and chloroplasts. *The Plant J* *36*, 616-628.
- Moffitt, J. R., Chemla, Y. R., Athavan, K., Grimes, S., Jardine, P. J., Anderson, D. L., and Bustamante, C. (2009). Intersubunit coordination in a homomeric ring ATPase. *Nature*.
- Mootha, V. K., Bunkenborg, J., Olsen, J. V., Hjerrild, M., Wisniewski, J. R., Stahl, E., Bolouri, M. S., Ray, H. N., Sihag, S., Kamal, M., *et al.* (2003). Integrated analysis of protein composition, tissue diversity, and gene regulation in mouse mitochondria. *Cell* *115*, 629-640.
- Moss, G. P. (1989). IUPAC-IUB Joint Commission on Biochemical Nomenclature (JCBN). The nomenclature of steroids. Recommendations 1989. *Eur J Biochem* *186*, 429-458.
- Nakai, M., Kinoshita, K., and Endo, T. (1995). Mitochondrial receptor complex protein. The intermembrane space domain of yeast MAS17 is not essential for its targeting or function. *J Biol Chem* *270*, 30571-30575.

- Nakai, T., Yasuhara, T., Fujiki, Y., and Ohashi, A. (1995). Multiple genes, including a member of the AAA family, are essential for the degradation of unassembled subunit 2 of cytochrome *c* oxidase in yeast mitochondria. *Mol Cell Biol* *15*, 4441-4452.
- Nebauer, R., Schuiki, I., Kulterer, B., Trajanoski, Z., and Daum, G. (2007). The phosphatidylethanolamine level of yeast mitochondria is affected by the mitochondrial components Oxa1p and Yme1p. *FEBS J* *274*, 6180-6190.
- Neher, S. B., Flynn, J. M., Sauer, R. T., and Baker, T. A. (2003). Latent ClpX-recognition signals ensure LexA destruction after DNA damage. *Genes Dev* *17*, 1084-1089.
- Neuhoff, V., Stamm, R., Pardowitz, I., Arold, N., Ehrhardt, W., and Taube, D. (1990). Essential problems in quantification of proteins following colloidal staining with coomassie brilliant blue dyes in polyacrylamide gels, and their solution. *Electrophoresis* *11*, 101-117.
- Neupert, W., and Herrmann, J. M. (2007). Translocation of proteins into mitochondria. *Annu Rev Biochem* *76*, 723-749.
- Neuwald, A. F., Aravind, L., Spouge, J. L., and Koonin, E. V. (1999). AAA+: A class of chaperone-like ATPases associated with the assembly, operation, and disassembly of protein complexes. *Genome Res* *9*, 27-43.
- Nishii, W., Maruyama, T., Matsuoka, R., Muramatsu, T., and Takahashi, K. (2002). The unique sites in SulA protein preferentially cleaved by ATP-dependent Lon protease from *Escherichia coli*. *Eur J Biochem* *269*, 451-457.
- Nolden, M., Ehses, S., Koppen, M., Bernacchia, A., Rugarli, E. I., and Langer, T. (2005). The *m*-AAA protease defective in hereditary spastic paraplegia controls ribosome assembly in mitochondria. *Cell* *123*, 277-289.
- Nunnari, J., Fox, T. D., and Walter, P. (1993). A mitochondrial protease with two catalytic subunits of nonoverlapping specificities. *Science* *262*, 1997-2004.
- Ogura, T., Whiteheart, S. W., and Wilkinson, A. J. (2004). Conserved arginine residues implicated in ATP hydrolysis, nucleotide-sensing, and inter-subunit interactions in AAA and AAA+ ATPases. *J Struct Biol* *146*, 106-112.
- Ogura, T., and Wilkinson, A. J. (2001). AAA+ superfamily of ATPases: common structure-diverse function. *Genes to Cells* *6*, 575-597.
- Okuno, T., Yamanaka, K., and Ogura, T. (2006). An AAA protease FtsH can initiate proteolysis from internal sites of a model substrate, apo-flavodoxin. *Genes Cells* *11*, 261-268.
- Ondrovicova, G., Liu, T., Singh, K., Tian, B., Li, H., Gakh, O., Perecko, D., Janata, J., Granot, Z., Orly, J., *et al.* (2005). Cleavage site selection within a folded substrate by the ATP-dependent Lon protease. *J Biol Chem* *280*, 25103-25110.
- Osman, C., Haag, M., Potting, C., Rodenfels, J., Dip, P. V., Wieland, F. T., Brugger, B., Westermann, B., and Langer, T. (2009). The genetic interactome of prohibitins: coordinated control of cardiolipin and phosphatidylethanolamine by conserved regulators in mitochondria. *J Cell Biol*.
- Osman, C., Wilmes, C., Tatsuta, T., and Langer, T. (2007). Prohibitins Interact Genetically with Atp23, a Novel Processing Peptidase and Chaperone for the F₁F₀-ATP Synthase. *Mol Biol Cell* *18*, 627-635.
- Ott, R. G., Athenstaedt, K., Hrastnik, C., Leitner, E., Bergler, H., and Daum, G. (2005). Flux of sterol intermediates in a yeast strain deleted of the lanosterol C-14 demethylase Erg11p. *Biochim Biophys Acta* *1735*, 111-118.

- Oudshoorn, P., Van Steeg, H., Swinkels, B. W., Schoppink, P., and Grivell, L. A. (1987). Subunit II of yeast QH2:cytochrome-c oxidoreductase. Nucleotide sequence of the gene and features of the protein. *Eur J Biochem* *163*, 97-103.
- Palermo, V., Falcone, C., and Mazzoni, C. (2007). Apoptosis and aging in mitochondrial morphology mutants of *S. cerevisiae*. *Folia Microbiol (Praha)* *52*, 479-483.
- Papadopoulos, V., Amri, H., Boujrad, N., Cascio, C., Culty, M., Garnier, M., Hardwick, M., Li, H., Vidic, B., Brown, A. S., *et al.* (1997). Peripheral benzodiazepine receptor in cholesterol transport and steroidogenesis. *Steroids* *62*, 21-28.
- Papadopoulos, V., Amri, H., Li, H., Boujrad, N., Vidic, B., and Garnier, M. (1997). Targeted disruption of the peripheral-type benzodiazepine receptor gene inhibits steroidogenesis in the R2C Leydig tumor cell line. *J Biol Chem* *272*, 32129-32135.
- Parks, L. W., and Casey, W. M. (1995). Physiological implications of sterol biosynthesis in yeast. *Annu Rev Microbiol* *49*, 95-116.
- Parks, L. W., Smith, S. J., and Crowley, J. H. (1995). Biochemical and physiological effects of sterol alterations in yeast--a review. *Lipids* *30*, 227-230.
- Pavlik, P., Simon, M., Schuster, T., and Ruis, H. (1993). The glycerol kinase (GUT1) gene of *Saccharomyces cerevisiae*: cloning and characterization. *Curr Genet* *24*, 21-25.
- Pearce, D. A., and Sherman, F. (1995). Degradation of cytochrome oxidase subunits in mutants of yeast lacking cytochrome *c* and suppression of the degradation by mutation of *yme1*. *J Biol Chem* *270*, 1-4.
- Plun-Favreau, H., Klupsch, K., Moiso, N., Gandhi, S., Kjaer, S., Frith, D., Harvey, K., Deas, E., Harvey, R. J., McDonald, N., *et al.* (2007). The mitochondrial protease HtrA2 is regulated by Parkinson's disease-associated kinase PINK1. *Nat Cell Biol* *9*, 1243-1252.
- Prakash, S., and Matouschek, A. (2004). Protein unfolding in the cell. *Trends Biochem Sci* *29*, 593-600.
- Pratje, E., and Guiard, B. (1986). One nuclear gene controls the removal of transient pre-sequences from two yeast proteins: one encoded by the nuclear the other by the mitochondrial genome. *EMBO J* *5*, 1313-1317.
- Prinz, W. A. (2007). Non-vesicular sterol transport in cells. *Prog Lipid Res* *46*, 297-314.
- Pronk, J. T., Yde Steensma, H., and Van Dijken, J. P. (1996). Pyruvate metabolism in *Saccharomyces cerevisiae*. *Yeast* *12*, 1607-1633.
- Rainey, R. N., Glavin, J. D., Chen, H. W., French, S. W., Teitell, M. A., and Koehler, C. M. (2006). A New Function in Translocation for the Mitochondrial γ -AAA Protease Yme1: Import of Polynucleotide Phosphorylase into the Intermembrane Space. *Mol Cell Biol* *26*, 8488-8497.
- Rawlings, N. D., and Barrett, A. J. (1995). Evolutionary families of metallopeptidases. *Methods Enzymol* *248*, 183-228.
- Raychaudhuri, S., and Prinz, W. A. (2006). Uptake and trafficking of exogenous sterols in *Saccharomyces cerevisiae*. *Biochem Soc Trans* *34*, 359-362.
- Reinders, J., Wagner, K., Zahedi, R. P., Stojanovski, D., Eyrich, B., van der Laan, M., Rehling, P., Sickmann, A., Pfanner, N., and Meisinger, C. (2007). Profiling phosphoproteins of yeast mitochondria reveals a role of phosphorylation in assembly of the ATP synthase. *Mol Cell Proteomics* *6*, 1896-1906.

- Reiner, S., Micolod, D., Zellnig, G., and Schneiter, R. (2006). A genomewide screen reveals a role of mitochondria in anaerobic uptake of sterols in yeast. *Mol Biol Cell* *17*, 90-103.
- Rijken, P. J., De Kruijff, B., and De Kroon, A. I. (2007). Phosphatidylcholine is essential for efficient functioning of the mitochondrial glycerol-3-phosphate dehydrogenase Gut2 in *Saccharomyces cerevisiae*. *Mol Membr Biol* *24*, 269-281.
- Rojo, E. E., Guiard, B., Neupert, W., and Stuart, R. A. (1998). Sorting of D-lactate dehydrogenase to the inner membrane of mitochondria. Analysis of topogenic signal and energetic requirements. *J Biol Chem* *273*, 8040-8047.
- Ronnow, B., and Kielland-Brandt, M. C. (1993). GUT2, a gene for mitochondrial glycerol 3-phosphate dehydrogenase of *Saccharomyces cerevisiae*. *Yeast* *9*, 1121-1130.
- Röttgers, K., Zufall, N., Guiard, B., and Voos, W. (2002). The ClpB homolog Hsp78 is required for the efficient degradation of proteins in the mitochondrial matrix. *J Biol Chem* *277*, 45829-45837.
- Rouser, G., Fkeischer, S., and Yamamoto, A. (1970). Two dimensional thin layer chromatographic separation of polar lipids and determination of phospholipids by phosphorus analysis of spots. *Lipids* *5*, 494-496.
- Russell, S. M., Burgess, R. J., and Mayer, R. J. (1980). Protein degradation in rat liver during post-natal development. *Biochem J* *192*, 321-330.
- Sambrook, J., and Russell, D. (2001). *Molecular Cloning: A Laboratory Manual* (Cold Spring Harbor, NY: Cold Spring Harbor Laboratory Press).
- Sauer, R. T., Bolon, D. N., Burton, B. M., Burton, R. E., Flynn, J. M., Grant, R. A., Hersch, G. L., Joshi, S. A., Kenniston, J. A., Levchenko, I., *et al.* (2004). Sculpting the proteome with AAA(+) proteases and disassembly machines. *Cell* *119*, 9-18.
- Schägger, H. (2001). Blue-native gels to isolated protein complexes from mitochondria. *Methods Cell Biol* *65*, 231-244.
- Schägger, H., and von Jagow, G. (1991). Blue native electrophoresis for isolation of membrane protein complexes in enzymatically active form. *Anal Biochem* *199*, 223-231.
- Schlame, M. (2008). Cardiolipin synthesis for the assembly of bacterial and mitochondrial membranes. *J Lipid Res* *49*, 1607-1620.
- Schmidt, M., Lupas, A. N., and Finley, D. (1999). Structure and mechanism of ATP-dependent proteases. *Curr Opin Chem Biol* *3*, 584-591.
- Schneider, A., Behrens, M., Scherer, P., Pratje, E., Michaelis, G., and Schatz, G. (1991). Inner membrane protease I, an enzyme mediating intramitochondrial protein sorting in yeast. *EMBO J* *10*, 247-254.
- Schneider, A., Oppliger, W., and Jenö, P. (1994). Purified inner membrane protease I of yeast mitochondria is a heterodimer. *J Biol Chem* *269*, 8635-8638.
- Schneider, H. C., Berthold, J., Bauer, M. F., Dietmeier, K., Guiard, B., Brunner, M., and Neupert, W. (1994). Mitochondrial Hsp70/MIM44 complex facilitates protein import. *Nature* *371*, 768-774.
- Schneiter, R., Brugger, B., Sandhoff, R., Zellnig, G., Leber, A., Lampl, M., Athenstaedt, K., Hrastnik, C., Eder, S., Daum, G., *et al.* (1999). Electrospray ionization tandem mass spectrometry (ESI-MS/MS) analysis of the lipid molecular species composition of yeast subcellular membranes reveals acyl chain-based sorting/remodeling of distinct molecular species en route to the plasma membrane. *J Cell Biol* *146*, 741-754.

- Schulte, U., Arretz, M., Schneider, H., Tropschug, M., Wachter, E., Neupert, W., and Weiss, H. (1989). A family of mitochondrial proteins involved in bioenergetICS and biogenesis. *Nature* *339*, 147-149.
- Scott, K. A., Alonso, D. O., Sato, S., Fersht, A. R., and Daggett, V. (2007). Conformational entropy of alanine versus glycine in protein denatured states. *Proc Natl Acad Sci U S A* *104*, 2661-2666.
- Sesaki, H., Dunn, C. D., Iijima, M., Shepard, K. A., Yaffe, M. P., Machamer, C. E., and Jensen, R. E. (2006). Ups1p, a conserved intermembrane space protein, regulates mitochondrial shape and alternative topogenesis of Mgm1p. *J Cell Biol* *173*, 651-658.
- Sesaki, H., Southard, S. M., Hobbs, A. E., and Jensen, R. E. (2003). Cells lacking Pcp1p/Ugo2p, a rhomboid-like protease required for Mgm1p processing, lose mtDNA and mitochondrial structure in a Dnm1p-dependent manner, but remain competent for mitochondrial fusion. *Biochem Biophys Res Commun* *308*, 276-283.
- Shah, Z. H., Hakkaart, G. A. J., Arku, B., DeJong, L., Van der Speck, H., Grivell, L., and Jacobs, H. T. (2000). The human homologue of the yeast mitochondrial AAA metalloprotease Yme1p complements a yeast *yme1* disruptant. *FEBS Lett* *478*, 267-270.
- Sherman, F. (2002). Getting started with yeast. *Methods Enzymol* *350*, 3-41.
- Sickmann, A., Reinders, J., Wagner, Y., Joppich, C., Zahedi, R., Meyer, H. E., Schonfisch, B., Perschil, I., Chacinska, A., Guiard, B., *et al.* (2003). The proteome of *Saccharomyces cerevisiae* mitochondria. *Proc Natl Acad Sci USA* *100*, 13207-13212.
- Sikorski, R. S., and Hieter, P. (1989). A system of shuttle vectors and yeast host strains designed for efficient manipulation of DNA in *Saccharomyces cerevisiae*. *Genetics* *122*, 19-27.
- Singh, S. K., Grimaud, R., Hoskins, J. R., Wickner, S., and Maurizi, M. R. (2000). Unfolding and internalization of proteins by the ATP-dependent proteases ClpXP and ClpAP. *Proc Natl Acad Sci U S A* *97*, 8898-8903.
- Singh, S. K., Rozycki, J., Ortega, J., Ishikawa, T., Lo, J., Steven, A. C., and Maurizi, M. R. (2001). Functional domains of the ClpA and ClpX molecular chaperones identified by limited proteolysis and deletion analysis. *J Biol Chem* *276*, 29420-29429.
- Song, M. C., Ogishima, T., and Ito, A. (1998). Importance of residues carboxyl terminal relative to the cleavage site in substrates of mitochondrial processing peptidase for their specific recognition and cleavage. *J Biochem* *124*, 1045-1049.
- Song, Z., Chen, H., Fiket, M., Alexander, C., and Chan, D. C. (2007). OPA1 processing controls mitochondrial fusion and is regulated by mRNA splicing, membrane potential, and Yme1L. *J Cell Biol* *178*, 749-755.
- Sprague, G. F., and Cronan, J. E. (1977). Isolation and characterization of *Saccharomyces cerevisiae* mutants defective in glycerol catabolism. *J Bacteriol* *129*, 1335-1342.
- Stahl, A., Moberg, P., Ytterberg, J., Pnfilov, O., Brockenhuus von Löwenhielm, H., Nilsson, F., and Glaser, E. (2002). Isolation and identification of a novel mitochondrial metalloprotease (PreP) that degrades targeting presequences in plants. *J Biol Chem* *277*, 41931-41939.
- Stahlberg, H., Kutejova, E., Suda, K., Wolpensinger, B., Lustig, A., Schatz, G., Engel, A., and Suzuki, C. K. (1999). Mitochondrial Lon of *Saccharomyces cerevisiae* is a ring-shaped protease with seven flexible subunits. *Proc Natl Acad Sci USA* *96*, 6787-6790.
- Steensma, H. Y., Holterman, L., Dekker, I., van Sluis, C. A., and Wenzel, T. J. (1990). Molecular cloning of the gene for the E1 alpha subunit of the pyruvate dehydrogenase complex from *Saccharomyces cerevisiae*. *Eur J Biochem* *191*, 769-774.

- Steglich, G., Neupert, W., and Langer, T. (1999). Prohibitins regulate membrane protein degradation by the *m*-AAA protease in mitochondria. *Mol Cell Biol* *19*, 3435-3442.
- Sullivan, D. P., Ohvo-Rekila, H., Baumann, N. A., Beh, C. T., and Menon, A. K. (2006). Sterol trafficking between the endoplasmic reticulum and plasma membrane in yeast. *Biochem Soc Trans* *34*, 356-358.
- Suno, R., Niwa, H., Tsuchiya, D., Zhang, X., Yoshida, M., and Morikawa, K. (2006). Structure of the Whole Cytosolic Region of ATP-Dependent Protease FtsH. *Mol Cell* *22*, 575-585.
- Sutter, T. R., and Loper, J. C. (1989). Disruption of the *Saccharomyces cerevisiae* gene for NADPH-cytochrome P450 reductase causes increased sensitivity to ketoconazole. *Biochem Biophys Res Commun* *160*, 1257-1266.
- Suzuki, C. K., Rep, M., Van Dijl, J. M., Suda, K., Grivell, L. A., and Schatz, G. (1997). ATP-dependent proteases that also chaperone protein biogenesis. *Trends Biochem Sci* *22*, 118-123.
- Suzuki, C. K., Suda, K., Wang, N., and Schatz, G. (1994). Requirement for the yeast gene LON in intramitochondrial proteolysis and maintenance of respiration. *Science* *264*, 273-276.
- Tatsuta, T., Augustin, S., Nolden, M., Friedrichs, B., and Langer, T. (2007). *m*-AAA protease-driven membrane dislocation allows intramembrane cleavage by rhomboid in mitochondria. *EMBO J* *26*, 325-335.
- Tatsuta, T., Joob, D. M., Calendar, R., Akiyama, Y., and Ogura, T. (2000). Evidence for an active role of the DnaK chaperone system in the degradation of sigma(32). *FEBS Lett* *478*, 271-275.
- Tatsuta, T., and Langer, T. (2007). Studying proteolysis within mitochondria. *Methods Mol Biol* *372*, 343-360.
- Tatsuta, T., and Langer, T. (2008). Quality control of mitochondria: protection against neurodegeneration and ageing. *EMBO J* *27*, 306-314.
- Taylor, S. W., Fahy, E., Zhang, B., Glenn, G. M., Warnock, D. E., Wiley, S., Murphy, A. N., Gaucher, S. P., Capaldi, R. A., Gibson, B. W., and Ghosh, S. S. (2003). Characterization of the human heart mitochondrial proteome. *Nat Biotechnol* *21*, 281-286.
- Thomas, B. J., and Rothstein, R. (1989). Elevated recombination rates in transcriptionally active DNA. *Cell* *56*, 619-630.
- Thorsness, P. E., and Fox, T. D. (1993). Nuclear mutations in *Saccharomyces cerevisiae* that affect the escape of DNA from mitochondria to the nucleus. *Genetics* *134*, 21-28.
- Thorsness, P. E., White, K. H., and Fox, T. D. (1993). Inactivation of *YME1*, a member of the ftsH-SEC18-PAS1-CDC48 family of putative ATPase-encoding genes, causes increased escape of DNA from mitochondria in *Saccharomyces cerevisiae*. *Mol Cell Biol* *13*, 5418-5426.
- Tinkelenberg, A. H., Liu, Y., Alcantara, F., Khan, S., Guo, Z., Bard, M., and Sturley, S. L. (2000). Mutations in yeast ARV1 alter intracellular sterol distribution and are complemented by human ARV1. *J Biol Chem* *275*, 40667-40670.
- Tomatsu, S., Kobayashi, Y., Fukumaki, Y., Yubisui, T., Oorii, T., and Sakaki, Y. (1989). The organization and the complete nucleotide sequence of the human NADH-cytochrome b5 reductase gene. *Gene* *80*, 353-361.
- Tomoyasu, T., Yuki, T., Morimura, S., Mori, H., Yamanaka, K., Niki, H., Hiraga, S., and Ogura, T. (1993). The *Escherichia coli* FtsH protein is a prokaryotic member of a protein family of putative ATPases involved in membrane functions, cell cycle control, and gene expression. *J Bacteriol* *175*, 1344-1351.

- Tong, A. H. Y., Evangelista, M., Parsons, A. B., Xu, H., Bader, G. D., Pagé, N., Robinson, M., Raghibizadeh, S., Hogue, C. W. V., Bussey, H., *et al.* (2001). Systematic genetic analysis with ordered arrays of yeast deletion mutants. *Science* *294*, 2364-2368.
- Towbin, H., Staehelin, T., and Gordon, J. (1979). Electrophoretic transfer of proteins from polyacrylamide gels to nitrocellulose sheets: procedure and some applications. *Proc Natl Acad Sci U S A* *76*, 4350-4354.
- Trotter, P. J., and Voelker, D. R. (1995). Identification of a non-mitochondrial phosphatidylserine decarboxylase activity (PSD2) in the yeast *Saccharomyces cerevisiae*. *J Biol Chem* *270*, 6062-6070.
- Tucker, P. A., and Sallai, L. (2007). The AAA+ superfamily--a myriad of motions. *Curr Opin Struct Biol* *17*, 641-652.
- Tuller, G., and Daum, G. (1995). Import of sterols into mitochondria of the yeast *Saccharomyces cerevisiae*. *FEBS Lett* *372*, 29-32.
- Tuller, G., Hrastnik, C., Achleitner, G., Schiefthaler, U., Klein, F., and Daum, G. (1998). YDL142c encodes cardiolipin synthase (Cls1p) and is non-essential for aerobic growth of *Saccharomyces cerevisiae*. *FEBS Lett* *421*, 15-18.
- Vaden, D. L., Gohil, V. M., Gu, Z., and Greenberg, M. L. (2005). Separation of yeast phospholipids using one-dimensional thin-layer chromatography. *Anal Biochem* *338*, 162-164.
- Van Dyck, L., Dembowski, M., Neupert, W., and Langer, T. (1998). Mcx1p, a ClpX homologue in mitochondria of *Saccharomyces cerevisiae*. *FEBS Lett* *438*, 250-254.
- Van Dyck, L., and Langer, T. (1999). ATP-dependent proteases controlling mitochondrial function in the yeast *Saccharomyces cerevisiae*. *Cell Mol Life Sci* *55*, 825-842.
- Van Dyck, L., Pearce, D. A., and Sherman, F. (1994). *PIM1* encodes a mitochondrial ATP-dependent protease that is required for mitochondrial function in the yeast *Saccharomyces cerevisiae*. *J Biol Chem* *269*, 238-242.
- van Meer, G., Voelker, D. R., and Feigenson, G. W. (2008). Membrane lipids: where they are and how they behave. *Nat Rev Mol Cell Biol* *9*, 112-124.
- Voelker, D. R. (2004). Lipid synthesis and transport in mitochondrial biogenesis, Vol 8: Springer Berlin / Heidelberg).
- von Janowsky, B., Knapp, K., Major, T., Krayl, M., Guiard, B., and Voos, W. (2005). Structural properties of substrate proteins determine their proteolysis by the mitochondrial AAA+ protease Pim1. *Biol Chem* *386*, 1307-1317.
- von Janowsky, B., Major, T., Knapp, K., and Voos, W. (2006). The disaggregation activity of the mitochondrial ClpB homolog Hsp78 maintains Hsp70 function during heat stress. *J Mol Biol* *357*, 793-807.
- Wagner, A., Grillitsch, K., Leitner, E., and Daum, G. (2009). Mobilization of steryl esters from lipid particles of the yeast *Saccharomyces cerevisiae*. *Biochim Biophys Acta* *1791*, 118-124.
- Wagner, I., Arlt, H., van Dyck, L., Langer, T., and Neupert, W. (1994). Molecular chaperones cooperate with PIM1 protease in the degradation of misfolded proteins in mitochondria. *EMBO J* *13*, 5135-5145.
- Wallace, D. C. (2007). Why do we still have a maternally inherited mitochondrial DNA? Insights from evolutionary medicine. *Annu Rev Biochem* *76*, 781-821.

- Wang, J., Hartling, J. A., and Flanagan, J. M. (1997). The structure of ClpP at 2.3 Å resolution suggests a model for ATP-dependent proteolysis. *Cell* *91*, 447-456.
- Wang, J., Song, J. J., Franklin, M. C., Kamtekar, S., Im, Y. J., Rho, S. H., Seong, I. S., Lee, C. S., Chung, C. H., and Eom, S. H. (2001). Crystal structures of the HslVU peptidase-ATPase complex reveal an ATP-dependent proteolysis mechanism. *Structure (Camb)* *9*, 177-184.
- Wang, J., Song, J. J., Seong, I. S., Franklin, M. C., Kamtekar, S., Eom, S. H., and Chung, C. H. (2001). Nucleotide-dependent conformational changes in a protease-associated ATPase HslU. *Structure* *9*, 1107-1116.
- Wang, P., Zhang, Y., Li, H., Chieu, H. K., Munn, A. L., and Yang, H. (2005). AAA ATPases regulate membrane association of yeast oxysterol binding proteins and sterol metabolism. *Embo J* *24*, 2989-2999.
- Wang, X., Zuo, X., Kucejova, B., and Chen, X. J. (2008). Reduced cytosolic protein synthesis suppresses mitochondrial degeneration. *Nat Cell Biol*.
- Weber, E. R., Hanekamp, T., and Thorsness, P. E. (1996). Biochemical and functional analysis of the *YME1* gene product, an ATP and zinc-dependent mitochondrial protease from *S. cerevisiae*. *Mol Biol Cell* *7*, 307-317.
- Weber, E. R., Rooks, R. S., Shafer, K. S., Chase, J. W., and Thorsness, P. E. (1995). Mutations in the mitochondrial ATP synthase gamma subunit suppress a slow-growth phenotype of *yme1* yeast lacking mitochondrial DNA. *Genetics* *140*, 435-442.
- Wenzel, T. J., Luttik, M. A., van den Berg, J. A., and de Steensma, H. Y. (1993). Regulation of the PDA1 gene encoding the E1 alpha subunit of the pyruvate dehydrogenase complex from *Saccharomyces cerevisiae*. *Eur J Biochem* *218*, 405-411.
- Wenzel, T. J., van den Berg, M. A., Visser, W., van den Berg, J. A., and Steensma, H. Y. (1992). Characterization of *Saccharomyces cerevisiae* mutants lacking the E1 alpha subunit of the pyruvate dehydrogenase complex. *Eur J Biochem* *209*, 697-705.
- Wilcox, L. J., Balderes, D. A., Wharton, B., Tinkelenberg, A. H., Rao, G., and Sturley, S. L. (2002). Transcriptional profiling identifies two members of the ATP-binding cassette transporter superfamily required for sterol uptake in yeast. *J Biol Chem* *277*, 32466-32472.
- Wilson, W. A., Wang, Z., and Roach, P. J. (2002). Systematic identification of the genes affecting glycogen storage in the yeast *Saccharomyces cerevisiae*: implication of the vacuole as a determinant of glycogen level. *Mol Cell Proteomics* *1*, 232-242.
- Winzeler, E. A., Shoemaker, D. D., Astromoff, A., Liang, H., Anderson, K., Andre, B., Bangham, R., Benito, R., Boeke, J. D., Bussey, H., *et al.* (1999). Functional characterization of the *S. cerevisiae* genome by gene deletion and parallel analysis. *Science* *285*, 901-906.
- Wiseman, H., Cannon, M., Arnstein, H. R., and Halliwell, B. (1993). Enhancement by tamoxifen of the membrane antioxidant action of the yeast membrane sterol ergosterol: relevance to the antiyeast and anticancer action of tamoxifen. *Biochim Biophys Acta* *1181*, 201-206.
- Wiseman, H., Cannon, M., Arnstein, H. R., and Halliwell, B. (1993). Tamoxifen inhibits lipid peroxidation in cardiac microsomes. Comparison with liver microsomes and potential relevance to the cardiovascular benefits associated with cancer prevention and treatment by tamoxifen. *Biochem Pharmacol* *45*, 1851-1855.
- Wojtyra, U. A., Thibault, G., Tuite, A., and Houry, W. A. (2003). The N-terminal zinc binding domain of ClpX is a dimerization domain that modulates the chaperone function. *J Biol Chem* *278*, 48981-48990.

- Woods, R. A. (1971). Nystatin-resistant mutants of yeast: alterations in sterol content. *J Bacteriol* *108*, 69-73.
- Xia, D., Esser, L., Singh, S. K., Guo, F., and Maurizi, M. R. (2004). Crystallographic investigation of peptide binding sites in the N-domain of the ClpA chaperone. *J Struct Biol* *146*, 166-179.
- Yaffe, M. P., Ohta, S., and Schatz, G. (1985). A yeast mutant temperature-sensitive for mitochondrial assembly is deficient in a mitochondrial protease activity that cleaves imported precursor polypeptides. *EMBO J* *4*, 2069-2074.
- Yaffe, M. P., and Schatz, G. (1984). Two nuclear mutations that block mitochondrial protein import in yeast. *Proc Natl Acad Sci USA* *81*, 4819-4823.
- Yang, M., Jensen, R. E., Yaffe, M. P., Oppliger, W., and Schatz, G. (1988). Import of proteins into yeast mitochondria: the purified matrix processing protease contains two subunits which are encoded by the nuclear *MAS1* and *MAS2* genes. *EMBO J* *7*, 3857-3862.
- Yang, X., Iwamoto, K., Wang, M., Artwohl, J., Mason, J. I., and Pang, S. (1993). Inherited congenital adrenal hyperplasia in the rabbit is caused by a deletion in the gene encoding cytochrome P450 cholesterol side-chain cleavage enzyme. *Endocrinology* *132*, 1977-1982.
- Young, L., Leonhard, K., Tatsuta, T., Trowsdale, J., and Langer, T. (2001). Role of the ABC transporter Mdl1 in peptide export from mitochondria. *Science* *291*, 2135-2138.
- Yu, A. Y., and Houry, W. A. (2007). ClpP: a distinctive family of cylindrical energy-dependent serine proteases. *FEBS Lett* *581*, 3749-3757.
- Zeng, X., Neupert, W., and Tzagoloff, A. (2007). The Metalloprotease Encoded by *ATP23* Has a Dual Function in Processing and Assembly of Subunit 6 of Mitochondrial ATPase. *Mol Biol Cell* *18*, 617-626.
- Zeth, K., Ravelli, R. B., Paal, K., Cusack, S., Bukau, B., and Dougan, D. A. (2002). Structural analysis of the adaptor protein ClpS in complex with the N-terminal domain of ClpA. *Nat Struct Biol* *9*, 906-911.
- Zhang, X., Shaw, A., Bates, P. A., Newman, R. H., Gowen, B., Orlova, E., Gorman, M. A., Kondo, H., Dokurno, P., Lally, J., *et al.* (2000). Structure of the AAA ATPase p97. *Mol Cell* *6*, 1473-1484.
- Zinser, E., and Daum, G. (1995). Isolation and biochemical characterization of organelles from the yeast *Saccharomyces cerevisiae*. *Yeast* *11*, 493-536.
- Zinser, E., Paltauf, F., and Daum, G. (1993). Sterol composition of yeast organelle membranes and subcellular distribution of enzymes involved in sterol metabolism. *J Bacteriol* *175*, 2853-2858.
- Zinser, E., Sperka-Gottlieb, C. D., Fasch, E. V., Kohlwein, S. D., Paltauf, F., and Daum, G. (1991). Phospholipid synthesis and lipid composition of subcellular membranes in the unicellular eukaryote *Saccharomyces cerevisiae*. *J Bacteriol* *173*, 2026-2034.
- Zweytick, D., Leitner, E., Kohlwein, S. D., Yu, C., Rothblatt, J., and Daum, G. (2000). Contribution of Are1p and Are2p to steryl ester synthesis in the yeast *Saccharomyces cerevisiae*. *Eur J Biochem* *267*, 1075-1082.
- Zwickl, P., Baumeister, W., and Steven, A. (2000). Dis-assembly lines: the proteasome and related ATPase-assisted proteases. *Curr Opin Struct Biol* *10*, 242-250.

7 List of abbreviations

AAA	"ATPases associated with a variety of cellular activities"
ADP/ATP	adenosine-5'-diphosphate/adenosine-5'-triphosphate
b	base
BSA	bovine serum albumine
C-/N-terminal	carboxy/amino terminal
C-/N-terminus	carboxy/amino terminus
DMSO	dimethyl sulfoxide
DNA	deoxyribonucleic acid
DTT	dithiothreitol
EDTA	ethylene diamine tetraacetic acid
Fig.	figure
5'FOA	5'-fluoroorotic acid
FPLC/HPLC	fast protein liquid chromatography/high performance liquid chrom.
g	gramm
<i>g</i>	gravity
G418	antibiotic G418
GFP	green fluorescent protein
h/min/s	hour/minute/second
HA	influenza hemagglutinin peptide
HEPES	N-2-hydroxyethylpiperazine-N'-2-ethanesulfonic-acid
IgG	immunoglobulin G
kb/kDa	kilobases/kilodalton
M	molarity per liter
MDa	megadalton
mg/ml	milligram/milliliter
mtDNA	mitochondrial DNA
µg/µl	microgramm/microliter
MOPS	3-(N-Morpholino)propanesulfonic acid
mRNA	messenger RNA
NAT	nourseothricin
NADH	nicotinamide adenine dinucleotide
nm	nanometer
OD(600)	optical density at a wavelength of 600 nanometer
PAGE	polyacrylamid gelelectrophoresis
PCR	polymerase chain reaction
PMF	peptide mass fingerprint
PMSF	phenylmethanesulfonyl fluoride
PVDF	polyvinylidenfluorid
RNA	ribonucleic acid
rpm	rounds per minute
RT	room temperature
SP6	bacteriophage SP6-specific RNA polymerase
STI	soybean trypsin inhibitor
Tab.	table
TCA	trichloric acid
Tris	tris(hydroxymethyl)aminomethane
YP	yeast extract peptone
V	voltage

8 Attachment

Assorted library for Synthetic genetic analysis (SGA)

Morphology components		Peptidases		Synthetic lethal with prohibitins		Lipid related	
ORF	Name	ORF	Name	ORF	Name	ORF	Name
<i>YLL006w</i>	<i>MMM1</i>	<i>YNR020c</i>	<i>ATP23</i>	<i>YER093c-a</i>	<i>GEP8</i>	<i>YNL169c</i>	<i>PSD1</i>
<i>YAL010c</i>	<i>MDM10</i>	<i>YGR101w</i>	<i>PCP1</i>	<i>YGL057c</i>	<i>YGL057c</i>	<i>YGR170w</i>	<i>PSD2</i>
<i>YOL009c</i>	<i>MDM12</i>	<i>YBL022c</i>	<i>PIM1</i>	<i>YLR091w</i>	<i>YLR091w</i>	<i>YDL142c</i>	<i>CRD1</i>
<i>YLR368w</i>	<i>MDM30</i>	<i>YKR087c</i>	<i>OMA1</i>	<i>YMR293c</i>	<i>YMR293c</i>	<i>YPR140w</i>	<i>TAZ1</i>
<i>YHR194w</i>	<i>MDM31</i>	<i>YKL134c</i>	<i>OCT1</i>	<i>YOR205c</i>	<i>GEP3</i>	<i>YLR168c</i>	<i>GEP1</i>
<i>YOR147w</i>	<i>MDM32</i>	<i>YMR150c</i>	<i>IMP1</i>	<i>YMR187c</i>	<i>YMR187c</i>	<i>YDR185c</i>	<i>YDR185c</i>
<i>YDR393w</i>	<i>MDM33</i>	<i>YMR035w</i>	<i>IMP2</i>	<i>YHR034c</i>	<i>PIH1</i>	<i>YLR193c</i>	<i>UPS1</i>
<i>YGL219c</i>	<i>MDM34</i>	<i>YER017c</i>	<i>YTA10</i>	<i>YLR204w</i>	<i>QRI5</i>	<i>YHR100c</i>	<i>GEP4</i>
<i>YKL053c</i>	<i>MDM35</i>	<i>YMR089c</i>	<i>YTA12</i>	<i>YML061c</i>	<i>PIF1</i>		
<i>YOL027c</i>	<i>MDM38</i>	<i>YPR024w</i>	<i>YME1</i>	<i>YKR016w</i>	<i>YKR016w</i>	<i>YKL091c</i>	<i>SFH1</i>
<i>YBR179c</i>	<i>FZO1</i>	<i>YCL057w</i>	<i>PRD1</i>	<i>YMR224c</i>	<i>MRE11</i>	<i>YNL231c</i>	<i>PDR16</i>
<i>YOR211c</i>	<i>MGM1</i>	<i>YDR430c</i>	<i>MOP112</i>	<i>YNL170w</i>	<i>YNL170w</i>	<i>YNL264c</i>	<i>PDR17</i>
<i>YDR470c</i>	<i>UGO1</i>	<i>YDL104c</i>	<i>QRI7</i>	<i>YOL095c</i>	<i>HMI1</i>	<i>YLR380w</i>	<i>CSR1</i>
<i>YLL001w</i>	<i>DNM1</i>	<i>YNL239w</i>	<i>LAP3</i>	<i>YGR132c</i>	<i>PHB1</i>	<i>YJL145w</i>	<i>SFH5</i>
<i>YPL072w</i>	<i>UBP16</i>	<i>YLR188w</i>	<i>MDL1</i>	<i>YGR231c</i>	<i>PHB2</i>	<i>YMR008c</i>	<i>PLB1</i>
		<i>YPL270w</i>	<i>MDL2</i>			<i>YMR006c</i>	<i>PLB2</i>
						<i>YOL011w</i>	<i>PLB3</i>
						<i>YLR133w</i>	<i>CKI1</i>
						<i>YGR007w</i>	<i>MUQ1</i>
						<i>YDR147w</i>	<i>EKI1</i>
Others		Respiratory chain assembly		Cell wall components		Inositol related	
ORF	Name	ORF	Name	ORF	Name	ORF	Name
<i>YDR258c</i>	<i>HSP78</i>	<i>YER154w</i>	<i>OXA1</i>	<i>YLR342w</i>	<i>FKS1</i>	<i>YJL153c</i>	<i>INO1</i>
<i>YLR304c</i>	<i>ACO1</i>	<i>YHR051w</i>	<i>COX6</i>	<i>YMR307w</i>	<i>GAS1</i>	<i>YDR123c</i>	<i>INO2</i>
<i>YMR072w</i>	<i>ABF2</i>	<i>YBR003w</i>	<i>COQ1</i>	<i>YER019w</i>	<i>ISC1</i>	<i>YOL108c</i>	<i>INO4</i>
<i>YGR028w</i>	<i>MSP1</i>	<i>YLR393w</i>	<i>ATP10</i>	<i>YJR100c</i>	<i>YJR100c</i>	<i>YHL020c</i>	<i>OPI1</i>
<i>YGR033c</i>	<i>TIM21</i>	<i>YDR377w</i>	<i>ATP17</i>	<i>YIL154c</i>	<i>IMP2'</i>	<i>YJR073c</i>	<i>OPI3</i>
<i>YMR060c</i>	<i>SAM37</i>	<i>YKL016c</i>	<i>ATP7</i>	<i>YOL023w</i>	<i>IFM1</i>	<i>YDL096c</i>	<i>OPI6</i>
		<i>YPL132w</i>	<i>COX11</i>	<i>YEL030w</i>	<i>ECM10</i>	<i>YDR360w</i>	<i>OPI7</i>
						<i>YKR035c</i>	<i>OPI8</i>
						<i>YLR338w</i>	<i>OPI9</i>
						<i>YOL032w</i>	<i>OPI10</i>
						<i>YPR044c</i>	<i>OPI11</i>

9 Danksagung

An erster Stelle möchte ich mich bei Professor Dr. Thomas Langer für die Bereitstellung des Themas, sein großes Engagement und seine fortwährende Unterstützung und Förderung meiner wissenschaftlichen Arbeit bedanken.

Prof. Dr. Jürgen R. Dohmen, Prof. Dr. Reinhard Krämer und Dr. Matthias Cramer danke ich für die bereitwillige Annahme einer Position in meinem „Thesis Comittee“, und für die bereits bei der Entstehung dieser Arbeit erfolgte Hilfe und Unterstützung.

Großer Dank geht an alle jetzigen und ehemaligen Mitgliedern der AG Langer für das tolle Arbeitsklima und für all die Hilfe, Anregungen und Unterstützung bei wissenschaftlichen und nicht-wissenschaftlichen Problemen. Besonderer Dank gilt dabei den Leuten aus dem „großen“ Labor und allen Mitstreitern des Yme1 Projektes (Martin und Gina). Außerdem möchte ich mich für das bemühte Beantworten machter weit reichenden Frage (Brigitte); für aufmunternde und ironische Worte, sowie unterstützende Vorschläge in vielerlei Hinsicht (Susanne); für Hilfe an der Bestellfront (Sascha und Casi); für technische Unterstützung (Guzi); für wissenschaftliche Anmerkungen und Hilfen (Gerrit); für gegenseitig motivieren bis zuletzt (Ines); für das gemeinsame Ausharren über eine ganz schön lange Zeit (Sarah und Steffen) und für das Korrekturlesen dieser Arbeit (Martin und Mirko) bedanken.

Außerdem möchte ich mich bei allen Leuten, die daran beteiligt waren für die tollen gemeinsam verbrachten Momente bei Espresso- und Biertrinken (oder doch lieber Wein), beim Karnevalfeiern, bei Laborausflügen, bei mehr oder weniger wissenschaftlichen Diskussionsrunden und bei den immer wieder lustigen Weihnachtsfeiern bedanken.

Ein großes Dankeschön geht auch an meine Familie und meine Freunde für Verständnis, Unterstützung und daran glauben, dass ich das alles schon hinkriege.

Ganz besonderer Dank gilt auch dem „kleinen“ Marc für’s immer da sein und es ja doch nie richtig machen.

10 Eidesstattliche Erklärung

Ich versichere, dass ich die von mir vorgelegte Dissertation selbständig angefertigt, die benutzten Quellen und Hilfsmittel vollständig angegeben und die Stellen der Arbeit - einschließlich Tabellen, Karten und Abbildungen -, die anderen Werken im Wortlaut oder dem Sinn nach entnommen sind, in jedem Einzelfall als Entlehnung kenntlich gemacht habe; dass diese Dissertation noch keiner anderen Fakultät oder Universität zur Prüfung vorgelegen hat; dass sie - abgesehen von unten angegebenen Teilpublikationen - noch nicht veröffentlicht worden ist sowie, dass ich eine solche Veröffentlichung vor Abschluss des Promotionsverfahrens nicht vornehmen werde. Die Bestimmungen der Promotionsordnung sind mir bekannt. Die von mir vorgelegte Dissertation ist von Herrn Prof. Dr. Thomas Langer betreut worden.

Tanja Engmann
Köln im März 2009

11 Lebenslauf

Vor- und Zuname: Tanja Engmann

Geburtstag: 10. Februar 1978

Geburtsort: Iserlohn

Staatsangehörigkeit: deutsch

Schulbildung

1984 – 1988 Bartholomäusschule, Städtische Gemeinschaftsgrundschule, Iserlohn

1988 – 1997 Gymnasium Letmathe der Stadt Iserlohn

Juli 1997 Abitur

Hochschulausbildung

Oktober 1997 – Juli 2002	Studium der Biologie an der Ruhr-Universität-Bochum
August 2001 – Juli 2002	Diplomarbeit am Institut für Physikalischen Chemie in der medizinischen Fakultät der Ruhr-Universität-Bochum bei Prof. Dr. W.-H. Kunau, mit dem Thema: „Untersuchungen zur Interaktion zwischen Proteinen des peroxisomalen PTS2-Importes der Hefe <i>Saccharomyces cerevisiae</i> .“
Juli 2002	Abschluss als Diplom-Biologin
Juli 2002 – August 2003	Praktikum an der University of California San Diego, USA bei Prof. Dr. S. Subramani. Forschungsthema: „Biogenese und Abbau von Peroxisomen in der Hefe <i>Pichia pastoris</i> und an menschlichen Zellen.“
September 2003 – März 2009	Doktorarbeit am Institut für Genetik der Universität zu Köln bei Prof. Dr. Thomas Langer; Dissertation zum Thema: „Structural, physical and genetic interaction of the i-AAA protease Yme1 in <i>Saccharomyces cerevisiae</i> .“

Publikationen

Graef, M., Langer, T., and Engmann, T. (2008) The recognition of substrates by AAA proteases in mitochondria. In: ATP-dependent proteases. Ed.: Eva Kutejová. Research Signpost, Kerala, India. pp 179-195.

